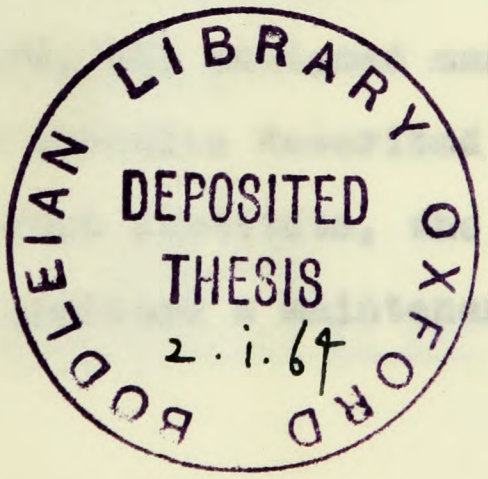
SOME EXPERIMENTS IN OPTICAL PUMPING

Thesis submitted for the degree of
Doctor of Philosophy
in the University of Oxford
by

R. C. GREENHOW



St. John's College.
June, 1963.

Clarendon Laboratory,
Oxford.

ACKNOWLEDGEMENTS

It is a pleasure to record my appreciation of the advice, assistance and encouragement received from the following people:-

Dr. D. Roaf, who supervised this work.

Dr. G. W. Series, for his constant help and interest.

Dr. K. R. Lea, who collaborated in most of the work reported here.

Dr. J. M. Vaughan, who was responsible, with my slight assistance, for all the work reported here involving the use of the high resolution Fabry-Perot spectrograph.

Dr. H. G. Kuhn, for permission to use the above spectrograph.

Mr. R. B. Partridge who collaborated in the later stages of this work.

Mr. D. Smith, who designed many of the electronic circuits described in this thesis.

The Rutherford Institute, who financed this work, and provided a maintenance grant.

CONTENTS

INTRODUCTION

PART ONE

OPTICAL PUMPING IN HE^4

CHAPTER ONE

(i)	The pumping process	1.1
(ii)	Rate equations	1.4
(iii)	Polarisation and "Alignment" Parameters	1.7
(iv)	Pumping time	1.8
(v)	Effect of relaxation on 'P' and 'A'	1.9
(vi)	Signal strengths	1.10
(vii)	Line shapes	1.12
(viii)	Effect of sample thickness	1.17
(ix)	Diffusion equation	1.18
	Table 1	1.21

CHAPTER TWO

(i)	The apparatus	2.1
(ii)	Experimental Procedure	2.2
(iii)	Details of the apparatus	2.5

CHAPTER THREE

(i)	Conditions for best optical pumping signals	3.1
(ii)	Thin samples	3.3
(iii)	Degree of polarisation	3.4
(iv)	Line widths	3.5
(v)	Line shapes	3.6
(vi)	Pumping transient	3.7
(vii)	Causes of relaxation	3.9
(viii)	Lamp investigation	3.12
(ix)	Summary	3.13

PART TWO

OPTICAL PUMPING IN HE^3

CHAPTER FOUR

(i)	The pumping process	4.1
(ii)	Rate equations	4.5
(iii)	Measurement of degree of polarisation	4.8
(iv)	Nuclear nutation	4.15

CHAPTER FIVE

(i)	Detection methods	5.1
(ii)	Determination of metastable density	5.6
(iii)	Items of equipment	5.8

CHAPTER SIX

(i)	Density of metastable atoms	6.1
(ii)	Observations of resonances in the metastable levels, using field modulation	6.4
(iii)	Pumping transient	6.7
(iv)	Longitudinal relaxation time	6.8
(v)	Origin of longitudinal relaxation	6.9
(vi)	Measurements of polarisation	6.10
(vii)	Correlation of results	6.12
(viii)	Measurements of transverse relaxation time	6.15
(ix)	Metastability exchange cross-section	6.18
(x)	Multiple Quantum Transitions	6.20
(xi)	Note on errors	6.21
(xii)	Summary	6.22

PART THREE

LIGHT MODULATION EFFECTS IN THE OPTICAL PUMPING OF He^4

CHAPTER SEVEN

(i)	Introduction	7.1
(ii)	Modulation at 2	7.2
(iii)	Theory of Dodd and Series	7.4
(iv)	Additional effects	7.4

CHAPTER EIGHT

(i)	Phase-sensitive detection	8.2
(ii)	Non-phase-sensitive detection	8.2
(iii)	Detection of signals modulated at more than 20 Kcs./sec.	8.3
(iv)	Items of equipment	8.4

CHAPTER NINE

(i)	High frequency modulation	9.1
(ii)	Modulation at $2\omega_0$	9.2
(iii)	Modulation at $4\omega_0$	9.4
(iv)	Modulation at ω_0	9.4

CHAPTER NINE (continued)

(v)	Modulation at $3\omega_0$	9.5
(vi)	Cross-beam modulation	9.5
(vii)	Summary	9.6
Appendix		A.1
References		R.1
Abstract		Ab.1

Introduction

Optical pumping on He^4 was first reported by Colegrove and Franken (ref. 2). They illuminated $^3S_1$ metastable He^4 atoms present in a low pressure gas discharge with unpolarised light from a He^4 lamp. The gas was situated in a weak magnetic field, and as a result of the non-uniform spectral density of the incident radiation the magnetic states of the $^3S_1$ level became unequally populated. Their experiments were limited to the production of alignment. This work was repeated by us, and extended to the production of polarisation. This was done as a preliminary to an attempt to produce nuclear polarisation in He^3. The original idea for the latter project was to perform optical pumping on the 2^1S_o metastable level of He^3, using 20,582 Å radiation to excite $2^1S_o - 2^1P_1$ transitions. It was hoped that nuclear polarisation would be transferred to the ground state (1^1S_o), since the decay from the 2^1P_1 state is predominantly to that level. Before attempting this experiment, efforts were made to detect polarisation in the triplet metastable level in He^3 but they met with no success. The conclusion was reached that spin exchange collisions with the ground state atoms, and subsequent depolarisation of these, provided a relaxation route so efficient, that no appreciable polarisation could be maintained by the lamps available. At this point it was reported, by Schearer (ref. 26) that nuclear polarisation

had been observed in ground state He^3 atoms, using optical pumping in the $^3S_1$ metastable level. The transfer mechanism was just the process which we had concluded was causing the relaxation in our experiments, i.e. spin exchange collisions. In fact the relaxation time of the ground state atoms was very long, but it required several seconds for the rare metastable atoms to polarise the ground state atoms, through the spin exchange collisions. This long pumping time, and the fact that the resonance lines were very much broader than those in He^4, had prevented us from detecting the resonances. Further attempts met with success, and are reported in part two of this thesis.

In the course of the work it was suggested to us, by Dr. G. W. Series, that the He^4 optical pumping system may provide an opportunity to study, in absorption, phenomena which he and his collaborators had been studying in fluorescence. These concerned resonance radiation which was modulated as a result of an r.f. perturbation acting upon the emitting atoms. In our case the perturbation was to act upon absorbing atoms. Exploratory experiments were successfully performed, and are reported in part three of this thesis.

The three sections of the thesis, which are accounts of optical pumping in He^4, optical pumping in He^3, and modulation experiments on He^4, are each divided further into three chapters. So far as possible these are concerned with theoretical considerations, experimental details, and results and discussion.

CHAPTER ONE

THEORETICAL CONSIDERATIONS

(i) The pumping process

(a) The levels

Optical pumping in He^4 differs from many other optical systems in that the polarization or alignment is produced in a metastable level, and not a ground level. The $^3S_1$ metastable level is used and this is populated by exciting a weak discharge in the low pressure He^4 gas. About 1 in 10^5 of the He^4 atoms may be in the $^3S_1$ metastable state at any given time. The remainder, in the ground state, act as a buffer gas. The 10,830Å optical radiation resulting from the transitions $^3S_1 - {}^3P_{0,1,2}$

(b) The pumping light

Light emitted or absorbed in the above transitions is referred to as D_0, D_1, or D_2 light depending on the J value of the upper level involved.

Reference to Fig. 1 shows that the fine structure interval $^3P_0 - {}^3P_1$ is .99 cm^{-1} (1.17Å), while that between $^3P_1$ and $^3P_2$ is .03 cm^{-1} (.03Å) (Ref. 1). The width at half intensity of the lines emitted by our lamps was about .1 cm^{-1} so that the D_0 line was well resolved from the D_1 and the D_2 lines but the two latter lines were not resolved at all. The Doppler absorption width at half intensity in the pumping cell, at room temperature, was about .06 cm^{-1} so that in absorption

PART ONE

OPTICAL PUMPING IN HE^4

CHAPTER ONE

THEORETICAL CONSIDERATIONS

(i) The pumping process

(a) The levels

Optical pumping in He^4 differs from many other optical systems in that the polarisation or alignment is produced in a metastable level, and not a ground level. The $^3S_1$ metastable level is used and this is populated by exciting a weak discharge in the low pressure He^4 gas. About 1 in 10^5 of the He^4 atoms may be in the $^3S_1$ metastable state at any given time. The remainder, in the ground state, act as a buffer gas. The 10,830Å optical radiation used for pumping results from the transitions $^3S_1 - {}^3P_{0,1,2}$.

(b) The pumping light

Light emitted or absorbed in the above transitions is referred to as D_0, D_1, or D_2 light depending on the J value of the upper level involved.

Reference to Fig. 1 shows that the fine structure interval $^3P_0 - {}^3P_1$ is .99 cm^{-1} (1.17Å), while that between $^3P_1$ and $^3P_2$ is .08 cm^{-1} (.09Å) (Ref. 1). The width at half intensity of the lines emitted by our lamps was about .16 cm^{-1} so that the D_0 line was well resolved from the D_1 and the D_2 lines but the two latter lines were not resolved at all. The Doppler absorption width at half intensity in the pumping cell, at room temperature, was about .06 cm^{-1} so that in absorption

the D_1 and D_2 lines are partially resolved. Most of the following analysis concerns optically thin pumping cells, in which case the intensities of the pumping light, in the regions of the D_1 and D_2 absorption lines, are at all times effectively equal. We therefore speak of D_0 and D_3 light, the latter being a combination of D_1 and D_2 light. Theoretically, the ratios of the intensities of the D_0, D_1 and D_2 lines are 5:3:1, so that the intensity ratio between D_0 and D_3 light, denoted by K, should be approximately 1/8. In practice it was found to vary between 1 and .25 according to lamp conditions. (See Chapter III).

(c) Polarisation

Fig. 2a is a Heisenberg representation of all the states involved in the $^3S_1 - {}^3P_{0,1,2}$ transitions in He^4. Consider metastable He^4 atoms situated in a magnetic field directed along the z-axis. Absorption of right-handed circularly polarised (σ^+) radiation incident along the z-axis excites transitions in which $\Delta m = +1$. These are shown in the diagram as sloping upwards to the right. The subsequent behaviour of the atoms in the ^3P states depends on whether or not their orientations are destroyed by collisions before the atoms decay. The effect of collisions is to disorient the orbital angular momentum of the atoms with respect to their spins. Thus an atom excited to a given state of the ^3P levels has a probability of decaying from another. This process will

be referred to as mixing in the excited states. Simple kinetic theory shows that at 1 mm. Hg. a Helium atom undergoes 6.10^6 collisions/sec., so that the collision time $\tau_c \simeq 10^{-7}$ secs. Since the lifetime of an atom in the ^3P levels, τ_r, is 10^{-7} secs., we can see that at pressures below $\frac{1}{2}$ mm. Hg. very little mixing will occur whilst for pressures above 2 mm. Hg. mixing will be almost complete. This effect does not exclude polarisation but it does limit the degree of polarisation attained.

We can now distinguish the following two cases:-

$\tau_r \ll \tau_c$ Since the process of excitation has favoured the states of higher M_J in the ^3P levels, spontaneous decay favours the states of higher M_J in the ^3S level. In the absence of any relaxation process for the ^3S states, many repetitions of the pumping cycle would result in complete polarisation, with all the atoms in the $|1, 1\rangle$ $^3S_1$ state. (The Dirac notation is used to refer to the states $|J, M_J\rangle$ of the specified level).

$\tau_r \gg \tau_c$ Populations are equalised in the excited states, so that the decay is isotropic. Any non-statistical distribution of the populations resulting in the ^3S states is therefore entirely due to unequal absorption of the pumping light by these states. Since the transitions involved comprise all the possible σ^+ transitions within a multiplet this situation will only occur for a non-uniform spectral density in the

exciting light. That is, K ≠ 1.

(d) Alignment

The effect of using unpolarised radiation to pump the sample is to excite $\Delta m = \pm 1$ transitions equally. This results in an alignment, in which case populations of the $|1, 1\rangle$ and $|1, -1\rangle$ states are increased equally at the expense of the $|1, 0\rangle$ state. In other respects the process is similar to that of polarisation, except that under no circumstances can complete alignment result, since atoms in the $|1, 1\rangle$ and $|1, -1\rangle$ states can always absorb σ^- or σ^+ quanta, and decay into the $|1, 0\rangle$ state.

(ii) Rate Equations

The pumping process can be described in terms of "rate equations" in which the rate of change of population of a given state is expressed in terms of the pumping and relaxation processes. Four cases will be considered; they are polarisation, (using circularly polarised radiation) and alignment, (using unpolarised radiation), each in the limit of no mixing and complete mixing, in the excited states. Use is made of the transition probabilities given in figs. 2a, b, c. The following analysis is an extension of that given by Colegrove and Franken, in ref. 2.

Let R_+ R_0 and R_- be the relative absorption rates out of the $^3S_1$ $|1, 1\rangle$, $|1, 0\rangle$ and $|1, -1\rangle$ metastable states. Then let C be a constant proportional to the light intensity, such

that CR_+ etc. give the absolute absorption rates from the $^3S_1$ states. We define the mean lifetime of an atom in any of the metastable states as τ_R. The populations of the three states are n_+, n_o, and n_-, where

$$n_+ + n_o + n_- = n \quad \text{a constant.}$$

The rate equations when there is complete mixing in the excited states are:-

$$\frac{dn_+}{dt} = -CR_+n_+ + \frac{C}{3}(R_+n_+ + R_on_o + R_-n_-) + (\frac{n}{3} - n_+)\frac{1}{\tau_R}$$

$$\frac{dn_o}{dt} = -CR_on_o + \frac{C}{3}(R_+n_+ + R_on_o + R_-n_-) + (\frac{n}{3} - n_o)\frac{1}{\tau_R} \qquad 1(a,b,c)$$

$$\frac{dn_-}{dt} = -CR_-n_- + \frac{C}{3}(R_+n_+ + R_on_o + R_-n_-) + (\frac{n}{3} - n_-)\frac{1}{\tau_R}$$

The first term in each equation gives the rate of change due to the optical excitation. The second terms give the rate of repopulation due to the decay from the excited states. This is the same in each equation because the effect of complete mixing is to equalise the populations in the excited states. The last terms account for relaxation in the metastable states, allowing for their continuous creation so that their total number remains constant. The relaxation time τ_R is assumed to be the same for the three states.

The steady state populations are calculated by setting the time differentials to equal zero. We obtain

$$(CR_+ + \frac{1}{\tau_R})\, n_+ = (CR_o + \frac{1}{\tau_R})\, n_o = (CR_- + \frac{1}{\tau_R})\, n_- \qquad (2)$$

giving

$$n_+ : n_o : n_- = (CR_+ + \frac{1}{\tau_R})^{-1} : (CR_o + \frac{1}{\tau_R})^{-1} : (CR_- + \frac{1}{\tau_R})^{-1}$$

We now distinguish between the two cases:-

(a) Alignment with complete mixing

From Table 1 and taking account of the ratio K between the intensities of the D_0 and D_3 light, we have $R_+ : R_o : R_-$ = (10 + 2K):12:(10 + 2K). These ratios are for absorption of unpolarised light directed along the z-axis.

It follows that,

$$n_+ : n_o : n_- = \left[12 + \frac{1}{C\tau_R}\right] : \left[(10+2K) + \frac{1}{C\tau_R}\right] : \left[12 + \frac{1}{C\tau_R}\right] \qquad (3)$$

(b) Polarisation with complete mixing.

Similarly, for right handed circularly polarised light directed along the z-axis, $R_+ : R_o : R_-$ = 6:6:4+2K so that,

$$n_+ : n_o : n_- = \left[(4+2K) + \frac{1}{C\tau_R}\right] : \left[(4+2K) + \frac{1}{C\tau_R}\right] : \left[6 + \frac{1}{C\tau_R}\right] \qquad (4)$$

This polarisation is the reverse of that to be expected for σ^+ light, owing to the mixing in the excited states.

The rate equations for no mixing are more complicated because account must be taken of the different rates of re-population of the metastable states by decay from the excited states. We first calculate the relative populations of all the ^3P states in terms of the instantaneous population of the metastable states, n_+, n_o, and n_-, then the proportions of these populations which decay to each metastable state, using the transition probabilities in fig. 2c. This yields the following rate equations:-

(c) Alignment with no mixing.

$$\frac{dn_+}{dt} = -(10+2K)Cn_+ + \frac{C}{6}\left[(10+4K)n_- + 18n_o + (46+4K)n_+\right] + (\tfrac{n}{3} - n_+)\frac{1}{\tau_R}$$

$$\frac{dn_o}{dt} = -12\,Cn_o + \frac{C}{6}\left[(4+4K)n_- + 36n_o + (4+4K)n_+\right] + (\tfrac{n}{3} - n_o)\frac{1}{\tau_R}$$

$$\frac{dn_-}{dt} = -(10+2K)Cn_- + \frac{C}{6}\left[(46+4K)n_- + 18n_o + (10+4K)n_+\right] + (\tfrac{n}{3} - n_-)\frac{1}{\tau_R}$$

5(a,b,c)

Their steady state solution is,

$$n_-:n_o:n_+ = (9 + \frac{1}{C\tau_R}):(2:2K:\frac{1}{C\tau_R}):(9+\frac{1}{C\tau_R}) \qquad (6)$$

(d) Polarisation with no mixing.

$$\frac{dn_+}{dt} = -6Cn_+ + \frac{C}{6}\left[(10+4K)n_- + 18n_o + 36n_+\right] - (\tfrac{n}{3} - n_+)\frac{1}{\tau_R}$$

$$\frac{dn_o}{dt} = -6Cn_o + \frac{C}{6}\left[(4+4K)\,n_- + 18n_o\right] - (\tfrac{n}{3} - n_o)\frac{1}{\tau_R}$$

$$\frac{dn_-}{dt} = -(4+2K)Cn_o + \frac{C}{6}(10+4K)n_- - (\tfrac{n}{3} - n_-)\frac{1}{\tau_R}$$

7(a,b,c)

Their steady state solution is:-

$$n_+:n_o:n_- = \left[(21+12K)C\tau_R + (10+2K) + \frac{1}{C\tau_R}\right]:\left[3+2K+\frac{1}{C\tau_R}\right]:\left[3+\frac{1}{C\tau_R}\right] \qquad (8)$$

(iii) Polarisation and Alignment Parameters

We now define polarisation and alignment parameters, 'P' and 'A'.

$$P = \frac{n_+ - n_-}{n_+ + n_o + n_-} = \frac{n_+ - n_-}{n} \qquad (9)$$

$$A = \frac{2(n_\pm - n_o)}{n_+ + n_o + n_-} = \frac{2(n_\pm - n_o)}{n} \qquad (10)$$

We can now calculate the alignment and polarisation for the four cases listed above, together with their maximum theoretical values, obtained by setting $\tau_R \to \infty$. These results are listed in Table I.

(iv) Pumping time

(a) Alignment, (complete mixing)

To determine the rate at which equilibrium is achieved, the rate equations must be solved explicitly for n_+, n_o and n_-, in terms of 't'. For alignment we have $R_+ = R_-$ so that the equations are symmetrical in n_+ and n_-. Thus at all times, $n_+ = n_-$, and equations (1a,b,c) reduce to two:-

$$\frac{dn_\pm}{dt} = (-\tfrac{1}{3} R_\pm C + \frac{1}{\tau_R}) n_\pm + \tfrac{1}{3} R_o C n_o + \frac{n}{3\tau_R} \qquad 11(a,b)$$

$$\frac{dn_o}{dt} = \tfrac{2}{3} R_\pm C n_\pm - (\tfrac{2}{3} R_o C + \frac{1}{\tau_R}) + \frac{n}{3\tau_R}$$

These can be solved by standard methods, and give the results:-

$$n_\pm = X \exp.\left[- \tfrac{1}{3} C(2R_o + R_\pm) - \frac{1}{\tau_R} \right] t + Y \qquad 12(a,b)$$

and $n_o = n - 2n_\pm$

Thus the time dependence of the alignment is contained in the expression:- $\exp\left[- \tfrac{1}{3} C(2R_o + R_\pm) - \frac{1}{\tau_R} \right] t$

For this reason we define a pumping time, τ_p by

$$\frac{1}{\tau_P} = \frac{C}{3}(2R_o + R_+) = \qquad (13)$$

so that

$$A(t) = A(\infty)\left[1 - e^{-(\frac{1}{\tau_P} + \frac{1}{\tau_R})t} \right] = A(\infty)\left[1 - e^{-\frac{t}{\tau}}\right] \qquad (14)$$

τ is an average of the life times of the metastable states, under the action of relaxation and pumping processes.

(b) Polarisation, (complete mixing)

By setting $R_+ = R_o$ we can deduce that $n_+ = n_o$ always, so that again the equations (1a,b,c) reduce to two. This leads to:-

$$\frac{1}{\tau_P} = \frac{C}{3}(2R_- + R_o) \qquad (15)$$

(c) Alignment (no mixing)

Equations 5a,b,c are symmetrical in n_+, and n_- and on solving for n_+, and n_- we obtain a pumping time given by:-

$$\frac{1}{\tau_P} = \frac{C}{3}(2O+K) \qquad (16)$$

(d) Polarisation (no mixing)

The equations (7,a,b,c) do not reduce to two, but can easily be solved since the equation for n_- is independent of n_o and n_+. Thus:-

$$n_- = \frac{n}{3}\left(1 - \frac{\tau}{3\tau_R}\right)e^{-t/\tau} + \frac{n\tau}{3\tau_R}, \text{ where } \frac{1}{\tau} = \frac{C(7+4K)}{3} + \frac{1}{\tau_R} \qquad (17)$$

It is apparent that the solutions for n_o, and n_+ will also contain their time dependence in exponential terms $e^{-t/\tau}$ and so, therefore, will the polarisation 'P'. Thus the pumping time in this case is given by,

$$\frac{1}{\tau_P} = \frac{C}{3}(7+4K) \qquad (18)$$

(v) <u>The effect of Relaxation on 'P' and 'A'</u>

Consider the case of polarisation, with complete mixing.

From table II we find:-

$$P = C(R_- - R_0^+)/C(R_0^+ + 2R_-) + 3/\tau_R \qquad (19)$$

The maximum polarisation achieved occurs for $\tau_R \to \infty$

so that $$P_{max} = \frac{R_- - R_0^+}{R_0^+ + 2R_-} \qquad (20)$$

But $$\frac{1}{\tau_P} = \frac{C}{3}(2R_- + R_0^+) \qquad (15)$$

and eliminating R_-, and R_0^+ between eqs. 19, 20, 15 we have finally,

$$P = P_{max}\ \tau_R/(\tau_P + \tau_R)$$

Similar expressions hold for both cases of alignment. In the case of polarisation, with no mixing the expression is only approximate. This is because of the inequality of n_o and and n_-. (See below)

(vi) Signal Strengths

The polarisation or alignment signal is detected by observing the change in transparency of the sample, when the populations n_+, n_o and n_- are equalised by a resonant r.f. field, H_1. We take as a measure of the signal strength, S_{max}. the ratio $\Delta I/I$ where ΔI is the change in intensity of the transmitted light on resonance, and I is the total absorbed by the sample when it is unpolarised. The latter can be measured as the change in intensity of the transmitted light when the weak discharge is switched off.

Thus

$$S_{max.} = \frac{\Delta I}{I} = \frac{n_+R_+ + n_oR_o + n_-R_- - \frac{1}{3}(n_+ + n_o + n_-)(R_+ + R_o + R_-)}{\frac{1}{3}(n_+ + n_o + n_-)(R_+ + R_o + R_-)} \qquad (21)$$

For alignment $R_+ = R_-$ and $n_+ = n_-$, so that

$$S_{max.} = \frac{2(n_+ - n_o)(R_+ - R_o)}{(2n_\pm + n_o)(2R_\pm + R_o)} \qquad (22)$$

which is clearly proportional to the alignment 'A'.

Similarly it can be shown that in the case of complete mixing the signal is proportional to the polarisation. For polarisation with no mixing the proportionality is only approximate. The exact expression is,

$$S_{max.} = \frac{(n_+ + n_o - 2n_-)(R_+ - R_-)}{(n_+ + n_o + n_-)(2R_+ + R_o)} \qquad (23)$$

which is clearly proportional to the polarisation if $n_- = n_o$. From the relative populations given in table I it can be seen that this is a good approximation if K is small or the polarisation large.

Expressions for the signal strengths in terms of the polarisation or alignment are to be found in table I. A negative sign implies that there is a decrease in the transmitted light, at resonance. It is to be noted that in all cases the existence of a signal depends on the condition $K \neq 1$. In the two cases of complete mixing, the existence of the polarisation or alignment itself depends on this condition.

(vii) Line shapes

The resonance signal is obtained by subjecting the polarised atoms to an oscillating r.f. field, $2H_1$, perpendicular to the main field H_o. The change in absorption of the cell is then plotted as a function of the frequency $\frac{\omega}{2\pi}$ of the r.f. field.

It has been shown, (ref. 3) that the effect of the anti-resonant component of the oscillating field is, to a close approximation, merely to shift the frequency of resonance, by a factor $(1 - \frac{H_1^2}{16H_o^2})^{-1}$.

The effect of the resonant component is to mix the wavefunctions of the three metastable states, so that an atom originally in one of the states has certain probabilities of being in either of the other two. These probabilities are given by the Majorana formula, (ref. 4).

$$P(J,m,m',t) = (\cos \tfrac{1}{2}\alpha)^{4J}(J+m)!(J+m')!(J-m)!(J-m')!$$
$$\times \left[\sum_{n=0}^{2J} \frac{(-1)^n (\tan \tfrac{1}{2}\alpha)^{2n-m+m'}}{n!(n-m+m')!(J+m-n)!(J-m'-n)!} \right] \qquad (24)$$

$P(J,m,m',t)$ is the probability that an atom with total angular momentum J, in the state $|J,m\rangle$ at $t = 0$, will be in a state $|J,m'\rangle$ at time 't'. $\sin^2 \frac{\alpha}{2}$ is given by (ref. 5)

$$\sin^2 \frac{\alpha}{2} = \frac{(\gamma H_1)^2}{(\gamma H_1)^2 + (\omega - \omega_o)} \sin^2 \tfrac{1}{2}\left[(\gamma H_1)^2 + (\omega - \omega_o)^2\right]^{\frac{1}{2}} t \qquad (25)$$

For $J = 1$, we require the probabilities $P(1,m,m',t)$, i.e.

P(1,1,0,t), P(1,0,1,t), P(1,0,-1,t), P(1,-1,0,t); and P(1,1,-1,t), P(1,-1,1,t). The first four of these, for which $m - m' = \pm 1$, are identical, and we set them equal P(1), where

$$P(1) = 2 \cos^2 \frac{\alpha}{2} \sin^2 \frac{\alpha}{2} \qquad (26)$$

The last two, for which $m - m' = \pm 2$, are also identical, and are given by,

$$P(2) = \sin^4 \frac{\alpha}{2} \qquad (27)$$

We are interested in the average time an atom originally in a state $|1 \quad m\rangle$ spends in a state $|1\ m'\rangle$. We can easily calculate this in the limit $\gamma H_1 \gg \frac{1}{\tau_R} + \frac{1}{\tau_P}$. That is to say, the strength of the rotating field must be such that atoms make a great many transitions between states before they are lost by optical excitation or relaxation mechanisms.

Writing

$$\sin^2 \frac{\alpha}{2} = x \sin^2 \tfrac{1}{2} (b^2 + \delta^2)^{\frac{1}{2}} t \qquad (28)$$

where $b = \gamma H_1$; $\delta = (\omega - \omega_o)$; $x = \dfrac{b^2}{b^2 + \delta^2}$

and taking a time average, we obtain,

$$P(1)_{av.} = x - \tfrac{3}{4} x^2 \qquad P(2)_{av.} = \tfrac{3}{8} x^2 \qquad (29) \quad (30)$$

$P(1)_{av}$ is the proportion of time that an atom starting in the state $|1\ m\rangle$ spends in a neighbouring state. ($\Delta m = 1$).

$P(2)_{av.}$ is the proportion of time that an atom starting in the state $|1, \pm 1\rangle$ spends in the state $|1, \mp 1\rangle$ ($\Delta m = 2$)

The transition of an atom from a state $|1, m\rangle$ to a state

$|1, m'\rangle$ may alter its probability of absorbing a photon. Knowing the initial distribution of the atoms among the states $|1, m\rangle$ we can calculate the change in absorption of the sample as the parameter 'x' is varied (i.e. as either H_1 or ω is varied.) This gives us the line shape. A detailed calculation on these lines is given in ref. 2 for the case of alignment, with complete mixing. There it was found that a double humped signal, similar to that of Brossel and Bitter resulted (ref. 6). It is possible to foresee the general shape of any alignment signal, without detailed calculation, by the following argument. In general the expression for the signal will be a function of $P(1)_{av.}$ and $P(2)_{av.}$. However in the case of alignment, $n_+ = n_-$ so that exchange of atoms between these two states will not affect the light absorption at all. The signal S is therefore a function of $P(1)_{av.}$ only. We require the condition for $\frac{dS}{d\delta} = 0$

$$\text{i.e.} \quad \frac{dS}{d\delta} = \left(\frac{\partial S}{\partial P(1)_{av.}}\right)\left(\frac{\partial P(1)_{av.}}{\partial x}\right)\left(\frac{\partial x}{\partial \delta}\right) = 0 \qquad (31)$$

since $P(1)_{av.}$ is a function of x, which is a function of δ. $\frac{\partial x}{\partial \delta} = 0$ gives the condition that $\frac{-2\,\delta/b}{1 + (\delta/b)^2} = 0$ or $\delta = 0$

Therefore $\omega = \omega_o$ is one turning point of the signal function. (32)

The others are given by,

$$\frac{\partial P(1)_{av.}}{\partial x} = 1 - 3x/2 = 0$$

or,

$$(\omega - \omega_o) = \pm \frac{\gamma H_1}{\sqrt{2}} \qquad (33)$$

Thus the signal is double humped, the humps being separated by a frequency $\sqrt{2}\,\gamma H_1$. These conditions are, of course, subject to $\frac{\partial S}{\partial P(1)_{av.}} \neq \infty$ at these points. Detailed calculation supports this assumption.

We now consider the general case of polarisation. The population of each metastable state is different. Even in the case of complete mixing where the populations of two states are the same, these are adjacent states and we cannot exclude either $P(1)_{av.}$ or $P(2)_{av.}$ from the calculation.

A simplification is obtained, however, by noting that any distribution of populations n_+, n_o and n_- can be expressed as the sum of an alignment, and a polarisation,

since $(n_+ + n_o + n_-) = (n_- + n_o + n_-) + (\overline{n_+ - n_-} + 0 + 0)$ (34)

We now consider the $(n_+ - n_-)$ atoms which constitute the fraction of the sample which is 100% polarised. Let this number of atoms, in the $|1, +1\rangle$ state, be n'. Under the action of the rotating field H_1, a number $n'P(1)_{av.}$ will be in the state $|1, 0\rangle$ and a number $n'P(2)_{av.}$ in the $|1, -1\rangle$ state at any given time. The total rate of absorption can therefore be expressed as,

$$CR_+^* = C\left[(1 - P(1)_{av.} - P(2)_{av.})\,R_+ + P(1)_{av.}R_o + P(2)_{av.}R_-\right]$$

The signal as a function of R_+^* is, (35)

$$S = (C(n'R_+^* - n'R_+) \qquad (36)$$

i.e. it is the difference between the absorptions with and without the rotating field. Substituting 35 in 36,

$$S = n'C \left[P(1)_{av.}(R_o - R_+) + P(2)_{av.}(R_- - R_+) \right] \qquad (37)$$

But in our case $R_+ = R_o$ (Eq. 4) and so

$$S = n'C\, P(2)_{av.} \qquad (38)$$

This is a function of $P(2)_{av}$ only, and by a process similar to the preceding one, we deduce that there is only one turning point, which occurs when $x = 0$ or $\omega = \omega_o$

The full expression for the signal is:-

$$S = n'C \left[\frac{(\gamma H_1)^2}{(\gamma H_1)^2 + (\omega - \omega_o)^2} \right]^2 \qquad (39)$$

which is the square of a Lorentzian.

A more sophisticated derivation of the line shape, based on the results and methods of Dodd and Series, (Ref. 7), which takes account of the finite lifetime τ of the metastable atoms, gives

$$S \propto \frac{(\gamma H_1)^4}{\left[(\omega-\omega_o)^2 + (\gamma H_1)^2 + (1/\tau)^2\right]\left[(\omega-\omega_o)^2 + (\gamma H_1)^2 + (1/2\tau)^2\right]}$$

which reduces to the above expression when $\tau \to \infty$ (See p. 7.8)

Depending on the actual distribution of populations, an observed signal will be a mixture of the single and the double humped signals. Consequently, as the distribution varies from an alignment towards a polarisation, the signal varies from a double humped signal, with separation $\sqrt{2}\,\gamma H_1$, through signals with more closely spaced humps, to a pure squared Lorentzian.

It has been assumed in this analysis that all line broadening effects, such as those due to field inhomogeneities

or the finite lifetimes of the metastable atoms, are negligible compared to the broadening effect of the rotating field.

(viii) The effect of the Sample Thickness

The discussion has so far been concerned with thin samples, that is, samples in which the absorption of the D_0 and D_3 lines is sufficiently small so that their ratio K does not very appreciably throughout the sample. The effect of the variation of K with sample thickness has been discussed, for the case of alignment, by Colegrove and Franken, in ref. 2. There a simple argument is shown to lead to the following relation between D_0 and D_3, the intensities of these lines at the front of the sample, and I_0 and I_3, their intensities at a distance 'x' into the sample. I_0^* and I_3^* are the intensities when the disorienting r.f. field is applied to the sample.

$$I_0 I_3 = I_0^* I_3^* = D_0 D_3 e^{-\alpha x} \qquad (40)$$

where α is a constant.

The product of the intensities decays exponentially with x. A plot of I_0, I_3, I_0^* and I_3^* is shown in fig. 3. For alignment, atoms are 'pumped' into the less absorbing states, so that $I_3 > I_3^*$ and $I_0^* > I_0$. For polarisation with no mixing in the excited states, atoms are 'pumped' into the more absorbing states, and $I_3^* > I_3$, and $I_0 > I_0^*$. These are the two

situations (a) and (b) in fig. 3. The signal obtained for any sample thickness x is given by $(I_o + I_3) - (I_o^* + I_3^*)$, and this is plotted in figs 3c, d. It can be seen that the signal inverts once for polarisation and twice for alignment, as the sample thickness is increased.

(ix) Diffusion Equation

In considering possible mechanisms for the destruction of metastable atoms, it is necessary to consider loss by collisions with the walls. We therefore include here some calculations based on the diffusion equation, for use in later chapters.

The diffusion equation may be written:-

$$\frac{dn}{dt} = D\nabla^2 n - kn \qquad (41)$$

'n' is the density of metastable atoms. 'D' is the coefficient of diffusion appropriate to for metastable atoms diffusing in ground state He atoms, at a particular temperature and pressure. 'k' is a coefficient giving the rate of loss (per unit density) of metastable atoms within the sample. We require the solution of this equation for the boundary conditions n = 0 at the walls of the cell. For a spherical cell, with radius 'R', the solution is:-

$$n(r,\theta,\phi,t) = \sum_{n=0}^{\infty} \sum_{\alpha} \sum_{m=0}^{n} \left\{ P_n^m(\cos\theta)\left[A_{nm\alpha}\cos m\phi + B_{nm\alpha}\sin m\phi \right] j_n(\alpha r) \exp\left[-(D\alpha^2 + k)\, t \right] \right\} \qquad (42)$$

The P_n^m are associated Legendre functions. $j_n(r)$ is a Bessel function of order 'n', for spherical co-ordinates. It is

related to an ordinary Bessel function by the relation:-

$$j_n(\alpha r) = \sqrt{\frac{\pi}{2\alpha r}}\ J_{n+\frac{1}{2}}(\alpha r) \qquad (43)$$

The allowed values of α are determined by the boundary condition,

$$n(R,\theta,\phi,t) = 0, \quad \text{that is,} \quad \sqrt{\frac{\pi}{2\alpha r}}\ J_{n+\frac{1}{2}}(\alpha R) = 0 \qquad (44)$$

The coefficients $A_{nm\alpha}$ and $B_{nm\alpha}$ depend on the initial distribution of the diffusing atoms. If this is not known the simplest assumption is that all the atoms diffuse in the first mode, in which case the solution is the first term of equation (42):-

$$n(r,t) = n(0,0)\frac{R}{\pi r}\sin\frac{\pi r}{R}\exp\left[-\left(\frac{D\pi^2}{R^2} + k\right)t\right] \qquad (45)$$

since $J_{\frac{1}{2}}(\alpha r) = \sqrt{\frac{2}{\pi\alpha r}}\sin\alpha r$, giving $\alpha R = \pi$ (46)

This gives the distribution in time and space of the metastable atoms, after the discharge has been switched off, and assumes the initial distribution to be of the form:-

$$n(r,0) = n(0,0)\frac{R}{\pi r}\sin\frac{\pi r}{R} \qquad (47)$$

In considering the situation whilst the discharge is still on, it is necessary to make further assumptions, concerning the creation of the metastable atoms. The simplest solution is obtained if it is assumed that the creation can be accounted for by the addition of a term 'cn' to the r.h.s. of equation 41, which becomes:-

$$\frac{dn}{dt} = D\nabla^2 n + (c - k)n \qquad (48)$$

and has a solution

$$n(r,t) = n(0,0)\frac{R}{\pi r}\sin\frac{\pi r}{R}\exp\left[-\left(\frac{D\pi^2}{R^2} + k - c\right)t\right] \quad (49)$$

For equilibrium,

$$c = \frac{D\pi^2}{R^2} + k \quad (50)$$

which is an expression for the rate of loss of metastable atoms, (per unit density).

Table I

		Alignment		Polarisation	
		Mixing	No-Mixing	Mixing	No-Mixing
Relative Equilibrium Populations	n_+	$12 + 1/C\tau_R$	$9 + 1/C\tau_R$	$4+2K + 1/C\tau_R$	$(21+12K)C\tau_R + 10+2K+1/C\tau_R$
	n_o	$10+2K+1/C\tau_R$	$2+2K+1/C\tau_R$	$4+2K+1/C\tau_R$	$3+2K+1/C\tau_R$
	n_-	$12+1/C\tau_R$	$9 + 1/C\tau_R$	$6 + 1/C\tau_R$	$3 + 1/C\tau_R$
Absorption Rates	R_+	$10 + 2K$	$10 + 2K$	6	6
	R_o	12	12	6	6
	R_-	$10 + 2K$	$10 + 2K$	$4 + 2K$	$4 + 2K$
Equilibrium Alignment 'A' or Polarisation 'P'		$\frac{4(1 - K)}{(34+2K)+3/C\tau_R}$	$\frac{4(7 - 2K)}{20+2K+3/C\tau_R}$	$\frac{2(1 - K)}{2(7+2K)+3/C\tau_R}$	$\frac{(21+12K)C\tau_R+(7+2K)}{(21+12K)C\tau_R+(16+4K)+3/C\tau_R}$
Pumping time, τ_P		$\frac{3}{C(34+2K)}$	$\frac{3}{C(20+K)}$	$\frac{3}{C(7+2K)}$	$\frac{3}{C(7+4K)}$
Alignment or Polarisation in terms of A_{max} or P_{max} i.e. A, P ($\tau_R \to \infty$)		$\frac{A_{max}\tau_R}{R + P}$	$\frac{A_{max}\tau_R}{R + P}$	$\frac{P_{max}\tau_R}{R + P}$	Approx. $\frac{\tau_R}{\tau_R + \tau_P}$
A_{max} and P_{max} evaluated for $K = \frac{1}{2}$		.057	.572	-.063	1
Signal strength, in terms of A or P. -ve A sign means less transmitted light, on		$-\frac{1}{2}\frac{(1-K)}{(8+K)}A$	$-\frac{(1-K)}{4(8+K)}A$	$-\frac{2(1-K)}{(8+K)}\lvert P\rvert$	$\frac{(1-K)}{(8+K)}P$

1.21

CHAPTER TWO

EXPERIMENTAL

The Apparatus

(i) Two methods were used to display the optical pumping signals. Both methods involved modulation of the magnetic field H_o. For the initial search a phase sensitive detector was used. This had the advantage that it could detect signals which were of smaller amplitude than the noise. When the signal was sufficiently improved it could be displayed on the oscilloscope, with no band-width limitation other than that of the oscilloscope amplifiers. Block diagrams of the apparatus for these systems are given in fig. (4).

The He^4 was contained in a 100 ml. spherical pyrex cell, supported at the centre of a system of Helmholtz coils. These consisted of two co-axial pairs used to produce the main magnetic field and modulation field, surrounded by a system of three orthogonal pairs of square coils, which were used to cancel the earth's field. Some smaller coils, also with Helmholtz spacing, but with their axis perpendicular to that of the main field coils, were used to apply the radio-frequency field H_1. In these experiments on oscillating (as opposed to a rotating field), was used for convenience sake.

The He^4 cell was placed between two converging lenses, the lamp being at the focal point of one lens, and the detector at the focal point of the other. The optic axis was parallel to the axis of the main coils. Thus the light passing through

the cell would have been parallel but for the effect of the finite size of the lamp. In practice light rays diverging by as much as 10° from the axis were accepted.

The output of the detector was taken to a pre-amplifier when necessary, thence to the oscilloscope or the phase sensitive detector.

For polarisation experiments a polaroid filter and quarter-wave plate could be inserted between the lamp and the first lens. For alignment experiments no filters were necessary, although a filter to remove the visible part of the emission from the lamp was sometimes employed.

Population of the $^3S_1$ meta-stable level was accomplished by exciting a weak discharge in the pumping cell. For this purpose a further pair of coils were mounted, in contact with the cell and with their axis parallel to that of the main coils. These were excited by power from an R.F. oscillator.

(ii) Experimental Procedure

(a) Detection of Polarisation and Alignment Signals.

It was decided to work at rather low magnetic fields - up to about one gauss. This gave economies in the construction of coils and their power supplies, but necessitated accurate cancellation of the earth's field. Since this is about .4 gauss it would have seriously affected the net field seen by the sample. This cancellation was accomplished using a compass needle and a dip circle to adjust the currents in the

three sets of orthogonal coils, so that no net field remained at the centre of the system.

A weak discharge was then excited in the cell, and a small modulating magnetic field applied, its amplitude adjusted to be about equal to half the line width of the expected signal. A reference signal derived from the modulation field was applied, via a phase-shifter, to the phase sensitive detector, whose output could be observed on a panel meter, and chart recorder. An oscillating radio frequency field of a few milli-gauss in amplitude was now applied, and the main field swept slowly through the region of resonance. This was repeated with different adjustments of the variables, namely the discharge intensity, gas pressure in lamp and cell, r.f. field strength, modulation depth, and phase of reference signal. When a signal was detected and improved sufficiently it could be applied to the "Y" amplifier of the oscilloscope, the reference signal being applied to the "X" amplifier. In this way a plot of transmitted light intensity versus magnetic field could be displayed. In order to obtain an undistorted signal in this way, it was necessary to use a frequency and amplitude of field modulation such that the transit time through the signal was large compared with the characteristic pumping time of the sample. When the phase sensitive detector was used, the line shape obtained could be improved at the expense of signal amplitude by reducing the size of the

modulating field until it was a small fraction of the line width. The earth's field compensation could now be accurately adjusted by observing the "zero field" signal. This signal occurred on modulating the main field through zero from positive to negative values. Since its occurrence is the result of stray fields at some arbitrary angle to the direction of the light beam, these can be compensated by adjusting the currents in the compensating coils until the zero field signal is a minimum.

Measurement of Pumping Transient

The apparatus was set up so as to produce polarisation. With no field modulation, an oscillating r.f. field at the resonant frequency was applied. The amplitude of this was large enough to completely depolarise the sample, despite the fact that pumping radiation was still incident on the cell. The r.f. was then suddenly removed, in a time short compared with the transient to be measured. The transmission of the sample was then measured as a function of time on the oscilloscope.

In practice the r.f. was pulsed off for a portion of each sweep of the time base by a delayed gate obtained from the oscilloscope. Thus a repetitive trace of the pumping transient could be obtained on the oscilloscope, which was then photographed.

(iii) Details of the Apparatus

(a) The Pumping Cell

These were originally cylindrical in shape, being constructed from 2" glass tubing, with the light passing through the cell perpendicular to the axis of the tube. It was found that in drawing the tubing strains had been introduced, which modified the polarisation of the light entering the cell. 100 ml. spherical pyrex flasks were found to be much better in this respect and were adopted for all subsequent cells. These were pumped down to a pressure of about 10^{-5} mm. Hg., and then outgassed by heating them almost to softening point with a flame. They were then filled with He. to the required pressure as measured by a McLeod gauge, and sealed off. A Barium getter assembly was usually included in the flask. This consisted of Barium wire surrounded by a protective sheath of non-magnetic alloy. A similar wire horse-shoe connected the two ends of this so as to complete a loop. Thus an induction heater could induce a high current in this circuit, vapourising the Barium, which became deposited on the glass envelope. The getter was not attached to the glass envelope in any way, but was always flashed in the tail of the flask, where it remained during use of the cell. To isolate the getter and Barium film further from the cell a separate getter compartment was occasionally added to the cell, communicating via a narrow re-entrant orifice with the main chamber (Figs. 5), 7)

One or two cells were produced with their walls coated with General Electric "Dri-Film"; di-chloro-di-methyl-silane. This was accomplished by attaching two small containers to the system, adjacent to the cell. These containers contained water, and Dri-film, respectively and after evacuation of each in turn, were isolated from the rest of the system by stop-cocks. After out-gassing the cell in the usual way, the pumping line was shut off, and water vapour from the water container allowed to enter the cell. A visible film was not necessary. This container was then closed, and the Dri-Film container opened to the system. The vapour from this rapidly filled the cell, and could be observed reacting with the water on the surface. Finally the cell was re-evacuated, out-gassed by flame, and filled, as usual. The film thus obtained was invisible, but could be tested if required by removal of the cell before seal off and insertion of a drop of water. This was found not to wet the surface of the glass.

(b) Lamps

These were constructed from 1" diameter quartz tubing. Their general outline is shown in figs. 6a and b, +7. The re-entrant lamp was a later improvement designed to minimise self-reversal. (See account of lamp investigation in Chapter III). Both types were designed for view end-on. The second compartment was to increase the overall volume of the lamp and to house the getter away from the intense discharge. It was

not necessary to flash the getter unless the lamp appeared excessively contaminated on striking a discharge. In fact it was a disadvantage to do so since the pressure in lamps in which the getter had been flashed slowly decreased until it was no longer possible to strike the discharge. The life of non-gettered lamps was much longer.

The discharge was excited by placing the front part of the lamp in the coil of a tuned circuit driven at 18 Mcs./s. by an R.C.A. transmitter having a power output of about 300 watts. This was modified by the insertion of two extra smoothing stages in its H.T. supply. Large quantities of heat were evolved in the lamp, which necessitated making it of quartz to prevent softening and implosion.

To reduce the heating a little, a stream of air was directed at the lamp, but this caused a deterioration in the noise characteristics of the lamp, owing to the mechanical vibrations set up by the air. It may also have caused more self-reversal of the spectral lines emitted due to cooling of the outer layers of gas in the lamp. The quartz envelopes withstood the temperature well, but the copper coils oxidised rapidly if no cooling was employed.

In order to compress a number of coils (13), into the length of the lamp bulb, (1½"), an ideal material to use proved to be a helix of flat copper strip. The strip was ½" wide and .0015" thick, the plane of the strip being perpendicular to the

axis of the helix. This material is manufactured by Messrs. "Spiro-Gills Ltd." of Pulborough, Sussex, for use in heat exchangers.

A length of this material is too limp to be self supporting and so it was strengthened by drilling three holes through the turns, parallel to the axis of the helix, and inserting glass rods, with ceramic beads separating the turns (See fig. 7).

The circuit as originally designed used mica condensers, but these proved to be a source of noise due to instability under high power operation, and in the final design an air spaced condenser was used.

The discharge excited in the lamp by this arrangement was of the type known as a "Ring discharge".

In addition to this main lamp some experiments were performed with a smaller lamp. This was driven by a multi-vibrator oscillator, the circuit of which was the same as that given in fig. (8) but without the control valve in the anode circuit. The lamp itself was in the form of an electrode-less Geissler tube, as can be seen from fig. (9) which illustrates the whole assembly.

Detectors

A number of detectors was used in the course of the work. A Mullard 618V lead sulphide cell was used in the initial work, and proved fairly satisfactory. It is a photo-

conductive device, and at a wavelength of 10,830 Å, its response is about 30% of its maximum which is at about 2.5μ. Its chief limitation is in its frequency response - it has a time constant of about 75 secs. which excludes its use in high speed applications such as measurements of He^4 pumping transients and the modulation experiments described in part three of this thesis.

Another lead sulphide detector - the Kodak Ektron - was also used. This has similar characteristics to the Mullard 61SV, but is available in a number of different sizes of sensitive area. Also the impedance of the device can be chosen, within limits, by specifying the configuration of the sensitive area. In principle, one can choose the detector most suitable for the size and intensity of the image, and with a suitable impedance for the amplifiers it is to feed. In practice no better signals were obtained with this than with the Mullard 61SV, and in addition to the disadvantages of the 61SV, the Ektron is more fragile and more difficult to mount.

A better photo-conductive detector was found to be the Texas Instrument Photo-Duo-Diode, Type 1S701. This is a small n-p-n symmetrical junction diode. The sensitive area is very small, but effectively increased to a circle of diameter 2 mm. by a lens incorporated in the body of the diode. The device is illuminated end on. A number of them could be packed

together, giving a larger sensitive area, but a more important advantage than this was that by connecting several in parallel, the impedance of the assembly could be reduced sufficiently to match the input impedance of the pre-amplifier or oscilloscope. This was necessary since, even when brightly illuminated by the main lamp, the impedance of a single device was about 1.5 MΩ - rising to as much as 100 MΩ, when illuminated by the small lamp.

In practice there was little advantage in increasing the size of the assembly until it collected all the light forming the image of the lamp, since the signal to noise ratio of the system as a whole was always dominated by noise from the lamp. The sensitivity of these detectors was greater than that of the lead sulphide detectors, and, in addition, their frequency response was much better. It was constant up to about 5 Kc/s., but was only reduced by 3db. at 20 Kc/s. All the above detectors were powered from an H.T. battery in a shielding box. A 1 MΩ high stability resistor was connected in series with the detector and the signal voltage developed across this by the photo-current was applied, through a condenser, to the input of the pre-amplifier.

When very fast response times were required, there was no alternative but to use a photo-cell. There are no photo-cathodes with good sensitivity in the region of 10,830Å. The best available is the "S - 1 response" cathode, which has a

peak response at about 8000Å. At 10,830Å the response falls to 10% of its maximum. Signals could, however, be observed with such a detector, (an RCA 6570 photo-cell was used) and it was found helpful to include an amplifying stage in the photo-cell mounting box. This also had the effect of reducing the output impedance to a point where high frequency signals were not unduly attenuated by coaxial cable connecting the detector to the amplifier. The circuit used is shown in fig. (10).

In order to reduce hum, the valve heaters were driven by accumulators, and a battery supplied the H.T. for photo-cell and valve.

A disadvantage of all these detectors was the use of ferromagnetic components in their construction. The Mullard 61SV has some unidentifiable ferromagnetic inclusions internally. The Kodak Ektron and Texas Instruments Photo-Duo-Diode both use nickel-iron leads. In the former case these could probably be replaced by copper wires, but in the latter case the hickel-iron is used in glass to metal seals. The RCA 6570 photocell uses ferromagnetic materials extensively in its glass-metal seals and elsewhere.

The effect of the inclusions was usually to cause broadening and asymmetry of the optical pumping signal. These could not be removed by adjusting the compensating fields since they were the result of field inhomogeneity, and the

only solution was to remove the detector from the vicinity of the cell.

(d) Polarising Filters

Polaroid type HR infra-red plastic polariser was used. Two samples were tried. Polarisation signals were first obtained with a sample mounted between glass laminations, but a later sample, without glass laminations gave much better signals.

(e) Quarter-Wave Plates

These were manufactured by Messrs. H. S. B. Meakin Ltd. from mica sheets. A rough test of the efficiency of the combination of polariser and quarter-wave plate was conducted. It was necessary to restrict the bandwidth of the light used to the region of 10,830Å. This was achieved using the Texas Instruments detector, which does not respond to wavelengths longer than 11,200Å, and a Polaroid Type XRX 40 filter which does not transmit wavelengths shorter than 8,500Å. There are no lines in the spectrum of He. in this region with appreciable intensity, other than the 10,830Å line. The transmission of the circular polariser was measured for various positions of an analyser using approximately parallel chopped radiation from a small He. lamp. A ratio of 4:3 was found between maximum and minimum, indicating that the radiation was in fact elliptically polarised with this ratio of major to minor axes. The efficiency of the circular polariser under the experimental

conditions was limited by the angle of divergence of the light.

(f) Weak Discharge

Various methods were used to excite the weak discharge in the cell. These included D.C. excitation with aluminium electrodes. This tended to produce a noisy discharge, and moreover the discharge did not uniformly fill the cell, being localised near the anode. Much better characteristics were obtained with an electrodeless discharge, excited by R.F. For this purpose a multivibrator oscillator was built, driving a small pair of four-turn coils mounted in contact with the cell. The discharge intensity was adjusted by varying the current through a series valve in the anode circuit of the oscillator. The circuit is shown in fig. (8).

(g) Main Coils

These were wound upon Duralumin bicycle wheel rims. They were split at one point of their circumference and re-joined with insulating material. The object of this was to reduce eddy currents which may have been induced in a conducting rim. The coils were "potted" in Araldite epoxy resin as they were wound.

(h) Modulation Coils

These were wound upon removable formers, and "potted" in the same way. When the resin set the coils were completely self supporting.

(i) Earth's Field Compensation Coils

Again no formers were used, but the coils were wound over bobbins mounted on a cubical framework of ½" Duralumin rods.

The field at a distance 'b' along the axis from the plane of a square coil of side 'a' is given by:-

$$H = \frac{2\sqrt{2}}{\pi} \frac{n\,i\,a^2}{(a^2 + 4b^2)\,(a^2 + 2b^2)^{1/2}}$$

where

ni = ampere turns of coil.

Hence the field at the centre of a pair of co-axial square coils separated by a distance '2x' is given by:-

$$H = \frac{4\sqrt{2}}{\pi} \frac{n\,i\,a^2}{(a^2 + 4x^2)\,(a^2 + 2x^2)^{1/2}}$$

from which the condition for $\frac{d^2H}{dx^2} = 0$ can be found. It is

$$2x = .5444a$$

and this was the coil spacing used.

A summary of the characteristics of the coils used is given in the following table.

The coils were powered by batteries. The currents through them were controlled by simple transistor devices. A circuit diagram is given in fig. 11b.

	Mean Diam.	No. of Turns/ Coil	Resis- tance	Induc- tance	Sepa- ration	Calibration Constant
Main Coils						
In series	24.25"	500	49	7H		
In parallel			12.5	1.4H	12.125"	13.16G/Amp.
Mod. Coils.	19.75"	80	10.5	.01H	9.875"	
Compen- sation Coils	Vert 33.5"x37.5"	60	10.5	.025H	18"	
	N-S 32.1"x32.5"				17.25"	
	E-W 32.3"x34.5"				18.5"	

(j) R.F. Coils

The oscillating R.F. current was generated by a General Radio "Bridge Oscillator". This fed a small pair of Helmholtz coils, approx. 4" in diameter, mounted with their axis perpendicular to that of the main coils. The number of turns per coil could be selected from a number of values between one and a hundred, so as to obtain a good match between the oscillator and its load at various frequencies.

(k) Main Field Current Supply

This was built in the Electronic Workshop to the circuit shown in Fig. 11. The value of its output current could be set by hand, using the "Zero" control, or, by injecting a suitable varying voltage at one of the inputs, a slow field sweep could be generated. The other input could be simultaneously used to inject a sinusoidally varying voltage, thus superimposing a modulation on the slowly varying field.

If necessary the current could be varied continuously from positive to negative values. The circuit of the sweep voltage generator is shown in fig. (12).

A 12V car battery was used to drive the supply.

(l) Modulation Coil/Supply

Field modulation was either obtained as above, or more usually, by feeding the modulation coils with current from a 6 watt Dawe Audio Oscillator. The frequency used was usually in the range 20 c/s - 100 c/s.

(m) Phase Shifter

This was built according to the circuit of Fig. 13c By switching the condensers in the phase shift network, about 300° phase shift could be obtained for frequencies between 1 c/s - 10 Kc/s.

(n) Phase Sensitive Detector

The circuit of this is shown in fig. (13a,b.) The reference signal is amplified by a transistor power amplifier and the output of this used to drive a mechanical synchronous chopper. This rectifies any incoming signal from the signal amplifier and phase-splitter providing it is locked in phase with the reference signal. Random noise signals result in no net D.C. level, and can be smoothed by condensers across the output of the chopper. These determine the time constant of the detector. The D.C. output signal is amplified and displayed on a panel meter or chart recorder.

(o) R.F. Power Amplifier and Pulser

In order to switch the oscillating radiofrequency field on or off electronically, a small r.f. power amplifier was built according to the circuit of fig. (14). This could be switched off by the application of a negative voltage to the grids of the amplifying valves. If a short pulse of r.f. was required the amplifier was biased off with an h.t. battery, then switched on for the duration of a 100 V positive pulse.

CHAPTER THREE

RESULTS AND DISCUSSION

(i) Conditions for Best Optical Pumping Signals

(a) Purity of sample

Trouble was experienced initially in obtaining optical pumping signals. This was later attributed to impure samples of He^4 in the pumping cell, and was rectified by the addition of getters to the cell. Confirmation of the detrimental effect of impurities was later obtained from a cell which was not gettered, but none the less sufficiently pure to give good signals. Within a few minutes of striking the weak discharge, signals had reduced in amplitude by an order of magnitude - presumably due to the ejection of impurities which had been adsorbed on the walls by the action of the discharge. Evidence of the presence of impurities was given by a marked change in the colour of the discharge.

(b) Cell Pressure

A pure sample having been achieved, weak signals obtained with a phase sensitive detector were rapidly improved until they were visible on an oscilloscope. It was then easy to adjust the parameters for maximum signals. It was found that best signals were obtained with low pressures in the cell, so that there was little mixing in the excited states. This was to be expected in view of the results in Table One, p. 1.21 0.1 and 0.3 mm Hg. cells gave best results for alignment, and

polarization, respectively. Examples are given in Fig. 15. Some results were obtained with a cell filled to 0.05 mm. Hg. but the pressure quickly dropped, owing to adsorption of the He. at the walls, so that it was impossible to strike a discharge.

(c) Discharge Intensity

In a 1 mm. Hg. cell it was possible to vary the discharge intensity from a scarcely visible glow to such an intensity that it was fairly difficult to see through it. At its brightest the sample became optically dense to the 10,830 Å radiation, and very small signals were obtainable. At its weakest the sample was optically thin, and again fairly weak signals were obtained. With the lower pressure cells, it was not possible to increase the optical density to so great an extent, and usually the best signals were obtained with a moderately bright discharge. A more quantitative description of discharge intensities is postponed until Part Two of this thesis, in which an account is given of a determination of the absolute density of metastable atoms in a 1 mm. He^3 cell, for various conditions of discharge.

(d) Choice of Lamp Pressure

In terms of brightness, it was found that lamps filled to about 1 mm. Hg., pressure were the best. However, higher pressure lamps (up to 5 mm. Hg.) were often quieter, so that in terms of the signal to noise ratio, better signals were

sometimes obtained with these. Also, it was found that, with a given cell, lamps at different pressures required different settings of the discharge intensity in the cell, to give maximum signals. Furthermore, the signal amplitudes obtained varied quite widely, and were not necessarily related closely to the intensities of the different lamps. All this could be understood when it was realised that the lamps varied greatly in their spectral distribution, as measured by the ratio 'K' due to their different degrees of self-absorption, or self-reversal, (see p.3.12). Less variation of signal strength with lamp pressure was obtained with a new type of lamp, which had a re-entrant window. (Figure 6b and p.3.13). This seemed effective in reducing self-reversal, and hence the variation in K.

(ii) Thin Samples

Larger signals were invariably obtained with cell pressures, and discharge strengths such that the sample was by no means optically thin. Polarization signals were usually larger when 'inverted'. It was of more interest to observe thin samples, since these were more amenable to calculations.

With low pressure cells it was easy to obtain signals which were not inverted. It was found that the polarity of the signals was as predicted in Table One, p.1.21. Figs. (16a, b) show polarisation and alignment signals obtained from a 1 mm. Hg. cell. Conditions were identical in the two cases,

except that a circular polarizer was inserted between lamp and cell for fig. (16a) while for fig. (16b) a grill reducing the intensity of the pumping light by a factor of about 2 was substituted for the circular polarizer. These photographs are plots of transmitted light intensity (y axis) versus magnetic field (x axis). Light intensity increases in the positive (upwards) direction of the y axis.

(iii) Degree of Polarization

If K is known, it is possible to measure the degree of polarization for a thin sample from the formulae in Table 1, p.1.21. In practice K is not usually known accurately, but, providing it is not close to 1, some idea of the polarization can be obtained.

As an example, we take the polarization produced in a .1 mm. cell, using a 2 mm. re-entrant lamp. The r.f. was increased until the signal amplitude no longer increased, and a further increase of r.f. resulted in signal broadening only. The signal amplitude, "ΔI", in terms of the output voltage of the detector, was found to be 10 mV. This was compared to the total amount, 'I', that the light intensity was reduced by absorption in the unpolarized sample. This was easily measured by switching the weak discharge off, and noting the increased transmission of the sample. In this case it was found to be .8V. The intensity of light emitted by the discharge was so small as to be negligible. From Table 1 we have:-

$$\frac{\Delta I}{I} = \frac{1 - K}{8 + K} P ,$$

therefore

$$P = \frac{8 + K}{1 - K} \cdot \frac{1}{80}$$

Thus the polarization was at least 10% (K = 0).

Setting K = $\frac{1}{2}$, a reasonable value, then P = 21%.

(iv) Line Widths

The narrowest lines obtained were polarization signals from thin samples. Fig. 16a is an example. It was easy to broaden these by increasing the r.f. field strength, but on decreasing it, a minimum width was reached. Further decrease of the r.f. field strength merely reduced the overall amplitude of the signal, but not its width at half height. This residual width, as measured on an oscilloscope, was about 5 mG. It was checked by observing the signal with a phase sensitive detector. The advantage of this was that the field modulation could be reduced to a small fraction of the line width, and the r.f. strength reduced to very small values, so that both these lines broadening effects could be eliminated. In the experiment, the values of the various parameters were:-

Field Modulation (Peak to Peak)	.25 mG
" " Frequency	26 c/s.
Rotating Field Strength (H_1)	.2 mG

The line width measured between points of inflexion was

$4 \pm .4$ mG. (The phase sensitive detector output is the derivative of the signal, and the maxima are equivalent to points of inflexion of the signal.) In Chapter I it was shown that the line shape was given by:-

$$s \propto \frac{(\gamma H_1)^4}{\left[(\omega-\omega_0)^2+(\gamma H_1)^2+(1/\tau)^2\right]\left[(\omega-\omega_0)^2+(\gamma H_1)^2+(\tfrac{1}{2}\tau)^2\right]}$$

It can be shown that the width at half height is given by:-

$$2(\omega'-\omega_0) = .836/\tau \quad \text{in the limit} \quad \gamma H_1 \ll 1/\tau \ ,$$

whereas the width at points of inflection is:-

$$2(\omega''-\omega_0) = .55/\tau$$

Thus the linewidth at half height is calculated to be $6.1 \pm .6$ mg. or about 17 kcs/sec.

For a line width of 17 Kc/s. we therefore have:-

$$\tau = 7.9 \times 10^{-6} \text{ sec.}$$

This is very much shorter than the value of τ obtained in section (vi) from measurements of the pumping transient. We therefore conclude that the observed line width is due to other causes. The most probable cause is the inhomogeneity of the magnetic field over the volume of the sample.

(v) Line Shapes

These were qualitatively as predicted by the theory of Chapter I. Fig. 16a and 16b, obtained from a thin sample, show clearly that the alignment signal is double humped, but the polarization signal is not. The double humped signal was very useful as a direct measure of the strength of the r.f.

field using the relation $2(\omega-\omega_0) = \sqrt{2}\gamma H_1$ at the peaks of the humps. Fig. 17 shows the effect on an alignment signal of increasing the r.f. field H_1. The increasing separation of the humps is quite clear. It is difficult to make an independent determination of the value of H_1 at these frequencies, but it was found that the line splitting was linearly proportional to the r.f. voltage applied to the r.f. coils. A further test, with a signal obtained at 300 Kc/s., was conducted, using large diameter (24 cm.) r.f. coils, so that the r.f. field was fairly uniform, and could be calculated from the dimensions of the coils and the current through them. The latter was determined by measuring the voltage across a known resistor placed at the electrical centre of the two coils. With these precautions the calculated value of H_1 was found to agree (within 20%) with that measured from the line splitting. It was therefore considered justifiable to use the double-humped signal to measure the average r.f. field in the sample.

(vi) Pumping Transient

Some experiments were performed to determine the relaxation time of the metastable atoms in the presence of the discharge. These were performed with a 1 mm. Hg. cell. This pressure was chosen because the main purpose of the experiment was to obtain information for calculations concerning a similar 1 mm. Hg. cell, containing He^3. This is reported in Part Two of this thesis.

In eq. 14 , p.1.8 , we found that the approach to equilibrium polarization has a characteristic time, τ , where $1/\tau = 1/\tau_P + 1/\tau_R$. Furthermore, the polarization is given by an expression:-

$$P = \frac{\tau_R}{\tau_P + \tau_R} \qquad \text{(Table I p.1.21)}$$

Consequently, providing P is small,

$\tau_R \ll \tau_P$, and so $\tau \simeq \tau_R$

An example of a pumping transient obtained by the method of section (iib) Chapter II, is shown in Fig. 18. The r.f. field H_1 was switched off at the indicated point in less than 2×10^{-5} secs. The time constant τ of the exponential rise in the signal is given, in this case, by $1.7 \pm .1 \times 10^{-4}$ secs. It was found to vary between 2×10^{-4} secs., and 1×10^{-4} secs., depending on the discharge intensity, the longer time being appropriate to weaker discharges. The relaxation time of metastable atoms under the experimental conditions is therefore between .1 m secs. and .2 m secs. As remarked in section 5, this is an order of magnitude greater than the lifetime predicted by line width measurements.

Switching on the r.f. was a slower process, taking about 1.5×10^{-4} secs. and gave rise to the transient at the right of fig. 18. This depolarization transient is, none the less, sufficiently sharp to demonstrate that the response of the detection system was rapid enough not to distort the slower

pumping transient. The small oscillations are due to nutation of the polarized atoms about the effective field which, at resonance, is H_1. H_1 is, in fact, increasing during the period of this transient.

The signal to noise ratio of this part of the trace is not large enough for quantitative measurements, but it is worth noting that the decay time of the nutation is about .1 m sec. Assuming the time constant 'θ' of the decay of nutation to be given by

$$2/\theta = \frac{1}{\tau_R} + \frac{1}{\tau_2}$$

we may calculate τ_2, the transverse relaxation time of the metastables. (See p.4.15 for a discussion of nutation in a two level system. The situation in a three level system is in fact more complicated than this simple equation suggests.)

Under the experimental conditions the inhomogeneity of H_1 is probably an important factor in shortening the decay of the nutation, so that the experimental results indicate that τ_R and τ_2 are comparable in size.

(vii) Causes of Relaxation

(a) Diffusion to the walls.

The solution was given in Chapter One of a diffusion equation containing an absorption term, for a spherical cell of radius R, assuming zero density of metastable atoms at the walls of the cell. There it was shown that the rate of loss

of metastable atoms (per unit density) considering only the first decay mode, was given by:-

$$\left[\frac{D\pi^2}{R^2} + K\right]$$

D is the coefficient of diffusion for metastable atoms diffusing in He^4 gas, at the temperature and pressure of the cell. K is the rate of loss of metastable atoms within the bulk of the gas.

The relaxation time due to diffusion to the walls is therefore given by

$$\tau_D = \frac{R^2}{\pi^2 D}$$

The diffusion coefficient was measured by Phelps and Molnar, (Ref. 8) who assumed complete destruction of metastable atoms at the walls. They obtained D = 410 cm. sec., for a pressure of 1 mm. Hg. and a temperature of 300°K. This is in good agreement with a theoretical value calculated by Buckingham and Dalgarno (Ref. 9) which lends support to the hypothesis of complete loss of metastable atoms at the walls.

The radius of our cells is 3.2 cms., so that in our experiment

$$\tau_D = 2.5 \times 10^{-3} \text{ secs.}$$

Clearly, then, diffusion to the walls is insufficient to account for the observed relaxation time, even allowing for the fact that a fraction of the atoms decay by faster modes of diffusion than the fundamental one.

(b) Losses within the bulk of the gas.

Phelps and Molnar found that at high densities of metastable atoms ($\sim 10^{11}$/cc.), their destruction was largely due to collision between pairs of metastables. The effect of such collisions is that one atom becomes ionized, and the other de-excited. The occurrence of this process was found by Biondi (Ref. 10) whilst studying ionization processes in Helium. He found that there was an increase in electron density in the gas some time after the discharge was switched off. This he attributed to the ionization mentioned above. Phelps and Molnar estimated that the cross section for such destructive collisions was about 10^{-14} cm^2. at 300°K. For a cell at 1 mm. Hg. pressure in which 1 in 3×10^5 atoms are in the $^3S_1$ metastable level (metastable density $\sim 1 \times 10^{11}$) this predicts a lifetime of about 7.5 m. secs. against this means of destructions. This is still insufficient to account for the observed life of .1 - .2 m. secs.

The discrepancy between observed and predicted lifetimes is almost certainly accounted for by the action of the discharge. Phelps and Molner found that the rate of loss of metastable Argon atoms was particularly large in the region of discharge and a similar situation probably occurs in Helium. This is attributable to collision processes with discharge products, i.e. ions, electrons, and excited atoms. Charge-exchage collisions can result in the excitation of

the 2^1P level e.g. from which radiative decay is allowed. Impurities are also a cause of relaxation, although the getter should reduce these to a very low pressure. Hydrogen is particularly effective in quenching metastable Helium atoms. These give up their energy of excitation to dissociate H_2 molecules.

(viii) Lamp Investigation

The profiles of the 10,830 Å emission lines from a number of lamps, under different conditions, were obtained using a high resolution Fabry-Perot spectrograph. The output of the detector (R.C.A. photomultiplier 7102) was fed to a direct recording apparatus (Ref. 11). This traced out the line profile, which was scanned by varying the pressure in the etalon box. The etalon spacer used was .226 cm. and the effective number of reflections, N_{eff}, was about 70. This corresponds to an instrumental width of .03 cm^{-1}.

The most striking result of the investigation was that low pressure lamps were so badly self-reversed that the ratio K of the intensities of the D_o and D_3 lines was sometimes greater than one. (See Fig. 19a). This improved with increased lamp pressure, until at 5 mm. Hg., $K \simeq .25$ (Fig. 19b).

Since the lower pressure lamps were in fact brighter than those at higher pressure, means were sought to reduce the self-reversal of the former. In order to reduce the layer

of cooler gas between the hottest part of the discharge and the front of the lamp, a re-entrant lamp was constructed, as shown in Fig. 6b. The profiles of two lamps filled at 1 mm. pressure, and identical except that one had a re-entrant window, are shown in Figures 19c and 19d. There is seen to be a definite improvement in the profile for the re-entrant lamp.

Until the investigation, it had been customary to flash a getter in the lamps to purify the gas. It was noticed, however, that a lamp exhibited less self-reversal before it was gettered than afterwards. This is accounted for by the quenching of metastable atoms by impurities, thus reducing the optical density at 10,830Å of the absorbing layer. This phenomenon is well known to spectroscopists, who sometimes add Hydrogen to a Helium discharge in order to quench the metastables, and reduce self-reversal. This expedient also reduces the intensity of the He lines so that too much impurity in the lamp is detrimental. Subsequent lamps were therefore baked out in the usual way but not gettered.

IX Summary

The work on He^4 was undertaken as a preliminary to experiments aimed towards producing nuclear polarisation in He^3.

A versatile optical pumping apparatus was built, and the work of Franken and Colegrove on the alignment of He^4

(ref. 2) was repeated, and also extended to cover the case of polarisation. The line shapes and polarity of the optical pumping signals were found to agree qualitatively with those predicted by the simple theory developed in chapter one.

Lamp performance was investigated and as a result an improved design was found. Possible causes for the relaxation of the metastable atoms were considered and the conclusion reached that wall effects were negligible. The majority of the relaxation took place within the bulk of the gas.

At this stage it was felt that sufficient insight had been gained into the optical pumping of He^4 and efforts were then directed towards optically pumping He^3.

PART TWO

OPTICAL PUMPING IN HE^3

Note on Time-Constants.

For convenience of reference, some of the more important time constants used in the analysis of optical pumping in He^3 are gathered together here, with a brief definition. Further information is to be found at the given page references.

τ_R	Longitudinal relaxation time of the metastable atoms.	4.5
τ_P	Pumping time of metastable atoms.	4.5
τ	Characteristic time of metastable atoms.	4.5
T_1	Longitudinal relaxation time of ground-state atoms with no discharge.	4.6
T	Longitudinal relaxation time of ground-state atoms with discharge on.	4.6, 4.8
τ_t	Transverse relaxation time of metastable atoms.	4.6
T_2	Transverse relaxation time of ground-state atoms, without discharge.	6.18
T_2'	Transverse relaxation time of ground-state atoms, due to metastability exchange collisions.	4.6
T_2''	Resultant transverse relaxation time due to T_2 and T_2'	6.17
Θ	Time constant of the decay of nuclear nutation, at resonance.	4.17, 6.17

PART TWO

CHAPTER FOUR

Theoretical Considerations

(i) The Pumping Process

(a) The Levels

Optical pumping in He^3 is similar to that in He^4, in as much as the same levels and optical transitions are used. Polarization is produced in the $^3S_1$ metastable levels, by means of circularly polarized light which excites some of the $^3S_1 - {}^3P_{0,1,2}$ transitions. The He^3 nucleus has a nuclear spin ($I = \frac{1}{2}$) which gives rise to hyperfine structure in the levels, whilst its reduced mass, and other effects, cause an isotope shift of the spectral lines. (Ref. 1). A term diagram of the relevant energy levels is given in Fig. 20. The spectral lines are similar to those of He^4 to the extent that the D_1 and D_2 lines are unresolved, and that the D_0 line is separated from them by about 1 cm^{-1}. The hyperfine structure is so large that the two hyperfine components of the D_0 line are well resolved, even when emitted by a hot lamp, as in the experiments. The calculated fine and hyperfine structure of the $^3S_1 - {}^3P_{0,1,2}$ lines for He^3 (Ref. 1) is shown in Fig. 21a together with the fine structure of He^4, in order to show the isotope shift. This can be compared to the actual lamp profiles obtained as described on p.3.12 , and shown in Fig. 21b. It will be noted that only the D_0, $F = \frac{3}{2} \rightarrow \frac{1}{2}$

transition of He^3 overlaps any of the He^4 structure. This coincidence between the He^4 D_3 line and the D_0, $F = \frac{3}{2} \rightarrow \frac{1}{2}$ hyperfine line of He^3 is almost exact. The transition probabilities for all the hyperfine components of the multiplet (obtained from ref. 1) are given in Fig. 22a. Account has been taken of the perturbations arising from the fact that the hyperfine structure of these levels is comparable in size with the fine structure. They have been used to derive the relative transition probabilities for all the Zeeman hyperfine components of the multiplet and these are given in Fig. 22b.

The Zeeman hyperfine structure of the levels in a weak magnetic field is shown to the right in Fig. 20. The absorption of right-handed circularly polarized light from a He^3 lamp, directed along the magnetic field, gives rise to all the allowed σ^+ transitions between the $^3S_1$ and $^3P_{0,1,2}$ levels. Decay tends to favour the metastable states of higher M_F, in the same way as states of higher M_J were favoured in He^4. Here the similarity ends, since the existence of a nuclear spin gives rise to effects in He^3 which do not occur in He^4. As a result of the hyperfine coupling, optical pumping in the metastable levels creates a nuclear polarisation which is rapidly transferred to the ground state through the process of metastability exchange.

(b) Metastability Exchange

Metastability exchange is the name given to a process which may occur when a metastable atom undergoes a collision with a ground-state atom. In the course of a collision a diatomic He molecule is formed in which the electrons of both atoms are shared. Providing that the interaction is long enough, there is a probability of ½ that the emerging nuclei have exchanged electrons. The nuclei may be distinguished by the directions of their spins. This is possible because the duration of a collision is so short that the nuclear orientations are the same before and after a collision (Ref. 12).

We have seen that when optical pumping is performed on the metastable atoms in a weak magnetic field, so that F is a good quantum number, then their nuclei become polarised through their hyperfine coupling with the electrons. However this is only true provided that the exchange collisions are not so frequent that the nuclei become uncoupled from the electrons. The hyperfine splitting in the $^3S_1$ levels (6740 Mc/s.) is a measure of the hyperfine interaction so that the lifetime of a metastable atom between collisions must be large compared with 10^{-10} secs. This is the interval between collisions for an atom in He at a pressure of about 1000 mm. Hg. so that this condition is well satisfied at pressures of a few mm. Hg.

The cross-section for a metastability exchange is likely

to be large since it depends on the electron exchange interaction and not on magnetic dipole coupling. It was estimated to be within a factor five of 10^{-15} cm^2. by Colegrove and Franken (Ref. 2). This may be compared with the classical gas-kinetic collision cross-section, which is $1.4\ 10^{-15} cm^2$.

(c) Use of He^4 light to pump He^3

At pressures above about .5 mm. Hg. mixing in the excited states becomes important, as in the case of He^4. Atoms may be excited out of states of higher M_F, and after mixing in the excited states decay to states of lower M_F. Use of He^4 radiation to pump the He^3 minimises this effect since only those atoms which are in the $^3S_1$ $|F = \frac{3}{2}$, $M_F = -\frac{3}{2}, -\frac{1}{2}>$ states can absorb σ^+ He^4 light. (Fig. 20). A further advantage is that since the states of higher M_F are transparent to the He^4 light, the transparency of the sample, and hence the size of the signal, is more sensitive to the degree of polarization.

The low oscillator strengths of the transitions excited by He^4 light ensure that the sample is usually optically thin. This fact together with the small number of transitions involved, made calculation of the polarization from observations of the signal strength much simpler for He^4 light. In particular, it did not require a knowledge of 'K' the intensity ratio between the D_3 and D_0 lines.

(d) Detection of Polarisation

As in the case of He^4, the polarization was detected by equalising the populations by saturating the magnetic dipole transitions with an applied r.f. field at the resonance frequency. There was a choice of three frequencies for any given field. The two hyperfine $^1S_0$ levels have different g values, 1.9 Mc/G and 3.6 Mc/G, and the ground state has a g value of 3.2 Kc/G. Because of the close coupling between these three levels, depolarisation of one of them by a r.f. field depolarized them all, and hence changed the transparency of the sample to the pumping radiation.

(ii) Rate Equations

The large number of metastable states in He^3 and the interaction between these and the ground states, makes the solution of rate equations for He^3 extremely complex. It is useful to consider a simplified model of the processes which actually occur. We restrict the six metastable states to two, with populations n_+ and n_- and consider their interaction with the two ground states, with populations N_+ and N_-. We define the following times:-

τ_P (10^{-3} secs)	Pumping time of metastables	Assuming no Interaction with ground state (56)
τ_R (10^{-4} secs)	Relaxation time of metastables	
τ (10^{-4} secs)	$1/\tau = 1/\tau_P + 1/\tau_R$	

τ_2 ($\sim 10^{-7}$ secs) Life time of metastable atoms before undergoing collisions in which there is a probability $\frac{1}{2}$ of metastability exchange.

T_2' ($\sim 10^{-2}$ secs) Lifetime of ground state before undergoing collisions in which there is a probability $\frac{1}{2}$ of metastability exchange.

Clearly $N\tau_2 = n\,T_2'$ (57)

T (~ 5 secs) Characteristic time for the approach to equilibrium polarization, of the coupled systems.

T_1 (~ 100 secs) Ground state (longitudinal) relaxation time.

The figures in brackets are approximate values typical of a 1 mm. Hg. He^3 cell. Let

$$N = N_+ + N_- \text{ and } n = n_+ + n_-. \quad \text{Also } N \gg n \qquad (58a,b)$$

We may now write the following rate equation, for the population n_+:-

$$\frac{dn_+}{dt} = \underset{(a)}{\frac{n_-}{\tau_P}} - \underset{(b)}{\frac{n_+}{\tau_R}} + \underset{(c)}{\frac{n}{2\tau_R}} + \underset{(d)}{\frac{N_+ n_-}{2N\tau_2}} - \underset{(e)}{\frac{N_- n_+}{2N\tau_2}} \qquad (59)$$

The separate terms are:-

(a) The rate at which atoms are pumped from the n_- state into n_+ state, by the optical radiation.

(b) and (c) Terms allowing for the destruction and creation of metastable atoms so that $n_+ + n_- = n$, a constant.

(d) This is the rate of increase of n_+ due to the metastability exchange of n_- metastable atoms with N_+ ground

state atoms. The factor $\frac{1}{2}$ is the fraction of the metastable collisions between N_+ and n_- which result in such an interchange.

(e) As (d), but for n_+ metastable atoms.

Similarly, we have+-

$$\frac{dn_-}{dt} = -\frac{n_-}{\tau_P} - \frac{n_-}{\tau_R} + \frac{n}{2\tau_R} + \frac{N_- n_+}{2N\tau_2} - \frac{N_+ n_-}{2N\tau_2} \qquad (60)$$

$$\frac{dN_+}{dt} = \frac{N_-}{2T_1} - \frac{N_+}{2T_1} + \frac{n_+ N_-}{2nT_2'} - \frac{n_- N_+}{2nT_2'} - \frac{N_+}{N}\frac{n}{\tau_R} + \frac{n}{2\tau_R} \qquad (61)$$

$$\frac{dN_-}{dt} = \frac{N_+}{2T_1} - \frac{N_-}{2T_1} + \frac{n_- N_+}{2nT_2'} - \frac{n_+ N_-}{2nT_2'} - \frac{N_-}{N}\frac{n}{\tau_R} + \frac{n}{2\tau_R} \qquad (62)$$

We now define the polarizations p and P in metastable and ground levels respectively:-

$$p = \frac{n_+ - n_-}{n} \qquad P = \frac{N_+ - N_-}{N} \qquad (63)\ (64)$$

Subtracting 1b from 1a, and 2b from 2a, and substituting 3a, b in the results, we obtain:-

$$\frac{dp}{dt} = \frac{1}{\tau_P} - \left(\frac{1}{\tau_P} + \frac{1}{\tau_R} + \frac{1}{2\tau_2}\right) P + \frac{1}{2\tau_2} P \qquad (65)$$

$$\frac{dP}{dt} = -\left(\frac{1}{T_1} + \frac{n}{N\tau_R} + \frac{1}{2T_2'}\right) P + \frac{n}{2N\tau_2} p \qquad (66)$$

These may be solved by making a number of approximations based on the expected values of the various time constants. The details of the calculation are to be found in Appendix 1. The solutions are:-

$$p = Ae^{-t/2\tau_2} + Be^{-t/T} + \frac{\tau_R}{\tau_P + \tau_R} \qquad (67)$$

$$P = -\frac{2}{T_2} Ae^{-t/2\tau_2} + Be^{-t/T} + \frac{\tau_R}{\tau_P + \tau_R} \qquad (68)$$

$$\text{where } \frac{1}{T} = \frac{1}{T_1} + \frac{n}{N}\left(\frac{1}{\tau_P} + \frac{2}{\tau_R}\right) \qquad (69)$$

These results show that under the experimental conditions, the equilibrium polarizations in the metastable and ground levels are equal to the value which would have been reached by the metastable atoms alone (see p. 1.21). That is $\frac{\tau_R}{\tau_P + \tau_R}$. Furthermore, detailed analysis shows that $B \gg A$, so that the second exponential dominates the first in each equation and the approach to equilibrium polarization is given by T, as defined in equation 8.

Thus the pumping time of the combined systems is the pumping time of the metastable atoms multiplied by the ratio $\frac{N}{n}$. The relaxation time of the combination is given by (69) with $\tau_P \rightarrow \infty$

The results of the above calculation are assumed to hold for the actual system with suitable alterations to the definitions of the various characteristic times. The pumping time τ_P becomes an average of the pumping times out of the metastable states. τ_R and τ_2 are assumed to be the same for all the metastable states. T_1 and T_2 are unaltered since they already apply to a two level system.

(iii) Measurement of Degree of Polarization

(a) Measurements. The problem is to relate measurements of the signal amplitude to the polarization in the ground state.

The observations we can make are similar to those for He^4. They are:-

(a) the amplitude of the signal, on depolarizing the sample,

(b) the total absorption of the sample, when unpolarized, (measured by noting the change in intensity of transmitted light when the discharge is switched on).

The signal, ΔI, depends upon the actual distribution of atoms amongst the metastable states $|F, M_F\rangle$. In particular, $|\frac{3}{2}, -\frac{3}{2}\rangle$, $|\frac{3}{2}, -\frac{1}{2}\rangle$ are the only absorbing states if a He^4 lamp is used to monitor the polarization. It is therefore important to determine the actual populations of the metastable states for a given polarization of the ground state.

(b) Relative Populations

The lifetime of a metastable atom between collisions in which metastability is exchanged is between 10^{-6} and 10^{-7} secs., for a sample at 1 mm. Hg. pressure. On the other hand, a typical pumping time τ_P for the metastable atoms is 10^{-3} secs., whilst the relaxation time, τ_R, may be 10^{-4} secs. Clearly then, the exchange with the ground states dominates the distribution of populations in the metastable levels.

The exchange processes may be described by equations relating the populations of the metastable and ground states, and their time differentials. We designate the populations

of the $|\frac{3}{2}, M_F\rangle$ and $|\frac{1}{2}, M_F\rangle$ metastable states by n_{M_F} and m_{M_F} respectively, and the populations of the ground states by N_{M_F}.

$$\sum n_{M_F} + \sum m_{M_F} = n \qquad \text{a constant} \qquad (70)$$

and $$\sum N_{M_F} = N \qquad \text{a constant} \qquad (71)$$

The rate equation for the state $|\frac{3}{2}, \frac{3}{2}\rangle$ is then:-

$$\frac{dn_{3/2}}{dt} = k\left[- a n_{3/2} N + b\, n_{\frac{1}{2}} N_{\frac{1}{2}} + c m_{\frac{1}{2}} N_{\frac{1}{2}} \right] \qquad (73a)$$

k is a constant related to the cross-section for metastability exchange. The first term expresses the fact that an atom may be lost from the $|\frac{3}{2}, \frac{3}{2}\rangle$ state by a collision with a ground state atom in the $|\frac{1}{2}, -\frac{1}{2}\rangle$ state. The second term accounts for gains in the population of the $|\frac{3}{2}, \frac{3}{2}\rangle$ state due to collisions between atoms in the $|\frac{3}{2}, \frac{1}{2}\rangle$ metastable state and the $|\frac{1}{2}, \frac{1}{2}\rangle$ ground state. Terms are included for all collisions in which the z component of angular momentum is conserved and which result in a change of population in the $\frac{3}{2}, \frac{3}{2}$ state. The coefficients a, b, c, of the separate terms express the relative probabilities that a collision between atoms in the two given states will result in a change in population of the $|\frac{3}{2}, \frac{3}{2}\rangle$ state.

In evaluating these coefficients it is useful to express the $|J, I, F, M_F\rangle$ states (which we have abbreviated to $|F, M_F\rangle$ states above), super-positions of $|J, I, M_J, M_I\rangle$ states. This can be done making use of the Wigner coefficients given, for example in Condon and Shortley, p.76 (Ref. 13).

We have:-

$\lvert F \;\; M_F\rangle$		$\lvert M_J, M_I\rangle$	$\lvert M_J, M_I\rangle$		F, M_F	M_J, M_I
$\lvert\frac{3}{2}, \frac{3}{2}\rangle$	=	$\lvert 1, \frac{1}{2}\rangle$				
$\lvert\frac{3}{2}, \frac{1}{2}\rangle$	=	$\sqrt{\frac{2}{3}}\lvert 0, \frac{1}{2}\rangle + \sqrt{\frac{1}{3}}\lvert 1, -\frac{1}{2}\rangle$		$\lvert\frac{1}{2}\;\frac{1}{2}\rangle$	=	$\lvert 0, \frac{1}{2}\rangle$
$\lvert\frac{3}{2}, -\frac{1}{2}\rangle$	=	$\sqrt{\frac{2}{3}}\lvert 0, -\frac{1}{2}\rangle + \sqrt{\frac{1}{3}}\lvert -1, \frac{1}{2}\rangle$		$\lvert\frac{1}{2}, -\frac{1}{2}\rangle$	=	$\lvert 0, -\frac{1}{2}\rangle$
$\lvert\frac{3}{2} -\frac{3}{2}\rangle$	=	$\lvert -1, -\frac{1}{2}\rangle$				
$\lvert\frac{3}{2}, \frac{1}{2}\rangle$	=	$\sqrt{\frac{2}{3}}\lvert 1, -\frac{1}{2}\rangle - \sqrt{\frac{1}{3}}\lvert 0, \frac{1}{2}\rangle$				
$\lvert\frac{1}{2}, -\frac{1}{2}\rangle$	=	$\sqrt{\frac{2}{3}}\lvert -1, \frac{1}{2}\rangle + \sqrt{\frac{1}{3}}\lvert 0, -\frac{1}{2}\rangle$				

72 a-h.

The coefficients of the states $\lvert M_J, M_I\rangle$ are probability amplitudes. The square of a coefficient expresses the probability that an atom with wave function $\lvert F, M_F\rangle$ will be found at a given time to be in the state $\lvert M_J, M_I\rangle$. We assume that at each collision there is a probability of $\frac{1}{2}$ that there is an exchange of electrons. It is then clear that collisions represented by the first term of eq. (73a) have a probability of $\frac{1}{2}$ or resulting in the transfer of an atom from the state $\lvert 1, \frac{1}{2}\rangle$ to the state $\lvert 1, -\frac{1}{2}\rangle$ (in the $\lvert M_J M_I\rangle$ representation). Therefore a = $\frac{1}{2}$.

The second term is more complicated because the $\lvert F = \frac{3}{2}, M_F = \frac{1}{2}\rangle$ state is a superposition of two $\lvert M_J, M_I\rangle$ states. (Eq. 72b). Referring now to states in the $\lvert M_J, M_I\rangle$ representation, exchange of electrons between an atom when it is in the metastable $\lvert 0, \frac{1}{2}\rangle$ state and a ground state atom in the $\lvert 0, \frac{1}{2}\rangle$ state can have no effect. But one third of the

time the metastable atom $|F = \frac{3}{2}, M_F = \frac{1}{2}\rangle$ is in the $|1, -\frac{1}{2}\rangle$ state, therefore the total probability for creation of an atom in state $|1, \frac{1}{2}\rangle$ is $\frac{1}{3} \cdot \frac{1}{2} = \frac{1}{6}$, i.e. b = 1/6.

Similar considerations allow the calculation of all the coefficients for all the rate equations, which are given on the next page.

By setting the time differentials equal to zero, the steady state solution of these equations may be found by inspection to be:-

$$n_{3/2}:n_{\frac{1}{2}}:n_{-\frac{1}{2}}:n_{-3/2}:m_{\frac{1}{2}}:m_{-\frac{1}{2}} = 1:\alpha:\alpha^2:\alpha^3:\alpha:\alpha^2 \qquad (74)$$

$$N_{\frac{1}{2}}:N_{-\frac{1}{2}} = 1:\alpha \qquad (75)$$

α is given in terms of the ground state polarisation by

$$P = \frac{1-\alpha}{1+\alpha} \qquad (76)$$

It has been pointed out (ref. 14) that this is statistically the most probable distribution of a given quantity of angular momentum, between two systems, in each of which the total number of particles is a constant. It is a Boltzman distribution in angular momentum and the"angular momentum spin temperatures" T_s of the two systems are the same. That is:-

$$\frac{n_{M_F}}{n_{M'_F}} = \frac{N_{M_F}}{N_{M'_F}} = e^{\Delta M_F/T_s} = \frac{1}{\alpha^{\Delta M_F}}$$

where $\Delta M_F = M_F - M'_F$

Therefore $T_s = (\log \alpha)^{-1}$

$$\frac{dn_{3/2}}{dt} = K\left[-\tfrac{1}{2}\, n_{3/2} N_{-1/2} + \tfrac{1}{6} n_{1/2} N_{1/2} + \tfrac{1}{3} m_{1/2} N_{1/2}\right]$$

$$\frac{dn_{1/2}}{dt} = K\left[\tfrac{1}{6} n_{3/2} N_{-1/2} - \tfrac{1}{6} n_{1/2} N_{1/2} - \tfrac{1}{3} n_{1/2} N_{-1/2} + \tfrac{2}{9} n_{-1/2} N_{1/2} + \tfrac{1}{9} m_{-1/2} N_{1/2}\right]$$

$$\frac{dn_{-1/2}}{dt} = K\left[\tfrac{1}{6} n_{-3/2} N_{1/2} - \tfrac{1}{6} n_{-1/2} N_{-1/2} - \tfrac{1}{3} n_{-1/2} N_{1/2} + \tfrac{2}{9} n_{1/2} N_{-1/2} + \tfrac{1}{9} m_{1/2} N_{1/2}\right]$$

$$\frac{dn_{-3/2}}{dt} = K\left[-\tfrac{1}{2} n_{-3/2} N_{1/2} + \tfrac{1}{6} n_{-1/2} N_{-1/2} + \tfrac{1}{3} m_{-1/2} N_{-1/2}\right] \qquad 73(a\text{-}h)$$

$$\frac{dm_{1/2}}{dt} = K\left[-\tfrac{1}{3} m_{1/2} N_{1/2} - \tfrac{1}{6} m_{1/2} N_{-1/2} + \tfrac{1}{3} n_{3/2} N_{-1/2} + \tfrac{1}{9} n_{-1/2} N_{1/2} + \tfrac{1}{18} m_{-1/2} N_{1/2}\right]$$

$$\frac{dm_{-1/2}}{dt} = K\left[-\tfrac{1}{3} m_{-1/2} N_{-1/2} - \tfrac{1}{6} m_{1/2} N_{1/2} + \tfrac{1}{3} n_{3/2} N_{1/2} + \tfrac{1}{9} n_{1/2} N_{-1/2} + \tfrac{1}{18} m_{1/2} N_{-1/2}\right]$$

$$\frac{dN_{1/2}}{dt} = K\Big[-N_{1/2}\left(\tfrac{1}{6} n_{1/2} + \tfrac{1}{3} n_{-1/2} + \tfrac{1}{2} n_{-3/2} + \tfrac{1}{3} m_{1/2} + \tfrac{1}{6} m_{-1/2}\right) + N_{1/2}\left(\tfrac{1}{2} n_{3/2} + \tfrac{1}{3} n_{1/2} + \tfrac{1}{6} n_{-1/2} + \tfrac{1}{6} m_{1/2} + \tfrac{1}{3} m_{-1/2}\right)\Big]$$

$$\frac{dN_{-1/2}}{dt} = K\Big[-N_{-1/2}\left(\tfrac{1}{6} n_{-1/2} + \tfrac{1}{3} n_{1/2} + \tfrac{1}{2} n_{3/2} + \tfrac{1}{3} m_{-1/2} + \tfrac{1}{6} m_{1/2}\right) + N_{-1/2}\left(\tfrac{1}{2} n_{-3/2} + \tfrac{1}{3} n_{-1/2} + \tfrac{1}{6} n_{1/2} + \tfrac{1}{6} m_{-1/2} + \tfrac{1}{3} m_{1/2}\right)\Big]$$

The metastability exchange processes provide the analogue of thermal contact between the two systems.

The distribution also has the property that the nuclear polarisation is the same in the metastable levels as in the ground level. This is to be expected since the effect of the exchange processes is to allow the nuclei to pass freely between the ground and metastable levels.

The derivation above ignores the energy difference between the metastable hyperfine levels. This is justifiable in this case because

$$kT \gg h\nu \qquad \left(\frac{h\nu}{kT} \simeq 10^{-3} \text{ at } 300^{\circ}K\right)$$

(c) Degree of Polarization

The optical pumping signal can now be calculated. Since only the $|\frac{3}{2}, -\frac{3}{2}\rangle$ and $|\frac{3}{2}, -\frac{1}{2}\rangle$ states absorb circularly polarised He^4 light, and the relative absorption coefficients of these are 3:1 (fig. 22), then

$$\frac{\Delta I}{I} = \frac{4.1/6\ (1 + 2\alpha + 2\alpha^2 + \alpha^3) - (3\alpha^3 + 1.\alpha^2)}{4.\ 1/6\ (1 + 2\alpha + 2\alpha^2 + \alpha^3)}$$

$$= \frac{(1-\alpha)(2 + 6\alpha + 7\alpha^2)}{2(1+\alpha)(1 + \alpha + \alpha^2)} \qquad (77)$$

Substituting $P = \frac{1-\alpha}{1+\alpha}$ (76)

gives $\frac{\Delta I}{I} = \frac{1}{2}\ \frac{P(15 - 10P + 3P^2)}{3 + P^2}$ (78)

This function is plotted in Fig. 23.

If P is small $\frac{\Delta I}{I} \simeq \frac{5P}{2}$ (79)

This expression is at variance with that given in ref. 15, namely

$$\frac{\Delta I}{I} = \frac{P(6 - 2P)}{3 + P^2} \qquad (80)$$

$$\simeq 2P \qquad \text{if P is small.}$$

This expression may be obtained if it is assumed (incorrectly) that in addition to the $|\frac{3}{2}, -\frac{3}{2}\rangle$ and $|\frac{3}{2} -\frac{1}{2}\rangle$ states, the $|\frac{1}{2} - \frac{1}{2}\rangle$ metastable state is also absorbent to the He^4 radiation, and that this radiation is equally intense in the region of both the hyperfine components of the $^3S_1 - {}^3P_o$ line in He^3. It is also necessary to use the unperturbed transition probabilities for excitation from these states, which are in the ratio 3:1:2. The perturbed ratios given in Fig. 22 are 4.75:1.58:5 or 3:1:3.16.

(iv) Nuclear Nutation

(a) The Bloch Equations

In the experiments observations were made of the nutation of the nuclei, when a pulse of r.f. at the resonance frequency was applied to the polarised sample. The motion of a system of spins under the action of an external field, H_o and a field H_1, rotating with angular frequency about H_o, is described by the Bloch equations. (Eqs. 42 of Ref. 16).

$$\frac{dM_z}{d\tau} - v + \alpha M_z = M_o$$

$$\frac{du}{d} + \beta u + \delta' v = 0$$

$$\frac{dv}{d\tau} + M_z + \beta v - u\delta' = 0 \qquad (82a,b,c)$$

where $\tau = \gamma H_1 t$, $\alpha = 1/\gamma H_1 T_1$, $\beta = 1/\gamma H_1 T_2$

$$\delta' = \omega - \omega_o / \gamma H_1 = \frac{\omega - \omega_o}{\omega_1} = \frac{\delta}{\omega_1} \qquad (83a-d)$$

M_o is the initial magnetisation. M_z, u and v are the instantaneous components of magnetisation in a co-ordinate system rotating about the z axis with angular frequency and are given by:-

$$u = M_x \cos\omega t - M_y \sin\omega t$$
$$v = -M_x \sin\omega t - M_y \cos\omega t \qquad (84a,b)$$

M_z is the same in both the rotating and the laboratory co-ordinate systems. The times T_1 and T_2 are the longitudinal and transverse relaxation times of the ground state atoms. Their values depend on the conditions under which they are observed. For instance the presence of the metastable atoms with which they undergo metastability exchange will affect their values, and so also will the pumping light.

In our experiments the polarisation P, and hence the magnetisation M_z is observed.

(b) Exact Resonance

The solution of eqs. 82 a,b,c, for M_z is simple for the case of exact resonance, i.e. $\delta' = 0$, in which case the equations reduce to two, and solving for M_z we obtain:-

$$\frac{d^2M_z}{d\tau^2} + (\alpha + \beta)\frac{dM_z}{d\tau} + (\alpha\beta + 1) M_z - \alpha\beta M_o = 0 \qquad (85)$$

Providing $(\alpha-\beta)^2 < 4$ i.e. $\omega_1 > \frac{1}{2}\left(\frac{1}{T_1} + \frac{1}{T_2}\right)$ (86)

this has the solution

$$M_z = \frac{\alpha\beta}{\alpha\beta+1} M_o + e^{-\frac{1}{2}(\alpha+\beta)\tau}\left[A \cos\sqrt{1 - \frac{(\alpha-\beta)^2}{4}}\tau + B \sin \sqrt{1 - \frac{(\alpha-\beta)^2}{4}}\tau\right] \quad (87)$$

Using the initial conditions to evaluate A and B, and substituting for α, β and τ from eqs.83 a,b,c

$$M_z = \varepsilon M_o + (1-\varepsilon) M_o \exp\left[-\tfrac{1}{2}\left(\frac{1}{T_1} + \frac{1}{T_2}\right)t\right]\left[\cos\omega' t + \frac{1}{2\omega'_1}\left(\frac{1}{T_1} + \frac{1}{T_2}\right)\sin\omega'_1 t\right] \quad (88)$$

where $\varepsilon = (1 + \omega_1^2 T_1 T_2)^{-1}$ and $\omega'_1 = \sqrt{\omega_1^2 - \tfrac{1}{4}\left(\frac{1}{T_2} - \frac{1}{T_1}\right)^2}$ (89)(90)

Under the conditions $\omega_1^2 T_1 T_2 \gg 1$, and $\omega_1 \gg \frac{1}{2}\left(\frac{1}{T_2} \pm \frac{1}{T_1}\right)$ (90)(91)

which hold in all cases where the nutation is clearly observable, then $\varepsilon \to 0$ and $\omega'_1 \to \omega_1$ so that

$$M_z \simeq M_o \exp\left[-\tfrac{1}{2}\left(\frac{1}{T_1} + \frac{1}{T_2}\right)t\right] \cos\omega_1 t = M_o e^{-t/\theta} \cos\omega_1 t \quad (92)$$

which defines θ. The z component of the magnetic moment therefore oscillates, with frequency γH_1 and the oscillations are damped with decay constant θ^{-1} which is the mean of T_1^{-1} and T_2^{-1}.

(c) <u>The general Solution</u>

The solution when $\delta \neq 0$ is much more complicated, but it has been shown (ref. 17) that the solution is of the form:-

$$M_z = Ae^{-a\tau} + Be^{-b\tau}\cos s\tau + Ce^{-b\tau}\sin s\tau + D \quad (93)$$

At exact resonance A = 0 and the solution reduces to the form of (87). Off resonance the nutation frequency is given by:-

$$\omega^*_1 = \sqrt{\omega_1^2 + (\omega - \omega_o)^2} \qquad (94)$$

The damping of the nutation in this case has the time constant θ^* where

$$\frac{1}{\theta^*} = \frac{1}{T_2} - \tfrac{1}{2}\left(\frac{1}{T_2} - \frac{1}{T_1}\right) \frac{\omega_1^2}{\omega_1^2 + (\omega - \omega_o)^2} \qquad (95)$$

If $T_1 >> T_2$ then

$$\frac{1}{\theta^*} = \frac{1}{T_2}\left[1 - \frac{\omega_1^2}{2\left[\omega_1^2 + (\omega - \omega_o)^2\right]}\right] \qquad (96)$$

Therefore for an accurate measurement of θ the deviation from resonance must be small so that $(\omega - \omega_o)^2 \ll \omega_1^2$ (97)

The first term of (93) is given by

$$Ae^{-a\tau} \simeq \frac{\delta'^2 M_o}{1 + \delta'^2}\left[1 - \frac{1 + \delta'^2}{\delta'^2 + \beta/\alpha}\right] \exp\left[-\frac{\beta + \alpha\delta^2}{1 + \delta^2}\right] \qquad (98)$$

In the experiments on nutation, exact resonance could be obtained by adjusting the frequency until this feature of the signal disappeared (see p.5.6).

(d) <u>Field Inhomogeneities</u>

The above analysis assumes that ω_o and ω_1 are constant over the sample. In practice there will be a certain inhomogeneity ΔH_1 and ΔH_o in H_1 and H_o. The effect of ΔH_1 is to vary the nutation frequencies of atoms in different parts of the sample. Consequently as time elapses phase differences develop and the macroscopic transverse

magnetisation is damped more rapidly than would otherwise be the case. H_1 should therefore be sufficiently homogeneous to satisfy the condition:-

$$\Delta H_1 \ll \frac{\pi}{\gamma^2 H_1 \theta} \qquad (99)$$

At exact resonance the expression for the nutation (92) is independent of H_o, but since $\omega_o = \gamma H_o$ the damping is affected through the relation (94). This shows that provided H_1 is homogeneous, the effect of ΔH_o is small if $\omega_1 >> \Delta\omega_o$ or

$$H_1 >> \Delta H_o \qquad (100)$$

CHAPTER FIVE

EXPERIMENTAL DETAILS

(1) Detection methods

A number of different methods was used to observe Optical Pumping signals in He^3, depending upon the type of measurement to be made. The experimental details are described below. Most of the apparatus was identical with that used for the experiments with He^4.

(a) Field Modulation

Under certain circumstances it was possible to observe signals due to magnetic resonance in the metastable levels by a method similar to that used for He^4 and described on p. 2.3. There were a number of difficulties associated with this method. At the low magnetic fields most readily available with the apparatus, the $F = 3/2$ and the $F = \frac{1}{2}$ resonances were so broad with high pressure cells that they tended to overlap. At higher fields where they did not overlap, the higher resonance frequency made it difficult to generate the high r.f. power required by the short-lived metastable atoms.

A second difficulty was connected with the coupling between the metastable and ground levels. In order to see a signal by field modulation it was necessary either to modulate so slowly that the polarisations in the ground and metastable levels were at all times in equilibrium (1/10 - 1/100 c/sec.) or else so fast that the two

polarisations were effectively uncoupled. The first was impracticable. The second was only useful if the coupling time ($\frac{N}{n}\tau_2$) was reasonably long. For a .1 mm. Hg. cell this is about 1 sec. For a 1 mm. Hg. cell it is .1 sec. We therefore required modulation frequencies of above about 10 c/sec. and 100 c/sec. respectively. Only the first was practicable since the modulation time had also to be long compared with the pumping time, which was about 5 m secs. This method of detection was therefore limited to low pressure cells.

(b) Sudden depolarisation

The signal could be observed without the use of field modulation, by monitoring the transmitted light on an oscilloscope, using a slow time base sweep, whilst applying a short burst of r.f. power. When the latter was adjusted to the resonance frequency a sharp change in the light intensity could be detected. This method is applicable to resonance in both metastable levels, or to nuclear resonance in the ground state. A large value of H_1 could be used to locate the signal roughly, and exact resonance obtained by progressively reducing H_1 until it was just sufficient to saturate the transitions over a narrow frequency band. It was necessary to allow sufficient time (10 - 60 secs.) for the sample to be "pumped" between successive bursts of r.f. The sharp change in light intensity when the r.f. was applied

was measured. This gave ΔI which was used in the measurement of polarization. The measurement of I, which is the intensity of the total light absorbed by the sample, when unpolarized, was obtained by noting the initial change in intensity when the discharge was switched on. The light emitted by the discharge itself was negligible compared with the lamp intensity.

(c) Pumping Transient

When the r.f. pulse described in the previous section is switched off, the sample returns to equilibrium polarization. This is observed as a gradual increase in the transmission of the sample. This pumping transient is much longer than the corresponding transient in He^4, and has a time constant of between 5 and 30 secs. For the shorter times (up to 10 secs.) the pumping transient was recorded directly by photographing the transient as displayed upon an oscilloscope. The longer transients were recorded point by point. The sample was 'pumped' for a measured time interval, and then the degree of polarisation measured by the depolarisation technique described in the previous paragraph.

(d) Nuclear Relaxation Times

The longitudinal relaxation time of the ground state polarization measured by a similar technique. The procedure was to "pump" the sample for a time sufficient to ensure that the equilibrium polarization was achieved. The lamp was

then switched off. After a given time, measured with a stop-watch, a pulse of r.f. was applied to destroy any remaining polarization. This depolarization was observed using a subsidiary He^4 lamp (described on p. 2.8) in place of the main lamp. In this way the polarizations remaining after a number of different delay times were measured and plotted as a function of time. From this graph the decay constant could be obtained.

The subsidiary lamp was mounted to the side of the apparatus and was focussed onto a small mirror next to the main lamp. This deflected the monitoring beam nearly axially through the pumping cell. The arrangement is shown in Fig.23b.

The purpose of using this lamp instead of the main lamp was two fold. Firstly, it was possible to measure the polarization with a He^4 lamp regardless of whether the sample had been pumped with a He^3 lamp or a He^4 lamp. Secondly, its intensity was so low that it did not materially affect the rate of decay of the sample. Its effect in this respect may be estimated by the following argument. If the pumping time with the little lamp is τ_P'', and that with the main lamp τ_P', then the initial polarization will be P', where

$$P' = \frac{\tau_R}{\tau_R + \tau_P''} \qquad \text{(68, p. 4.8)}$$

Similarly, the equilibrium polarization with the little lamp is P" where

$$P'' = \frac{\tau_R}{\tau_R + \tau_P''} \qquad \text{(68, p. 4.8)}$$

During this decay, with the little lamp on, the polarization decays from P' to P", with time constant T" where

$$\frac{1}{T''} = \frac{1}{T_1} + \frac{n}{N}\left(\frac{1}{\tau''_P} + \frac{2}{\tau_R}\right) \qquad (69, \text{p. } 4.8)$$

In the experiments P' $\sim$ 5% and P" $\sim$ ¼%. Therefore

$$\frac{1}{\tau_R} \gg \frac{1}{\tau'_P} \gg \frac{1}{\tau''_P}$$

and $$\frac{1}{T''} \simeq \frac{1}{T_1} + \frac{n}{N}\frac{2}{\tau_R} = \frac{1}{T}$$

Thus if P is large enough to be measured and subtracted from each point of the decay curve, the error in T due to τ''_P is about ¼% which is much less than the experimental error. The maximum error which could be caused by ignoring P completely is about 5% which is barely significant.

The time T measured by the method outlined above was the relaxation time of the ground state with the discharge on. Measurements were not possible with the discharge off, but it was found feasible to switch off the main lamp and discharge together, and then at some subsequent time to switch the discharge on again. Then after a short delay the remaining polarization could be measured with the little lamp, as before. The time so measured was usually about two minutes. The delay between striking the discharge (with a Tesla coil) and making the measurement(about 2 secs.) was also measured, and allowed for if necessary by using the decay time with the discharge on, as measured above. This was not usually necessary if a weak discharge was used.

(e) Nutation

Application of a pulse of r.f. at the ground state resonance frequency gave rise to nutation of the nuclei at a frequency γH_1. Nutation frequencies of up to 2.5 K/c were observed, and the damping of the nutation had a time constant of about a tenth of a second. It was therefore necessary to synchronize the sweep of the oscilloscope with the r.f. pulse. This was achieved by using the delayed sweep facility of the Tektronix 545 oscilloscope. The sweep of time base 'B' was initiated by hand, and after a certain delay, this triggered time base 'A'. A 25V positive gate derived from time base 'A' was amplified to 100V, and used to gate a Dawe audio power oscillator, which supplied the power for nuclear resonance. Adjustment to exact resonance was made by observation of the shape of the nutation signal. Just off resonance the nutation was superimposed upon an exponential, with time constant approximately T_2. The amplitude of this exponential relative to that of the nutation is approximately $\left(\frac{\omega - \omega_0}{\omega_1^2}\right)^2$ providing $T_1 >> T_2$ (Eqn. 98 p.4.18). Therefore, by adjusting the r.f. frequency until no exponential was visible in the signal, it was possible to ensure that the resonance condition was approached as closely as required by the condition given in eq. (97) p.4.18 i.e. $(\omega - \omega_0)^2 \ll \omega_1^2$

(ii) Determination of Metastable Density

For the interpretation of the various relaxation times

measured, it was important to know the density of metastable atoms in the discharge. A direct measurement of this was made, using the Fabry-Perot spectrograph described on p. 3.12 . A bright He^3 lamp was used as the source, and a 1 mm. He^3 cell interposed between lamp and etalon. A trace was obtained of the lamp profile. This was Doppler broadened, and to some extent self-absorbed. A second trace was then obtained with the weak discharge excited in the cell. The effect of the layer of metastable atoms so created was to absorb radiation from the lamp and re-emit it in all directions. Since the cell was not at the focal point of the collecting lens, the fraction of light re-emitted in the forward direction was not focussed upon the spectrograph pin-hole, and had negligible effect.

From the two traces obtained it was possible to deduce the absorption coefficient as a function of the optical frequency, and hence (knowing the oscillator strength, f) the total number of absorbing atoms in the path of the light could be calculated. It was necessary to know the path length, which was not constant over a spherical cell, but by restricting the aperture to about a quarter of the diameter of the cell, a reasonable measurement could be made. A number of different measurements was made for different settings of the discharge intensity.

(iii) Items of Equipment

(a) Switching Arrangements

The lamp could be switched on and off by utilising the "keying" facilities of the transmitter. A remote switch operated a relay in the transmitter. When this was actuated, the screen grids of the output valve were earthed, thus biassing off the power amplifier.

The discharge was switched off by temporarily interrupting the H.T. supply of the discharge oscillator. This was also achieved by a remote switch. The discharge was not usually self-starting, so a probe connected to a Tesla coil was arranged near the cell. The discharge could then be struck at the required moment by a short burst of high voltage r.f. from the coil.

(b) Pulsing the R.F.

Pulsing the r.f. for electron resonance was achieved using the r.f. power amplifier described in p. 2.17. The lower nuclear frequencies were obtained from a Dawe audio oscillator and this was adapted to be pulsed directly. The grid circuit of the power amplifier could be interrupted between earth and the grid leak resistors. Injection of a 100 v. negative pulse at this point was sufficient to drive the output values beyond cut off.

(c) Pulse Amplifier

As described above, the r.f. power was pulsed using a

"gate" outputs from the oscilloscope. These were only 25V in amplitude so a simple pulse amplifier was built, to give 100V output. Its circuit is shown in fig. 24.

(d) D.C. Detection Circuit

Measurements of transients with time constants of several seconds required D.C. coupling throughout the detection circuit. In order to avoid overloading the high gain D.C. pre-amplifier of the oscilloscope, it was necessary to "back-off" the H.T. voltage applied to the detector. This was achieved with the simple circuit in Fig. 25. Also included in this unit were condensers for limiting the bandwidth of the system when necessary.

CHAPTER SIX

RESULTS AND DISCUSSION

Introduction

Time did not permit the measurement of all the numerous parameters of a number of cells filled to different pressures and with different discharge intensities. Accordingly a 1 mm. Hg. wall-coated cell, with its getter housed in a separate compartment, was selected and fairly complete measurements made on this. Where measurements were made with other cells and these gave significantly different results, these are also reported.

(i) Density of Metastable Atoms

An example of the traces obtained by the method described on p. 5.6 is shown in Fig. 26. The lower trace has been displaced downwards for clarity.

Assuming that the absorption is of the form:-

$$I = I_o \exp(-K_\nu x)$$

then

$$K_\nu = \frac{1}{x} \log \frac{I_o}{I} \qquad (101)$$

Using this formula the absorption coefficient was calculated, as a function of $\tilde{\nu}$, the reciprocal wave length, from measurements made on the traces. But

$$\int_0^\infty K_{\tilde{\nu}}\, d\tilde{\nu} = \frac{\pi e^2}{mc^2} nf \qquad \text{(Ref. 18)} \qquad (102)$$

where n is the density of the absorbing atoms, and f is the oscillator strength of the transition. Hence by graphical

integration n can be calculated. It is necessary to assume a value for 'f'. Ref. 19 gives .58 as the value of the absorption oscillator strength for the $^3S_1 - {}^3P_{0,1,2}$ transitions. From each trace it was possible to make two measurements of n, by taking the D_0 and D_3 components separately. The relative f-values of these were taken to be 1/9 and 8/9 respectively, from a consideration of their statistical weights.

There was found to be a large discrepancy (a factor of 2.5) in the values obtained from the two lines. The reason for this was that the width of the emission line was very little wider than that of the absorption line. Consequently the absorption coefficients obtained from the wings of the narrow D_0 lines were exaggerated. On the other hand the absorption in the D_3 line was rather strong, and it was feared that the instrumental width may have masked the depth of the trough in the centre.

As a check, a trace was obtained in a similar manner to the above but with a He^4 lamp as the source, Fig. 27a. One of the hyperfine components of the D_0 He^3 line was absorbent to the D_3 He^4 emission line, and in this case the width of the latter greatly exceeded that of the former, so that an accurate plot of the absorption profile could be obtained. This is shown in Fig. 27b. The Doppler width in He^3 at 290^oK is .065 cm^{-1} while the instrumental width was about

.03 cm^{-1}. The result of 'folding' these together is to give an expected width of .085 cm^{-1} which is very close to the observed width of .08 cm^{-1}. This curve was therefore integrated to give the absolute density of metastable atoms, at a particular setting of the discharge. It had been noted from the accurate points in the centre of the D_0 lines previously obtained that the intensity ratio of the two hyperfine components of this line was close to the theoretical ratio predicted by Fred at al. in ref. 1 . Accordingly, this ratio (19:15, Fig. 22a) was used to give the f-value of the measured component. Having obtained an absolute value for n, relative values of n were obtained from the absorption coefficients at the centres of the D_0 lines in the original traces.

It was assumed in the calculation of the Doppler width that the effective Doppler temperature in the discharge was the same as room temperature. This is justified, since experiments have shown that the life time of the metastable atoms is about 10^{-4} secs while the collision time is about 10^{-7} secs. Furthermore the natural width and the width due to resonance broadening caused by metastability exchange (each about $3 \times 10^{-5} cm^{-1}$) are both negligible compared with the Doppler width.

The density of metastable atoms in a 1 mm. Hg. cell was found to vary between 12.5 and 3.5×10^{10}/c.c. depending upon

the discharge setting. These figures correspond to ratios of 2.3 and 1 x 10^6 between the populations of ground and metastable levels ($\frac{N}{n}$).

It is rather difficult to estimate the accuracy of these measurements. The observed quantity is an average density over an ill-defined path length in a spherical cell. Apart from this, the agreement between the expected and observed line widths and intensity ratios is evidence of a fair degree of accuracy in the measurements. All things considered it is thought that the absolute, and relative, densities are correct to within 25% and 10% respectively.

(ii) Observations of Resonances in the Metastable Levels, using Field Modulation

(a) Signals obtained using He^3 Lamp

Fig. 28 is a signal obtained using a .1 mm. Hg. cell, and a 1.5 mm. Hg. He^3 lamp. The signals are in fact inverted under these circumstances, i.e. there is an increase in transmission at resonance. The explanation of this is similar to that given for the inversion of He^4 resonances on p. 1.17.

The radiofrequency was 1 Mc./sec., and the amplitude of the field modulation was about ½ gauss, centered at zero field. The resonances at 1.9 and 3.8 Mcs./G. can be seen clearly. Calculation of the ratio of the amplitudes of these signals has not been attempted. It would be a

complicated function of all the transition probabilities of Fig. 22 and also the relative intensities of all the spectral components of the pumping light. It would also be necessary to take into account the interaction between the metastable and ground levels.

(b) Signals obtained using He^4 Lamp

It is possible to predict the relative amplitude of the two resonances when the exciting lamp is filled with He^4. In this case atoms in the $F = 3/2$ level only are absorbent and affect the signal. Resonance in the $F = 1/2$ level gives rise to a signal in the following way. As soon as the $F = 1/2$ level is depolarised by the r.f., metastability exchanges take place. The rate equations 73 on p.4.13 show that 8/27 of such exchanges result in the excitation of ground state atoms to the $F = 3/2$ level. This is a very rapid process, and takes place in a time (10^{-5} secs.) short compared with the time taken to modulate the magnetic field through the signal (10^{-3} secs). Thus it is possible to see a signal in the $F = 1/2$ level despite the fact that there is insufficient time during the transit of the resonance for the depolarised $F = 1/2$ level to depolarise the ground-state (and hence the $F = 3/2$ metastable state).

The signal in the $F = 1/2$ level may now be estimated. Provided the r.f. transitions are not saturated the ratio of the signals in the $F = 1/2$ and $F = 3/2$ levels is expected to be

$$\frac{8}{27} \cdot \frac{\alpha}{\alpha^2 + 1} \simeq \frac{4}{27}$$ for small polarisation.

The second factor accounts for the relative number of atoms in the two metastable levels (p.42 eq. 74)

This result is not inconsistent with the observed ratio, as can be seen in Fig. 29, which is a photograph of the signals obtained under the same conditions as Fig. 28 except that a He^4 lamp was used.

If the modulation frequency or amplitude was decreased unduly the signal was reduced because of the depolarisation of the ground state as described on p. 5.1

Signals obtained with He^4 lamps were not inverted. Since the He^4 D_3 line only is absorbed signal inversion cannot take place.

(c) Line Widths

The signals obtained as described above are much broader than He^4 signals. This is because the phase lifetime of the metastable atoms is determined by the frequency of the metastability exchange processes.

The width of the F = 3/2 resonance in Fig. 28 is .15 Mc/sec. This is accounted for by r.f. broadening since the H_1 was of such a value that nearly maximum signal amplitude was obtained. (H_1 was measured as 25 mG., which is equivalent to a line width of about .1 Mc/sec.) A more accurate measurement of the limiting line width using a phase sensitive detector and chart recorder (as described on p. 3.5) yielded the value .078 Mc/sec.

for the line width between points of inflection. If we assume a Lorentzian line shape, this corresponds to a line width at half height of .135 ± .02 Mc/sec. This is equivalent to a lifetime of about 2.36 ± .6 $.10^{-6}$ secs. This may be compared to the collision time of the ground state He^3 atoms which is about 1.4 $.10^{-6}$ secs.

Fig. 30 was obtained under identical conditions as Fig. 29 except that a .33 mm. Hg. cell was used. The r.f. power was the same but the signals were much broader. This is to be expected as the lifetime of the metastable atoms is much shorter.

(d) Alignment

Very weak signals were observed when unpolarised light was used to pump the sample. These were attributed to alignment in the F = 3/2 metastable level, by a process similar to that in He^4. No signals were observed under these conditions in the F = 1/2 metastable state, as was to be expected, since alignment has no meaning for a state of spin 1/2.

(iii) Pumping transient

Observations were made of the pumping transient, after a short burst of r.f. had depolarised the sample. This method suffered from the fact that the noise output of the lamp was rather high in the frequency range 0-10 c/sec. Fig. 31 shows a signal obtained when the sample was depolarised by resonance in the ground state. A smoothing condenser was used in the

detection circuit (time constant ~ .1 sec.) in order to eliminate high frequency noise. This also had the effect of eliminating the nutation which would otherwise have been visible immediately after the initial depolarisation. Similar traces were obtained for resonance in the $F = 3/2$ metastable level, but without of course the nutation.

Three photographs of the pumping transient, taken under identical conditions, yielded the following results:-

8.4 secs. 7.6 secs. 8.8 secs.

These indicated the reliability of the method. Times greater than about 8 secs. were measured, point by point, as described on p. 5.3 .

The length of the pumping transient, T, varied greatly with discharge intensity. Values of T between 32 secs. and 3.3 secs. were measured with the 1 mm. Hg. cell. The former time corresponds to the weakest possible discharge.

(iv) Longitudinal Relaxation Time

Measurements of T_1 were made by observing the relaxation of the sample with the discharge and pumping light off. The method is described on p. 5.3 . This was a reasonably accurate and repeatable measurement, since it did not depend upon the brightness of the lamp nor the discharge setting. For the 1 mm. Hg. cell, two measurements of T_1 made with an interval of three months between them gave values:-

165 ± 10 secs. 158 ± 5 secs.

Relaxation with the discharge on was much faster, and times between 4 and 30 secs. were recorded. A semi-log plot of a typical decay is shown in Fig. 32. It has been corrected for P", as described on p. 5.5 .

(v) Origin of Longitudinal Relaxation

Whilst the discharge is on, the metastable atoms provide the major source of relaxation. Relaxation of metastable atoms is discussed on p. 3.9 .

No exhaustive investigation was conducted into the causes of relaxation when the discharge was off. However, to investigate the effect of the walls, two cells were constructed, filled to a pressure of 1.05 mm. Hg. and identical in all respects except that one cell was coated with Dri-film, as described on p. 2.6 . T_1 was measured for these two cells, with the results:-

Wall-coated cell	105 ± 10 secs.
Non-Wall-coated cell	82 ± 10 secs.

There appears to be a small improvement for the wall coated cell, although more measurements would be required to establish this. However this measurement shows that there is not a tremendous advantage to be gained by coating the walls of the cell.

Both the times quoted above are longer than the results for the 1 mm. Hg. cell quoted on p. 6.8 . The major difference between this cell and the other two was that the former had a

separate, re-entrant compartment to house the getter. This communicated with the cell via a capilliary ½ mm. wide and 1 cm. long. The getters of the other two cells were flashed at the end of the flask necks, which were about 7 cm. long and 1.8 cm. in diameter.

A rough calculation predicts the effect of the getter. We assume that all atoms diffusing to the end of the neck are completely depolarised. The opening into the neck is about 1/40 of the total surface area of the flask. Using a value of 800 $cm^2/sec.$ (estimated from kinetic theory) for the coefficient of self diffusion of He^3 at a pressure of 1 mm. Hg. we can calculate the characteristic diffusion time for a sphere of radius 10 cm. (the distance from the centre of the flask to the end of the neck.) From eq. 45, p. 1.19, this is evaluated as 1.2×10^{-2} secs. This must be multiplied by 40 giving a time of about ½ sec.

Clearly then the Barium film is an inefficient relaxation agent since the observed relaxation time is about 100 secs. However this calculation has shown that the getter could easily account for the difference in the relaxation times in the two types of cell.

(vi) Measurements of Polarisation

(a) Conditions for maximum polarisation

The polarisation of the samples was measured as described on p. 5.3 . It was invariably found that the highest

polarisation was achieved for the weakest possible discharge. This is understandable since:-

$$P = \frac{\tau_R}{\tau_P + \tau_R} \qquad (68 \text{ p. } 4.8)$$

and experiments on He^4 have shown that τ_R decreases with more intense discharges. Maximum polarisations of between 3% and 2½% were achieved in cells varying in pressure between .1 and 1 mm. Hg., using a 2 mm. Hg. lamp. At higher pressures the maximum polarisation was less, falling to 1.2% in a 2.4 mm. Hg. cell.

In Fig. 33 the polarisation achieved in the 1 mm. Hg. cell is plotted as a function of metastable density. From eq. 68 we see that if P is small (i.e. $\tau_P \gg \tau_R$) then $P \propto \tau_R$ so that relative values of τ_R (103) may be obtained from this graph.

(b) Relative merits of He^3 and He^4 lamps

Some experiments were performed with the He^4 lamp monitoring beam described on p. 5.4 , in order to determine the relative merits of He^3 and He^4 lamps, in pumping He^3. He^4 was found to be superior in all cells tested which were filled at .33 mm. Hg. and above. As an example, the polarisations produced in a .33 mm. Hg. cell were 1% and 2.3% using similar He^3 and He^4 lamps, respectively. The disparity was much greater for higher pressure lamps, and accordingly He^4 lamps were almost universally used in the experiments.

With a .1 mm. Hg. cell, He^4 and He^3 lamps gave about the same size signals, but the polarisation due to the latter was slightly higher.

There are two reasons for the superiority of He^4 lamps. The first arises as a result of the mixing processes which take place in the P states, and is dealt with on p. 4.4 . The other reason is that, as was shown on p. 6.2 , the sample is optically fairly dense to He^3 D_3 light. Consequently a certain amount of multiple scattering takes place, and since the scattered light is unpolarised it acts as a relaxation process. The first effect decreases with gas pressure, the second with metastable density. Consequently it is only for the lowest pressure cells that He^3 lamps are superior.

(vii) Correlation of results

(a) Effect of Metastable Density on Ground State Relaxation

The pumping transient and the decay of polarisation with the discharge are both governed by the relation:-

$$\frac{1}{T} = \frac{1}{T_1} + \frac{n}{N}\left(\frac{2}{\tau_R} + \frac{1}{\tau_P}\right) \qquad (69.\ p.4.8)$$

In the latter case $1/\tau_P = 0$ since the lamp is off. In either case, for small polarisation $\tau_P \gg \tau_R$. Therefore:-

$$\frac{1}{T} - \frac{1}{T_1} \simeq \frac{2n}{N\tau_R} \qquad (104)$$

and substituting the relation (103) in (104) we have

$$\frac{1}{T} - \frac{1}{T_1} \propto \frac{n}{P} \qquad (105)$$

Fig. 34 is a plot of 1/T v. n/P. The point at n/P = 0 is that obtained with the discharge off. The next two points were obtained from point by point measurements of the pumping transient. The rest were obtained from the decay of polarisation with the discharge on. The points lie approximately on a straight line with a small positive intercept of the 1/T axis, thus demonstrating the validity of eq. 69 in the range of metastable densities tested.

There is some evidence of divergence at the higher metastable densities in Fig. 34. The reason for this is thought to be connected with the discharge products. It was noticed that at high discharge intensities an increase in the apparent brightness of the discharge produced little increase in metastable density. As an example, the two points in the graph in Fig. 34 for 1/T = .167 and .25 correspond to metastable densities 1.12 and 1.24 x 10^{11}/c.c. i.e. a 10% difference. On the other hand, there was a 30% difference in discharge intensity. The latter quantity was determined by measuring the intensity of the light emitted by the discharge. At lower discharge settings the discharge brightness was roughly proportional to the metastable density. It is therefore suggested that at higher discharge intensities the discharge products contribute directly to the ground-state relaxation by collision processes, without the agency of the metastable atoms. This could account for the

shortened relaxation times observed to the right in Fig. 34.

(b) Comparison with He^4

It is of interest to compare the relaxation time of the metastable atoms in He^3 and He^4. We can do this through the relation given in eq. 69. We make use of the measurements of τ_R made on He^4 with a cell filled to the same pressure as the 1 mm. Hg. cell. At the same setting of the discharge which in He^3 gave a metastable density of 9.2×10^{10}/c.c. τ_R in He^4 was found to be 1.3×10^{-4} secs. With $T_1 = 160$ secs. (and $\tau_p = \infty$) eq. 69 gives 22 secs. as the value of T. The measured value of T at this discharge setting, was found to be 14 secs.

The theoretical prediction is in reasonable agreement with experiment, bearing in mind the assumptions made regarding the similarity of the discharges in the two cells. The agreement also depends upon the assumptions made in the derivation of eq. 69 concerning the creation and destruction of the metastable atoms in He^3. Excitation is largely by ionisation, with subsequent recombination and decay, or by the creation of excited atoms which also decay to the metastable level. Some collision processes may excite metastable atoms directly. In any case the nuclear polarisation which was present in the ground state is almost completely lost as a result of these radiative and collision processes, and all the metastable states are populated with

equal probability. The metastable atoms then become polarised by exchange collisions with the ground state atoms. Subsequent decay of these atoms to the ground level is again by a number of different routes, but the probability is that the nuclear polarisation is again lost. Thus the metastable atoms are doubly effective in relaxation since polarisation is lost both at their excitation and at their destruction. This accounts for the factor 2 in the last term of eq. 69.

(viii) Measurements of the Transverse Relaxation Time

(a) Measurements with the discharge on

Nutation of the ground state atoms in He^3 was observed by the method described on p. 5.6 . For an accurate measurement of θ three conditions were to be satisfied. (p. 4.18).

The inhomogeneity ΔH_o of the static field was to be such that:-

$$\Delta H_o \ll H_1 \qquad (100 \text{ p. } 4.19)$$

The inhomogeneity of the rotating field H_1 was to satisfy the condition:-

$$\Delta H_1 \ll \frac{\pi}{\gamma^2 H_1 \theta} \qquad (99 \text{ p. } 4.19)$$

Exact resonance was to be achieved within the limit:-

$$(\omega - \omega_o)^2 \ll (\gamma H_1)^2 \qquad (97 \text{ p. } 4.18)$$

The first condition was always satisfied for all values of H_1 which were large enough to give rise to several cycles of nutation within the time θ. The second condition was

checked by photographing a number of transients with different values of H_1. It was found that with the r.f. coils used hitherto (~ 10 cm. diam.) H_1 was insufficiently homogeneous. An increase of H_1 by a factor 3 reduced the length of the transient by a similar factor.

Larger coils of diameter 24 cm. were substituted, and a marked improvement was found. To estimate the effect of ΔH_1 a graph of ω_1 v. θ was plotted (Fig. 35). It can be seen that θ decreased as ω_1 increased. When $\omega_1/2 = 700$ c/s, θ was 2/3 of its extrapolated value at $\omega_1 = 0$. In the measurements H_1 was such that $\omega_1/2\pi \sim 100$ c/s, at which frequency the reduction in θ was less than 10%. The third condition was satisfied by observing the shape of the signal as described on p. 5.6 . Fig. 36a shows an off-resonance signal. The exponential base line can be clearly seen.

Two photographs of the nutation, taken with two different values of H_1 are shown in Figs. 36b,c. The nutation frequency agreed well with the frequency predicted by calculation from the current through the coils. In practice the nutation frequency itself was measured in order to determine H_1.

The decay constant θ^{-1} was obtained graphically from the photographs by plotting the log of the nutation amplitude against time. An example is shown in Fig. 37. Since the Decay of the nutation is governed by eq. 92. It was pointed

out in the derivation of this equation that T_1 and T_2 must be modified according to the experimental conditions. In the experiments the pumping light and the discharge were both on. Eq. 92 therefore becomes:-

$\frac{2}{\theta} = \left[\frac{1}{T_2} + \frac{1}{T_2''}\right] + \frac{1}{T}$ and substituting eqs. 57 and 69:-

$$\frac{2}{\theta} = \left[\frac{1}{T_2} + \frac{n}{N\tau_2}\right] + \left[\frac{1}{T_1} + \frac{n}{N}\left(\frac{2}{\tau_R} + \frac{1}{\tau_P}\right)\right] \qquad (106)$$

However even for the strongest discharges and lamps, when T was about 3 secs., θ, being about .1 secs, was little affected by τ_R, τ_P or T_1. Accordingly, T_2'' the transverse relaxation time with the discharge on, is defined by:-

$$\frac{1}{T_2''} \simeq \frac{1}{T_2} + \frac{n}{N}\frac{1}{\tau_2} \qquad (107)$$

and hence, $T_2'' \simeq \frac{\theta}{2}$ (108)

A number of measurements were made using the 1 mm. Hg. cell with different discharge settings. It was found that T_2'' varied with, n, the metastable density, as expected in view of eq. 107. The maximum value of T_2'' measured, with the weakest self sustaining discharge, was .16 secs. Fig. 38 is a graph of $1/T_2''$ v. n, for the 1 mm. Hg. cell. It is approximately linear, and passes close to the origin, thus verifying eq. (107) and demonstrating that the major cause of the transverse relaxation is the metastability exchange process.

(b) Measurements with the discharge off

The accuracy of the points in Fig. 38 is not great enough to permit a good estimate of T_2, by extrapolation to n = 0, but a value of $\frac{1}{2}$ sec ($1/T_2 = 2$ secs^{-1}) appears to be the lower limit. A reliable measurement of this quantity was not achieved, but an attempt was made using the following sequence of operations:-

The sample was pumped to equilibrium polarisation.

The discharge was turned off.

The r.f. was turned on, at time t = 0.

The discharge was turned on and the initial amplitude of nutation observed, at time t = t'.

The amplitude of nutation was then plotted as a function of t, and the decay constant deduced. The method was very inaccurate since after switching on the discharge the measurements had to be made within a time short compared with T_2'', (.1 secs.). However some results were obtained which verified that T_2 was at least $\frac{1}{2}$ sec.

(ix) Metastability Exchange Cross-Section

The cross-section for metastability exchange can be estimated from the measurements of T_2'' and n. If we assume that the transverse relaxation is dominated by metastability exchange collisions, as the previous results indicate, then

$$\frac{1}{T_2''} = Q \, v \, n \qquad (109)$$

where Q is the metastability exchange cross-section, v is the mean relative velocity of the atoms and n is the density or the metastable atoms. Taking the point on the graph of n v. $1/T_2''$ (Fig. 28) where $n = 10^{11}$/cc., we find $1/T_2'' = 15.8 \pm 1.5$ $secs^{-1}$. v is given by

$$v = \left[\frac{16\ kT}{\pi\ M}\right]^{-\frac{1}{2}} \qquad (110)$$

$$= 2.0 \times 10^5 \text{ for } He^3 \text{ at } 290^\circ K$$

Using these values we obtain

$$Q = (7.9 \pm 2) \times 10^{-16} cm^2$$

The cross-section defined in eq. 109 is twice the cross-section for actual exchange of metastability. Half of all the inelastic collisions result in no exchange, but still contribute to the relaxation of the transverse magnetisation.

The accuracy of this result depends mainly upon the accuracy of 'h' and we have seen that this is probably about 25%. This is the error quoted.

On the other hand, the line width of the metastable resonances gave as the value of τ_2, $2.36 \pm .4 \times 10^{-6}$ secs. which implies a cross-section given by

$$\frac{1}{\tau_2} = Q\ v\ N \qquad (111)$$

For a .1 mm. Hg. cell, $N = 3.5 \times 10^{15}$, and hence

$$Q = 6.1 \pm 1 \times 10^{-16} cm^2$$

The error quoted here is that of the line width measurement. There is also an unknown error in N, since we had no

means of measuring the pressure in the cell after it had been sealed off. Adsorption of He by the walls of the cell, and by the getter would lower the pressure and result in an under-estimate of Q. The two estimates of Q agree within the experimental error.

These values may be compared with the classical collision cross-section, derived from viscosity data, and assuming hard sphere molecules. It is $1.4 \times 10^{-15} cm^2$. (Ref. 20).

(x) Multiple Quantum Transitions

Some observations were made of nuclear resonance signals, when the frequency of the applied r.f. field was at approximately one third of the resonance frequency, ω_o. These were observed in the same way as the nutation signals, and an example is shown in Fig. 39a. This was obtained with a field of 1.5 G. and an r.f. frequency of 1.6 kc/sec. For comparison, Fig. 39b shows a signal at the same field, H_o but with the fundamental frequency, ω_o. The r.f. field strength, .25G was adjusted to be the same in the two cases.

The frequency of nutation of the triple quantum signal varied markedly (a factor of two or three) with apparently the same experimental conditions. Sometimes there was a more rapid fluctuation superimposed upon the slower one.

Resonances were also observed at frequencies approximately equal to $\omega_o/5$ and $\omega_o/7$. No resonances were observed for even submultiples of the resonance frequency.

The signals are interpreted as being due to absorption of more than one quantum from the oscillating r.f. field. This may be considered as consisting of two oppositely rotating fields, and the absorption of, say, two σ^+ quanta and one σ^- quantum in a $\Delta m = 1$ transition conserves both angular momentum and energy if the frequency $\omega = \omega_0/3$. Similarly for higher odd multiple quantum transitions. For the observation of even multiple transitions it is necessary to have a π component of the oscillating field parallel to H_0 so that a quantum may be absorbed. It was ascertained that the wave-form of the applied r.f. was sinusoidal in these experiments. This was necessary since harmonic frequencies could excite single quantum transitions indistinguishable at first sight from the multiple quantum transitions described above.

(xi) Note on Errors

Most of the measurements of times and polarisations were subject to errors of about 10%, and these are the error flags shown on the graphs. The errors in the metastable densities are harder to assess. They depend upon two factors. The first is the accuracy of the original measurements, which has already been discussed. The second is that all the measurements were related to each other in terms of the discharge setting, as measured by the arbitrary scale reading of the discharge level control. Throughout the experiments the discharge arrangements were unchanged, so far as was

possible, nevertheless the electronic components and the pumping cell itself were subject to ageing. The scatter of the points in Figs. 34 and 38 probably represent the consistency with which the discharge could be re-set.

(xii) Summary

Longitudinal relaxation of the polarisation is dominated by relaxation of the metastable atoms, despite their small number, even with the weakest attainable discharge. Little improvement in polarisation is gained therefore by the use of wall coatings although there is some evidence that these increase the relaxation time with the discharge off. It would be profitable to reduce the number of metastable atoms so long as τ_R is increased by so doing, or until $N\tau_R/n > T_1$ whichever happens first. This is not practicable with a discharge, but electron bombardment could be used to create the metastable atoms, and this method would have the advantage of not creating the discharge products which hasten the relaxation of the metastable atoms. Substantially greater polarisations may be achievable in this way. The other obvious way to increase the polarisation is, of course, to use more powerful lamps. The limitation in this respect is that the greater the angular divergence of the light the less effective it is in polarising the sample. Geometrical considerations therefore limit the size and number of the lamps which can profitably be used. For the same reason

extremely strong converging lens do not necessarily improve matters.

Nevertheless the design of the apparatus was probably at fault in that more light could have been concentrated upon the sample, especially if a smaller cell had been used. At the time of its construction a large cell was thought to be an advantage, in that wall effects would be less important. It now appears that these are very small. Also the apparatus was used for other experiments, such as those described in part III of this thesis in which it was desirable to have a rather small divergence of the pumping light, so that the geometry of the apparatus was well defined.

Relaxation of the transverse magnetisation set up by a rotating field was also found to be dominated by the action of the metastable atoms. This fact was utilised in measuring the cross-section for metastability exchange. This was measured in two different ways, and reasonable agreement was found between them. By improving the experimental procedure much greater accuracy could be achieved, particularly in the case of the line width measurement. Some means would have to be devised to measure the pressure in the cell.

These experiments have shown that the theory developed in Chapter Four is substantially correct in describing the optical process in He^3 and its relation to optical pumping in He^4.

PART THREE

LIGHT MODULATION EFFECTS IN THE OPTICAL PUMPING OF He^4

Chapter Seven

Theoretical Considerations

(i) Introduction

The starting point of the investigation of light modulation effects in the optical pumping of He^4 was the work of Dodd and Series (ref. 7), Dodd, Series and Taylor (ref. 21) and Kibble and Series (ref. 22). In their experiments, Hg. vapour, situated in a magnetic field, was illuminated with light of such polarisation and direction as to excite selectively transitions to one or more of the Zeeman states of the 6^3P_1 level. fig. 40. A rotating magnetic field of suitable frequency (ω_o), applied to the vapour, coupled states of different orientation, so that the wave functions of the excited atoms became coherent superpositions of the unperturbed eigenfunctions. This coherence manifested itself in the fluorescent light, as intensity modulation at the frequency ω_o and its harmonics. It was suggested that the He^4 optical pumping system may provide an opportunity to study similar effects in absorption, that is, when the coherence is introduced between the states of a lower level involved in an optical transition. The modulation would then be expected to occur in the absorbed light, and observations were to be made upon the transmitted light as usual in He^4 optical pumping experiments. The details of the modulation would depend upon the direction and polarisation of the light used for pumping, and observation.

(ii) Modulation at $2\omega_o$

The simplest case to be considered is illustrated in fig. 41. Unpolarised light is incident upon the sample in the direction of the static magnetic field, H_o. This tends to produce an alignment, in which the $|1, \pm 1\rangle$ states are preferentially populated at the expense of the $|1,0\rangle$ state (p. 1.4). A rotating field at the resonance frequency is now applied, so that the states $|1, \pm 1\rangle$ and $|1, 0\rangle$ are coupled. Consider now the optical transitions shown in fig. 41. They correspond to σ^+ and σ^- transitions from the $M_J = \pm 1$ states and clearly there are frequency differences of $2\omega_o$ between pairs of them. Furthermore, by virtue of the rotating field, the absorbing atoms have wavefunctions which are coherent superpositions of $|1,1\rangle$ $|1,0\rangle$ $|1, -1\rangle$. The 'quanta' of light absorbed are therefore to be represented, not as photons of sharp frequency, but as coherent superpositions of such photons. The phase differences between these are determined by the experimental conditions, and are related to the phase of the r.f. perturbation. This implies complementary effects in the fraction of the unpolarised incident light which is not absorbed by the sample. Since the two components are circularly polarised with opposite directions of rotation, they are orthogonal, and interference can be observed only with the aid of a linear analyser.

The two circularly polarised components may be represented

by

$$\underline{E_+} = \underline{i}\, E_o \cos\left[k_+ z + (\omega_K + \omega_o)t\right] + \underline{j}\, E_o \sin\left[K_+ z + (\omega_K + \omega_o)t\right]$$

$$\underline{E_-} = \underline{i}\, E_o \cos\left[k_- z + (\omega_K - \omega_o)t\right] - \underline{j}\, E_o \sin\left[K_- z + (\omega_K - \omega_o)t\right] \qquad (112a,b)$$

where ω_K is the angular frequency of the optical radiation $(K_+ \approx K_-)$ and k is the reciprocal wavelength. The two components are separated in frequency by $2\omega_o$. Their orthogonality may be demonstrated by evaluating:-

$$\int_o^{2\pi/\omega_K} \underline{E_+} \cdot \underline{E_-}\, dt = \int_o^{2\pi/\omega_k} E_o^2 \cos 2(kz + \omega_K t)\, dt = 0 \qquad (113)$$

The intensity of the two components combined is given by

$$\underline{E_+}^2 + \underline{E_-}^2 = 2 \qquad (114)$$

i.e. there is no modulation.

The intensity of the two components after passing through a plane analyser, with its axis at an angle α with the X axis is :-

$$(\underline{E_+} + \underline{E_-}).(\underline{i}\cos\alpha + \underline{j}\sin\alpha)^2 = 4\cos^2(\omega_K t + Kz)(1+\cos(2\omega_o t - 2\alpha) \qquad (115)$$

The light is therefore intensity modulated with frequency $2\omega_o$. The phase of the modulation depends upon the orientation of the analyser with respect to the X axis, and of course upon the phase of the r.f. perturbation. The phase of the σ^+ and σ^- components have been arbitrarily set equal, at $z = t = 0$, with E vectors parallel to the X axis.

(iii) Theory of Dodd and Series

The simple physical picture described above is inadequate to give us any information about the line shape of the modulation signal, or about modulation at any other frequencies. The He^4 and Hg. experiments are sufficiently similar to enable us to adapt the theory developed in ref. 7 to describe a simplified version of the He^4 experiment. The simplification is to consider a single excited P state only, with J = 0. We regard the optical pumping process as a means of preferentially populating certain of the metastable levels, and ignore the fact that in He^4 this is essentially a two stage process, i.e. absorption followed by emission. In Hg. it is a one stage process, i.e. absorption only.

Under these conditions the two experiments are very similar except that the J = 1 level lies below the J = 0 level, and we consider absorption of light instead of the emission of fluorescent light.

(a) General Solution

The general solution for the emission of fluorescent light from a system of angular momentum J, under the action of simultaneous perturbations due to a rotating magnetic field, optical radiation, and natural damping is given in ref. 7 (eq. 32) as:-

$$I = I_0 \sum_{\substack{m\mu n \\ m'\mu'n'}} \mathcal{F}_{nn'} \langle m|\mu\rangle\langle\mu|n\rangle\langle n'|\mu'\rangle\langle\mu'|m'\rangle \, g_{nmm'} \frac{\Gamma}{\Gamma + ix} \exp\left[-i(m-m'-n+n')\omega_0 t\right] \qquad (116)$$

where m, μ, n m', μ', n', take the values J, J-1, ... -J

$1/\Gamma = \tau_n$ the natural lifetime of the states.

$$x = (\mu - \mu')\, p + (n - n')\omega_o \qquad p^2 = \delta^2 + b^2 \qquad (117a,b)$$

The notation is that of ref. 7.

In the Hg. experiment $\mathcal{F}_{nn'}$ and $\mathcal{G}_{mm'}$ are the excitation and emission matrices. They depend upon the polarisation and direction of the incident and observed light. In calculations on He^4 an $\mathcal{F}_{nn'}$ matrix is used which describes as nearly as possible the action of the pumping process in populating the metastable states. It is at this point that we ignore the fact that optical pumping is a two stage process. This approximation is equivalent to rejecting certain information, which if it could be included in the theory, would allow a complete description of all the modulation effects in He^4.

$\mathcal{G}_{mm'}$ is now taken to be an absorption matrix, and its elements depend upon the type of light used to detect the signal (usually the same as that used to pump the sample), and the type of analyser used. The elements of $\mathcal{F}_{nn'}$ and $\mathcal{G}_{mm'}$ obtained from ref. 7, for various polarisers and analysers in the case of light incident along the z axis, are given below. The angle α is defined in this case as the angle between the rotating field vector H_1 and the axis of the plane analyser, at time zero.

In the He^4 experiment, Γ is given by :-

$$\Gamma = 1/\tau = 1/\tau_R + 1/\tau_P$$

(b) Modulation Frequencies

The frequencies of modulation are given by the index of the exponential in eq. 116. Using the elements of $\mathcal{F}_{nn'}$ and $\mathcal{G}_{mm'}$ given in the table below we can at once determine the allowed frequencies. (These are subject to the remaining factors of eq. 116 being non-zero under these conditions.)

MATRIX ELEMENTS of $\mathcal{F}_{nn'}$ and $\mathcal{G}_{mm'}$

$$|P|\begin{pmatrix}1&0&0\\0&0&0\\0&0&1\end{pmatrix} \quad (a)$$

$$\tfrac{1}{2}|P|\begin{pmatrix}1&0&(\cos\alpha-i\sin\alpha)\\0&0&0\\(\cos\alpha+i\sin\alpha)&0&1\end{pmatrix} \quad (b)$$

$$|P|\begin{pmatrix}1&0&0\\0&0&0\\0&0&0\end{pmatrix} \quad (c)$$

INCIDENT LIGHT	ANALYSER	$\mathcal{F}_{nn'}$	$\mathcal{G}_{mm'}$	MODULATION
Unpolarised	None	a	a	None
Unpolarised	Linear	a	b	$2\omega_o$
Circularly Polarised	None	c	c	None
Circularly Polarised	Linear	c	b	$2\omega_o$
Linearly Polarised	None	b	b	$2\omega_o$, $4\omega_o$ (when $\omega_o \ll \Gamma$ see p. 7.9)

The terms of eq. 116 have been evaluated for the case of unpolarised light, and the unmodulated term only for the case of circularly polarised light.

(c) Unpolarised light

The expression for the transmitted light is:-

$$I = I_o \left[(1 - A) + D \cos 2(\omega_o t - \alpha) \right] \qquad (118)$$

where $$A = \frac{b^2(4\delta^2 + b^2 + \Gamma^2)}{(\delta^2 + b^2 + \Gamma^2)(4\delta^2 + 4b^2 + \Gamma^2)} \qquad (119)$$

and $$D = \frac{b^2(2\delta^2 - b^2 - \Gamma^2)}{(\delta^2 + b^2 + \Gamma^2)(4\delta^2 + 4b^2 + \Gamma^2)} \qquad (120)$$

The functions A and D are identical with those in ref. 7. A describes the line shape of the unmodulated signal. It is identical with the Brossel-Bitter "double-humped" line shape. A similar shape has already been predicted on p. 1.14 for the alignment signal in He^4. The function D describes the envelope of the modulation which is at a frequency $2\omega_o$. This function is plotted in fig. 46a. It is to be noted that with the particular geometry used in this experiment there is no "quadrature" signal - i.e. there is no term in $\sin 2\omega_o t$. The effect of rotating the analyser is to vary the phase of the modulation.

(d) Circularly polarised light

When circularly polarised light is used both to pump the sample and monitor the signal, with no analyser, the expression for the transmitted light is:

$$I = I_o \left[1 - A - \tfrac{1}{2}F \right] \qquad (121)$$

where F is given by

$$F = \frac{3b^4}{(\delta^2 + b^2 + \Gamma^2)(4\delta^2 + 4b^2 + \Gamma^2)} \qquad (122)$$

The experimental situation corresponds to over-population of the $|1, 1\rangle$ and $|1, 0\rangle$ states (unequally), at the expense of the $|1, -1\rangle$ state. The signal shape is a combination of the Brossel-Bitter, and the Lorentzian squared shapes, as was predicted on p. 1.16 from simple physical arguments.

The Lorentzian squared type of signal occurs alone when e.g. the populations of the $|1, 1\rangle$ and $|1, 0\rangle$ states are the same, and that of the $|1, -1\rangle$ state is depleted. Experimentally this would be achieved, in the simplified He^4 system, with a σ^+ beam directed along the z axis, and an equally intense plane polarised beam directed along the x axis, with E vector parallel to H_0. This situation is represented by the excitation matrix

$$\mathcal{F}_{nn'} = |P|^2 \begin{pmatrix} 1 & 0 & 0 \\ 0 & 1 & 0 \\ 0 & 0 & 0 \end{pmatrix} \qquad (123)$$

Under these circumstances (with no analyser) the light transmitted in the z direction is given by the expression

$$I = I_0(1 - \tfrac{1}{2}F) \qquad (124)$$

This is the justification for the use of the function F to describe the line shape obtained for a pure polarisation. In terms of the experimental parameters F is given by:-

$$F = \frac{3}{4} \frac{(\gamma H_1)^4}{\left[(\omega-\omega_0)^2 + (\gamma H_1)^2 + (\frac{1}{\tau})^2\right]\left[(\omega-\omega_0)^2 + (\gamma H_1)^2 + (\frac{1}{2\tau})^2\right]} \quad 7.9$$

(125)

(iv) Additional Effects

(a) Low Magnetic Fields

In the general expression for the intensity of the transmitted light (eq. 116) the factor $\frac{\Gamma}{\Gamma + ix}$ is very small, unless $n = n'$, or $\omega_0 \ll \Gamma$, or $x = 0$ (since $x = (n-n')\omega_0 + (\mu-\mu')p$). So far we have considered the first case only. At low magnetic fields, such that $\omega_0 \ll \Gamma$ new phenomena occur. These have been studied in Hg. by Kibble and Series (ref. 22). The calculation for He^4 indicated that under these circumstances modulation at a frequency $4\omega_0$ occurs, if the incident light is linearly polarised. The envelope of this function is described by the function F, as in the case of Hg. It is the same function which describes the line shape of the unmodulated signal in the case of a pure polarisation, and is plotted in fig. 47a.

The use of terms with $n \neq n'$ in this calculation requires justification. It implies the existence of metastable atoms in coherent superposition states, before the effect of the r.f. perturbation is felt. A possible mechanism for this occurs in the optical pumping cycle, which, as was pointed out above, has been over simplified in the present theory. In the experimental system atoms are excited from states which are already mixed by the r.f. perturbation, to excited states from which

they decay. It is possible that the original coherence may be carried over, so that on decay to the ground states, some coherence already exists, before the action of the r.f. perturbation. Attempts to calculate this effect rigorously, allowing for the excitation - decay - excitation processes have not been successful.

(b) Scattered Light

A further possibility for the creation of an additional degree of coherence lies in the process of multiple scattering. It has been shown that the He^4 sample may be fairly dense optically, so that a certain amount of multiple scattering will certainly occur. If as was suggested above, coherence can be remembered throughout a cycle of absorption and emission, then it is also likely that the emitted photons carry some information relating to this coherence, and this will be imparted to the metastable atoms upon re-absorption. The question of multiple scattering for the case of fluorescence, in Hg. has been discussed by Dodd, Series and Taylor in ref. 21. They concluded that the form of the resonances remained unchanged.

(c) Off-Axis Light

The effect of light not strictly parallel to the magnetic field is to introduce additional non-diagonal elements in the $\mathcal{F}_{nn'}$ and $\mathcal{G}_{mm'}$ matrices. The possibility then arises of modulation at ω_o and $3\omega_o$. In the latter case it is again

necessary to consider terms in which $n \neq n'$, as were discussed above. Calculations have not been made of modulation at these frequencies.

Chapter Eight

Experimental Details

Detection systems

The shortcomings of detectors sensitive to 10,830 Å radiation enumerated in Chapter Two proved to be a serious handicap to the investigation of light modulation in He^4. The modulation appears at the fundamental and harmonics of the radio-frequency, and the frequencies used hitherto had been in the range .5 - 2 Mcs./sec. Since the frequency response of our best detector, the Texas Instruments diodes type 1S701 (p.2.9) was limited to about 20 kcs./sec. we were obliged to use frequencies less than this in order to be able to observe the modulation signals. However the width of the zero field signals (p.2.4) was at least 15 kcs./sec. so that an oscillating r.f. field at a frequency less than 20 kcs/sec. gave rise to further signals, at $\pm H_o$ each of which overlapped this. Furthermore each of these were modulated and there was interference between them. To avoid this complication a rotating r.f. field was used. The frequency was usually .5, 1, or 10 kcs./sec.

To observe the signals the apparatus was set up as usual for optical pumping (p.2.1). A linear analyser could be inserted between the cell and the detector. The field H_o was not modulated.

(i) Phase Sensitive Detection

Whenever convenient phase sensitive detection was used since this method yielded the maximum amount of information about the signal. A reference signal was obtained from the rotating field generator, and if the fundamental frequency of modulation was to be observed, this was fed directly to the P.S.D. Otherwise harmonics of this frequency were generated, and one of these used as the reference signal. The P.S.D. was limited in frequency to 2 kcs./sec. so that for observation of modulation at an angular frequency of $4\omega_0$ it was necessary to use a rotating field with frequency .5 kcs./sec.

The field H_0 was swept slowly through the resonance, and the output of the P.S.D. recorded by a pen recorder on chart. By varying the phase of the reference signal, it was possible to make independent observations of the two signals in quadrature.

(ii) Non-Phase-Sensitive-Detection

When it was necessary to observe modulation at frequencies greater than 2 kcs./sec. the signals were either displayed directly upon an oscilloscope or else detected with a non-phase-sensitive detector and recorded upon chart as before. In either case, to separate the different harmonics, and to improve the signal to noise ratio, a narrow band tuned amplifier was used. It was not possible to separate signals

in quadrature by these methods. If the modulation was of the form $X \sin \omega t + Y \cos \omega t$, the envelope detected was $(X^2 + Y^2)^{\frac{1}{2}}$ In both cases the field was swept slowly through the resonance as before.

(iii) Detection of signals modulated at more than 20 kcs./sec.

It was necessary to use photocells for detection of high frequency modulation. There were two alternatives. One was to use the S-1 response photocell RCA 6570, described on p. 2.11. The other was to observe the modulation in the 3889 Å spectral line of He^4. For this purpose a Mullard 90 AV vacuum photocell was used, together with an interference filter to prevent all but the 3889 Å radiation from striking the cell. The 10830 Å radiation was effective in optically pumping the sample, as before.

To display modulation signals at higher frequencies two different methods were tried.

(a) A tuned amplifier and tuned phase sensitive detector for 465 kcs./sec. was borrowed. An oscillating r.f. field at 232.5 kcs/sec. was used and the necessary reference signal at 465 kcs./sec. generated by means of a tuned frequency doubler. Detection of modulation at a frequency $2\omega_0$ was attempted partly because this was expected to have the greatest amplitude but also because it was very difficult to prevent direct pick-up of r.f. radiation at 465 kcs./sec. from saturating the tuned amplifier. Even with this precaution

a large standing signal was caused by direct pick-up of the first harmonic.

(b) Another method used an adaption of an ex-W.D. i.f. strip and detector, tuned to 9.7 Mcs./sec. The RCA 6570 photocell was mounted directly upon the chassis in order to reduce losses of signal due to lead capacitance. One of the difficulties with this method lay in the provision of an adequate load for the photocell at such high frequencies. A tuned circuit was used but since the impedance of the photocell was several MΩs. there was severe mismatch, and loss of signal.

(iv) Items of Equipment

(a) Rotating Field

A rotating field may be achieved by the use of two orthogonal pairs of coils, fed with oscillating currents in quadrature. In early experiments the rotating field was created with the use of a passive net-work (Fig. 42a). However each network was limited in use to one frequency, and an improvement on this was to drive one channel direct from the audio oscillator and the other from a power amplifier incorporating a phase shifter. The amplitudes and phase of the two channels were set up for a particular frequency using a twin beam oscilloscope with identical amplifiers.

Finally a two phase oscillator with twin power amplifiers was built, to the circuit of fig. 42b. The two phase oscillator consists essentially of two phase shifters in

series. The potentiometers controlling the phase shift of these are ganged together. The output of the second phase shifter is amplified and fed back to the input of the first. At any setting of the control knobs there is a particular frequency for which the feed-back is positive, and the device oscillates. Thus the phase shift controls become the frequency control of the oscillator. The oscillating voltages at the points X and Y are in quadrature and signals from these points are amplified in conventional power amplifiers and fed to the orthogonal pairs of coils.

(b) Tuned Amplifiers

At frequencies of a few kcs./sec. 'LC' tuned amplifiers are extremely cumbersome owing to the large values of inductance and capacitance required in the tuned circuits. Sharply tuned amplifiers can be made with the use of a "twin T", an RC device, shown in fig. 43a. At an angular frequency given by $\omega = \frac{1}{RC}$ the network has zero impedance to a signal injected at A-B. This is only strictly true when there is an infinite load across C-D. To construct a tuned amplifier the 'twin T' is incorporated in a 100% negative feed-back loop of a high gain wide band amplifier. The only frequency to be amplified is therefore the frequency of the twin T, the amplification of all other frequencies being approximately unity. The circuit of the amplifier constructed is given in Fig. 43b.

The 'Q' of the amplifier could be increased still further (at the expense of stability) by a slight adjustment to one of the components of the twin T. By this means a gain of about 2000 and a band width of ~ 10 c/sec. was achieved, at a frequency of 2 kc/secs. With a twin T of frequency ω_o inserted in the amplifier, the discrimination against input signals at $\omega/2$ and $2\omega_o$, was as much as 1000:1 in favourable circumstances. A large number of twin T's was constructed, using components accurate to 1%. They were constructed on tag boards fitted with plugs for rapid interchange.

It is worth noting that when such an amplifier is used in front of a P.S.D. the frequency stability of the oscillator supplying the r.f. and reference must be good compared with the bandwidth of the amplifier. The reason for this is that the output signal from the amplifier undergoes a sharp 180° phase shift as the frequency of the signal is varied through the centre frequency of the amplifier (ref. 23).

(c) Detector

To obtain a D.C. voltage proportional to the amplitude of the modulation, a detector utilising semiconductor diodes was built with the circuit given in fig. 44. It has a conventional valve output stage suitable for driving a pen recorder.

(d) Harmonic Generator

In order to generate reference signals at multiples of the r.f. frequency, the first step was to produce a ramp wave-

form using the circuit of fig. 45. The Fourier analysis of such a wave-form is:-

$$\sin \omega t - \frac{\sin 2\omega t}{2} + \frac{\sin 3\omega t}{3} - \frac{\sin 4\omega t}{4} \ldots\ldots$$

The separate components of this wave-form were then selected by a narrow band "twin T" amplifier similar to that described above.

An ideal P.S.D. eliminates completely all signal frequencies not synchronous with the reference except for odd higher multiples and odd sub-multiples, of the reference frequency. These are attenuated. In the experiments, it was required to observe, say, a modulation frequency $4\omega_o$ in the presence of a larger signal at $2\omega_o$; It was therefore important that the reference signal contained no component at $2\omega_o$ in order that the full performance of the P.S.D. could be realised. It was rather difficult in practice to eliminate the lower frequencies completely when selecting the higher harmonics from the ramp wave-form, and there was often up to a total of 5% of all the other harmonics present. This was not the ultimate limit on the discrimination of the detector since in practice the reference signal was used to saturate the reference signal amplifier in the P.S.D., thus producing a square wave. The "on" to "off" time ratio of this was the important factor, and this could be adjusted to unity within

less than 5% by observation on an oscilloscope. The ultimate limit was set by the symmetry in action of the synchronous switch used in the detector, which the makers claim to be better than 4%.

Chapter Nine

Results and Discussion

Introduction

The results reported in this chapter are mostly qualitative, and constitute a preliminary survey of modulation effects in the optical pumping of He^4. The aim was to discover what effects could be observed under a variety of experimental arrangements. More quantitative investigations of particular features are at present in progress.

Except where stated otherwise the modulation experiments were performed with the apparatus set up as described in Chapter Two. Low pressure He^4 cells (.1 and .3 mm. Hg.) and He^4 lamps were used. The modulation was observed in the transmitted fraction of the pumping light, which was always incident in the direction of the static magnetic field. A rotating field was invariably used for r.f. frequencies below 100 kc./sec.

(i) High Frequency Modulation

Experiments to detect modulation at high frequencies ($\omega_o \gg \Gamma$) were not successful. This was due in part to the inefficiency of the photodetectors, and the other experimental difficulties mentioned in Chapter Eight. However these experiments were by no means exhaustive, since at this stage it was learnt, from the work on Hg. (ref. 22) that with the use of rotating r.f. fields, signals obtained at extremely low

magnetic fields (i.e. such that $\omega_o \ll \Gamma$) were similar to those obtained at higher frequencies. Since signals were much easier to obtain at the lower frequencies work was concentrated upon these.

(ii) Modulation at $2\omega_o$

Modulation at $2\omega_o$ was detected in signals observed with both the 10,830 Å line and the 3889 Å line. Fig. 46b shows a signal obtained using the 3889 Å line, and phase sensitive detection. Unpolarised light and a linear analyser were used. It was observed that the width of the signal was roughly proportional to the strength of the rotating field. The latter was measured in terms of the voltage applied to the rotating field coils. Variation of the phase of the reference signal produced a small asymmetry in the line which was interpreted as being due to an anti-symmetrical signal in quadrature with the main symmetrical signal. There was clearly a marked disparity in the amplitudes of the two signals and it was not found possible to eliminate the larger one sufficiently to observe the smaller one clearly. The theory of chapter Seven predicts no quadrature signal at all. It was found that rotation of the analyser through 2π gave rise to a phase change of 4π as predicted in eq. 118. Removal of the analyser reduced the size of the signal greatly, and eliminated the large central feature completely. The residual side humps may be attributable to a small oscillating component

of the r.f. due to imperfections in the rotating field system. These results are in accord with the theory. In particular the shape of the modulation envelope is very similar to the curve D, plotted in fig. 46a.

(iii) Modulation at $4\omega_0$

Fig. 47b is an example of the $4\omega_0$ modulation envelope obtained, using a linear polariser, but no analyser. A rotating field at 500 cs/sec. was used, and non-phase-sensitive detection. The signal was observed in the 10,830 Å spectral line. Γ equals about 10 kcs./sec. for the $^3S_1$ level of He^4, so the condition $\omega_0 \ll \Gamma$ given on p. 7.9 is fulfilled in this case. The signal may be compared with the theoretical curve F plotted in fig. 47a. There is an obvious similarity.

A signal of quite a different shape was obtained with no polariser but with a linear analyser. The example given in Fig. 47c was obtained under conditions otherwise the same as those above. The shape appears to be similar to the line shape for modulation at $2\omega_0$. A theoretical interpretation for modulation at $4\omega_0$ under these experimental conditions has not yet been found. Measurements of the relative amplitudes of the $2\omega_0$ and $4\omega_0$ signals were made (for both circular and unpolarised light) when a small stop was placed in front of the lamp, to reduce the angular deviation of the incident light. No significant variation was found. It therefore appears that neither of these signals depend for

their existence upon off-axis light.

The signals described above, obtained with circularly polarised light disappeared almost completely on removal of the linear analyser, but using the P.S.D. it was possible to observe weak signals under these conditions. These were remarkably sensitive to the adjustment of the earth's field compensation coils. When the compensation was deliberately misaligned signals such as that in fig. 48. were obtained.

(iv) Modulation at ω_o

As an example of the modulation at ω_o we include a recording (fig. 49) made with non-phase sensitive detection, of the envelope of modulation at 10 kcs./sec. Unpolarised light, and a linear analyser were used. The amplitude of the signal was smaller than that of the modulation at $2\omega_o$ and $4\omega_o$.

Strictly speaking there should be no asymmetry present in a curve obtained with non-phase sensitive detection, regardless of the symmetry of the components. The asymmetry present in the experimental curves may be explained by a phenomenon first noticed in the work on Hg. Direct pick-up of r.f. radiation endows the detectors with a degree of phase sensitivity. This can be understood with reference to Fig. 50. When there is a large standing signal due to direct pick-up, a small genuine signal in quadrature with this will have much less effect than one which is in phase.

That this was the origin of the asymmetry was ascertained by rotating the analyser through 90°. The asymmetry changed sign, since the phase of the signal was reversed with respect to the direct pick-up. This confirms that there is an asymmetrical component present in the modulation at ω_o.

(v) Modulation at $3\omega_o$

Modulation at $3\omega_o$ appeared to consist of two components in quadrature. In this case they were of approximately the same amplitude. Examples of the two components are given in Figs. 51a, b. They were obtained using the 10,830 Å line for observation, phase sensitive detection, a 500 cs./sec. rotating field, unpolarised light, and a linear analyser.

Some evidence was found that the $3\omega_o$ signal reduced in size, relative to the $2\omega_o$ signal, when the angular divergence of the incident light was reduced by placing a small stop in front of the lamp. However this did not appear to be the case with the signal modulated at ω_o. It was pointed out on p. 7.10 that a possible explanation for the occurrence of both $3\omega_o$ and ω_o modulation signals lay in the presence of off-axis light.

(vi) Cross-Beam Modulation

Some experiments were performed with the apparatus set up so as to produce alignment, but with an independent unpolarised monitor beam in the x direction. Modulation was observed at the frequencies ω_o, $2\omega_o$, and $4\omega_o$. Figs. 52,a,b

show two signals in quadrature obtained at the fundamental frequency, which was 1 kc./sec. in this case. No analyser was used. Modulation has been observed under similar experimental conditions in the optical pumping of sodium, by Bell and Bloom (ref. 24). They interpreted their results phenomenologically using equations similar to the Bloch equations. Schearer (ref. 25) observed an x-beam modulation signal, at 1.4 Mcs./sec. in He^4 obtained a double rather than a triple peaked signal.

A similar experiment was performed with no x-beam, so that the scattered light alone was observed. This yielded somewhat different signals, shown in Figs. 53. The signal in quadrature with the main signal is clearly asymmetric, of the dispersion type. No attempt has been made so far to account for these signals in terms of the theory of ref. 7.

(vii) Summary

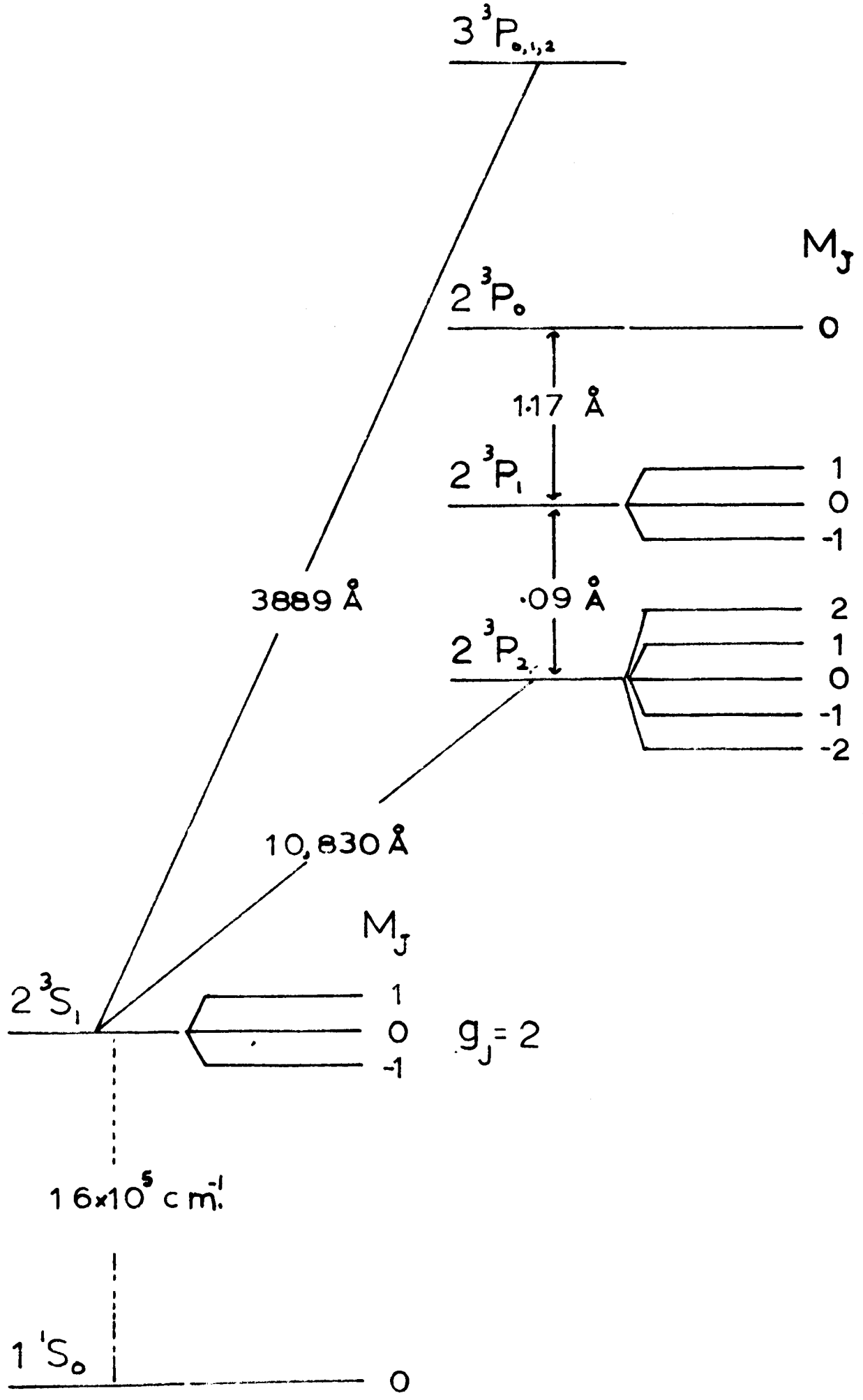
A chart showing the experimental conditions under which modulation signals have been observed, to date, is given below. Many of the observations were made visually, with an oscilloscope and no record was made of line shapes.

Beam		Wavelength of Observation	Polariser	Analyser	Rotating Field Frequency	Modulation Frequencies			
Pumping	Observation					ω_o	$2\omega_o$	$3\omega_o$	$4\omega_o$
Z	Z	10830 Å	-	Lin.	500 c/s 10 kc/s	x x	x x	x x	x x
Z	Z	3889 Å	-	Lin.	500 c/s	x	x	x	x
Z	Z	10830 Å	Circ.	Lin.	500 c/s		x		x
Z	Z	10830 Å	Lin.	-	500 c/s				x
Z	X	10830 Å	-	-	1 kc/s	x	x		x
Z	X Fluorescence	10830 Å	-	-	1 kc/s	x	x		

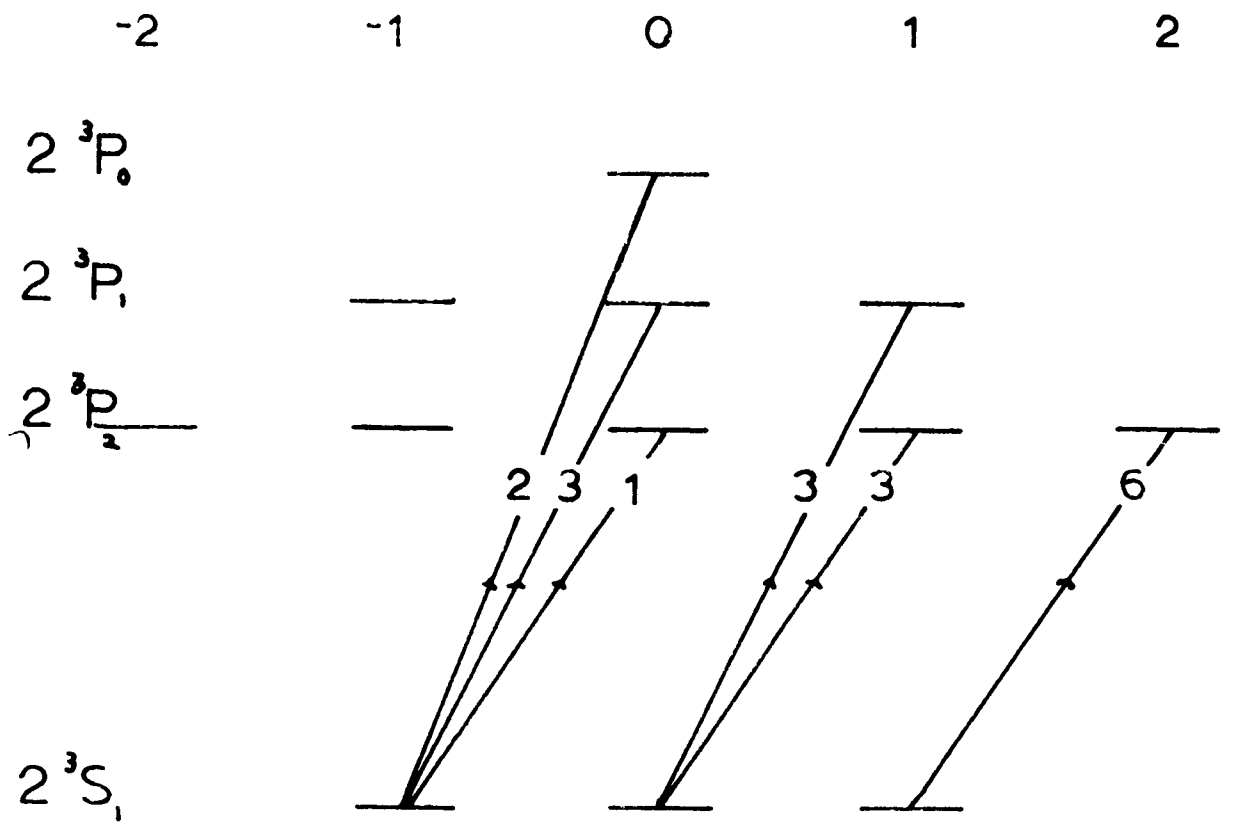
The theory developed in Chapter Seven is reasonably successful in describing the situations to which it is applicable. However the chief conclusion to be drawn from these preliminary experiments is that the modulation phenomena are so complex that some simplifying measures are required. It is true that the experiments upon Hg. indicated that the phenomena observed at low magnetic fields ($\omega_0 \ll \Gamma$) were similar to those at higher frequencies, providing that a rotating r.f. field was used to avoid the interference of a counter rotating component. Nevertheless new phenomena are also observed, and in any case the rotating fields used are by no means perfect, so that a small anti-resonance component is always present to confuse the observations.

A much simpler situation from the point of view of theoretical interpretation would be obtained by working at higher magnetic fields. Under these circumstances there would be little effect from an anti-resonant component of the r.f. perturbation. More important than this, effects present only when $\omega_0 \ll \Gamma$ would disappear. This requires a frequency $\omega_0 \sim 100$ kcs./sec.

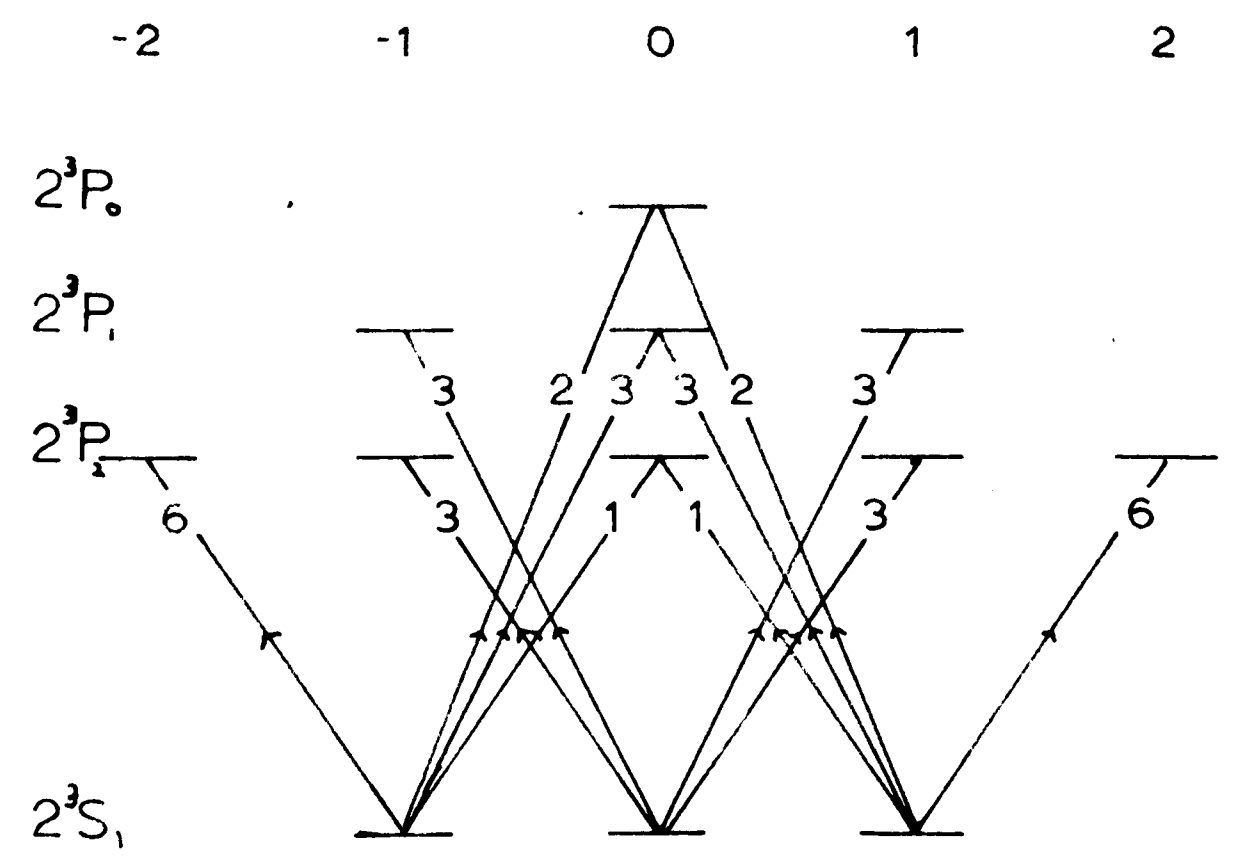
In addition to this, it is thought that the coherence effects due to the two stage optical pumping process would disappear as ω_0 becomes greater than the width of the excited (^3P) energy levels. This condition requires a frequency $\omega_0 \sim 10$ Mcs./sec.



1 HE^4 TERM DIAGRAM

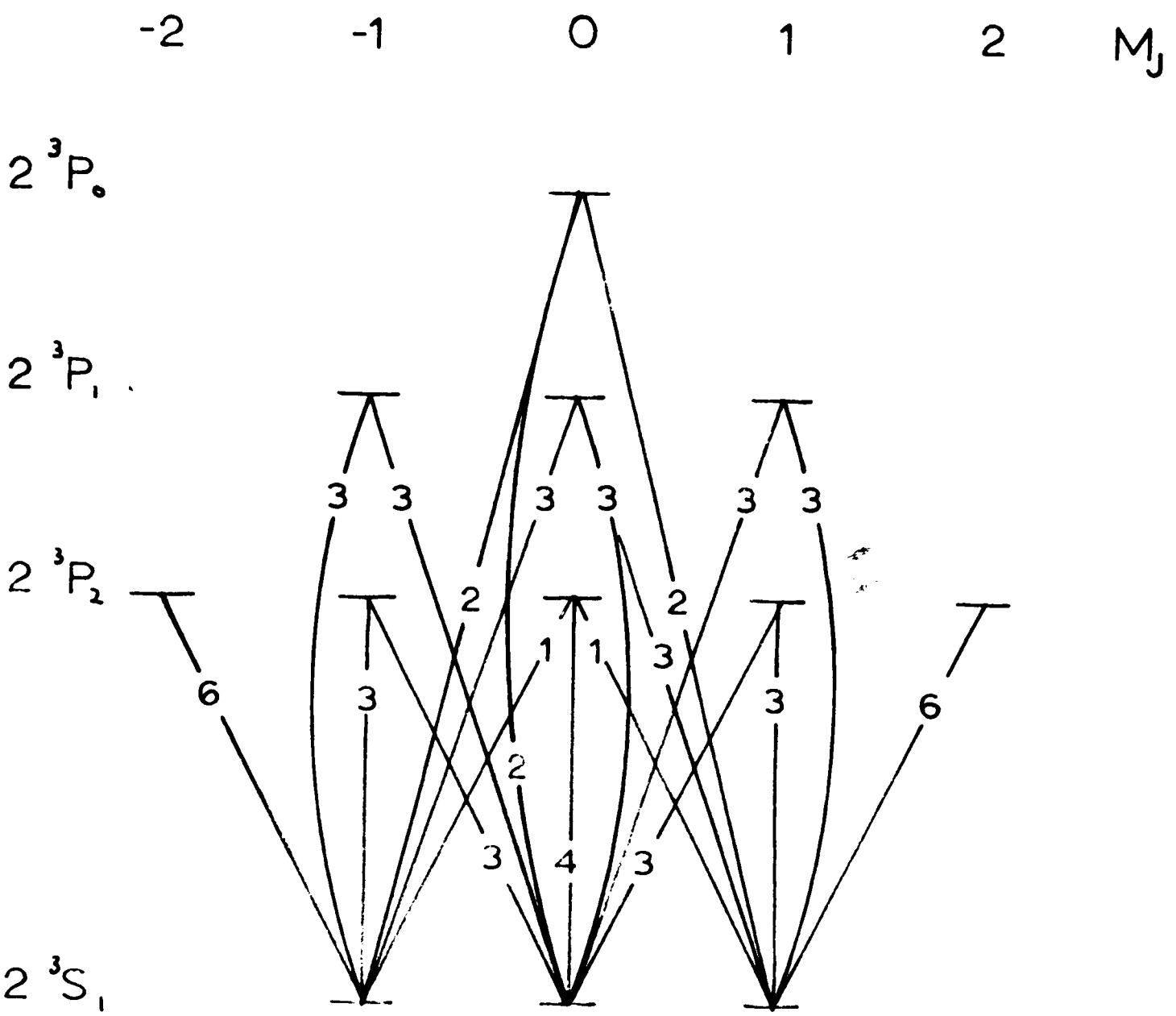


2a σ^+ POLARIZED LIGHT
INCIDENT IN Z DIRECTION

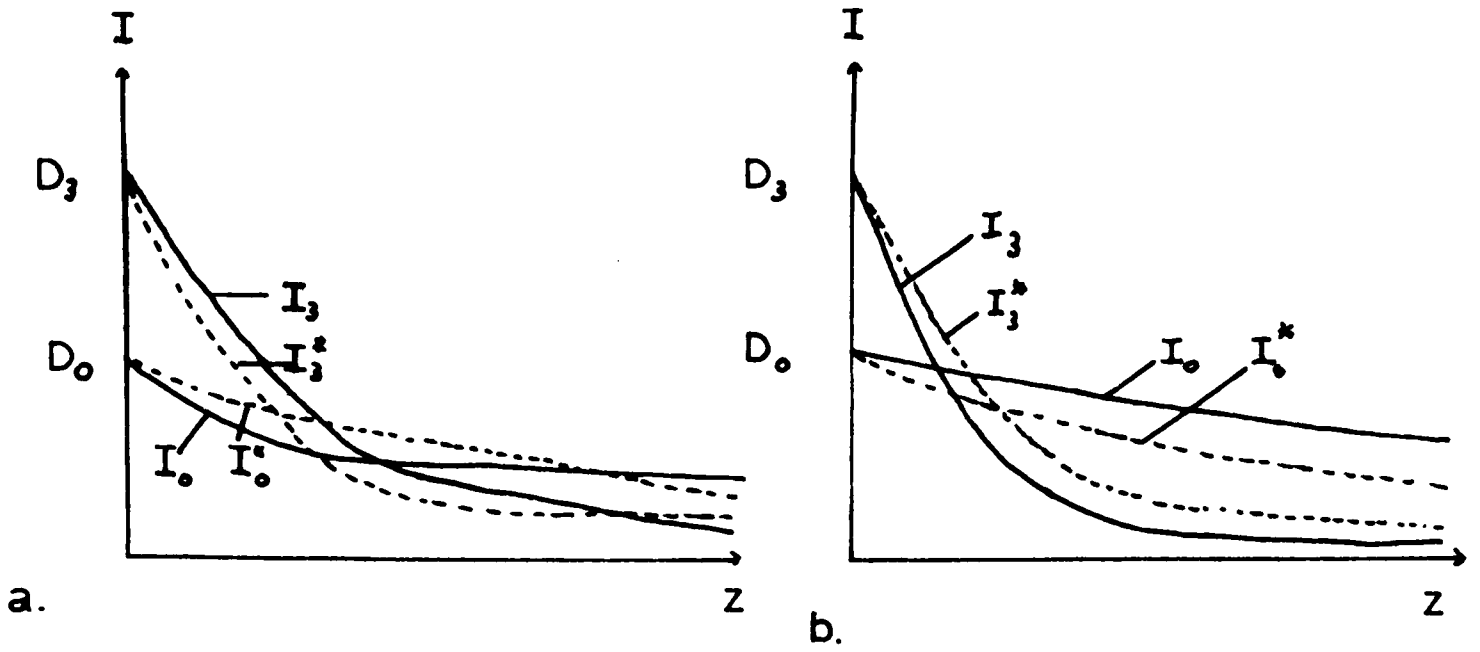


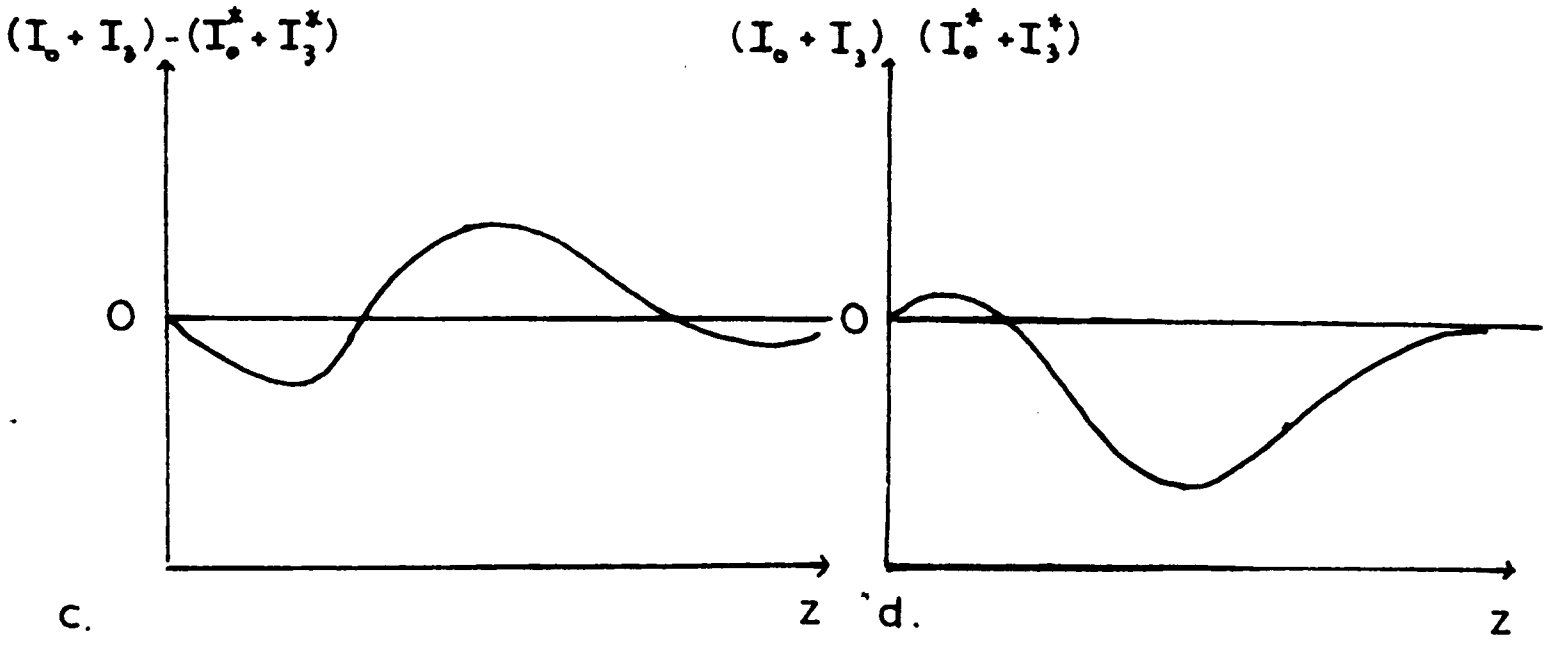
2b UNPOLARIZED LIGHT
INCIDENT IN Z DIRECTION

2ab RELATIVE ABSORPTION PROBABILITIES HE^4



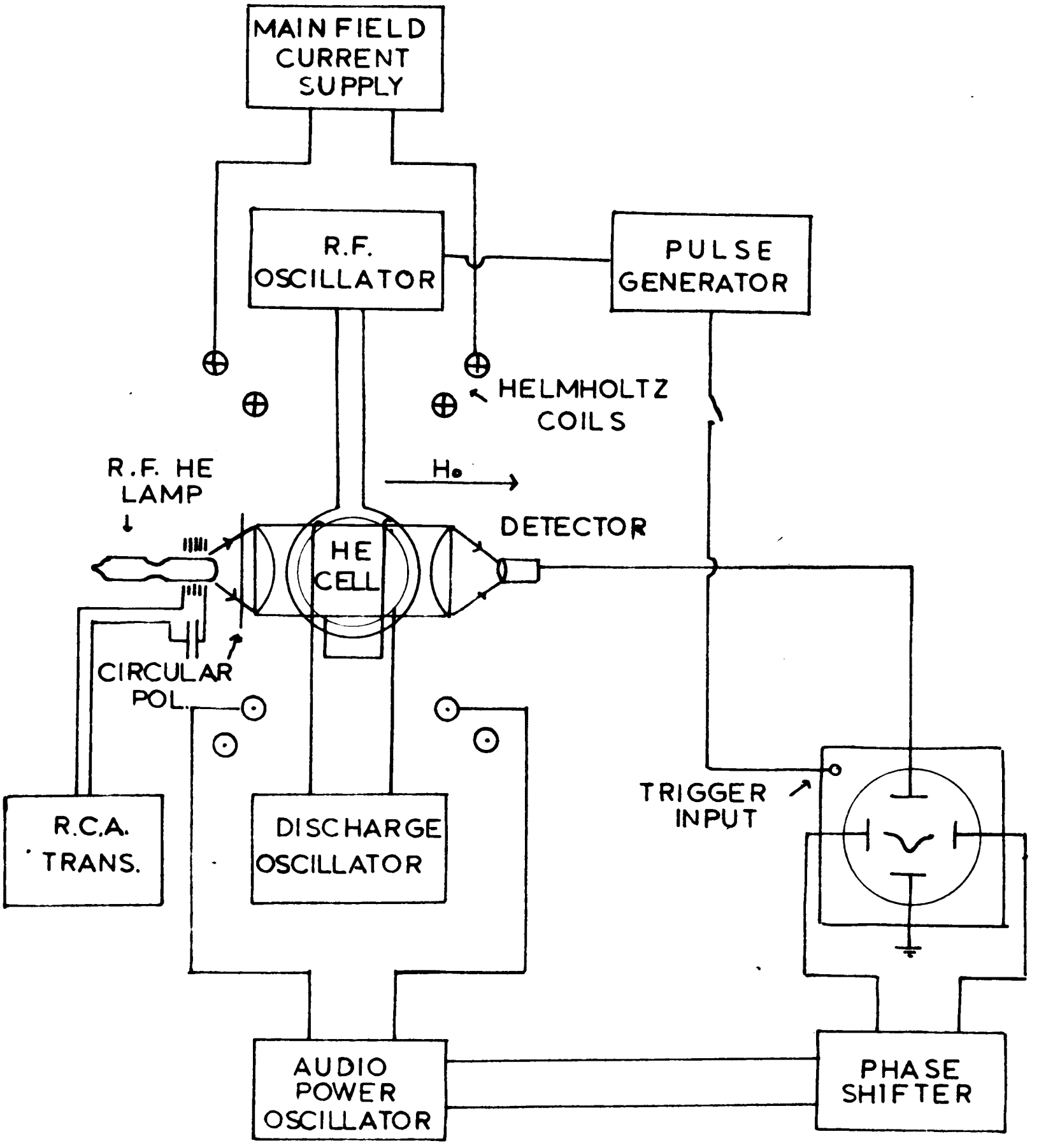
2c RELATIVE PROBABILITIES FOR SPONTANEOUS EMISSION



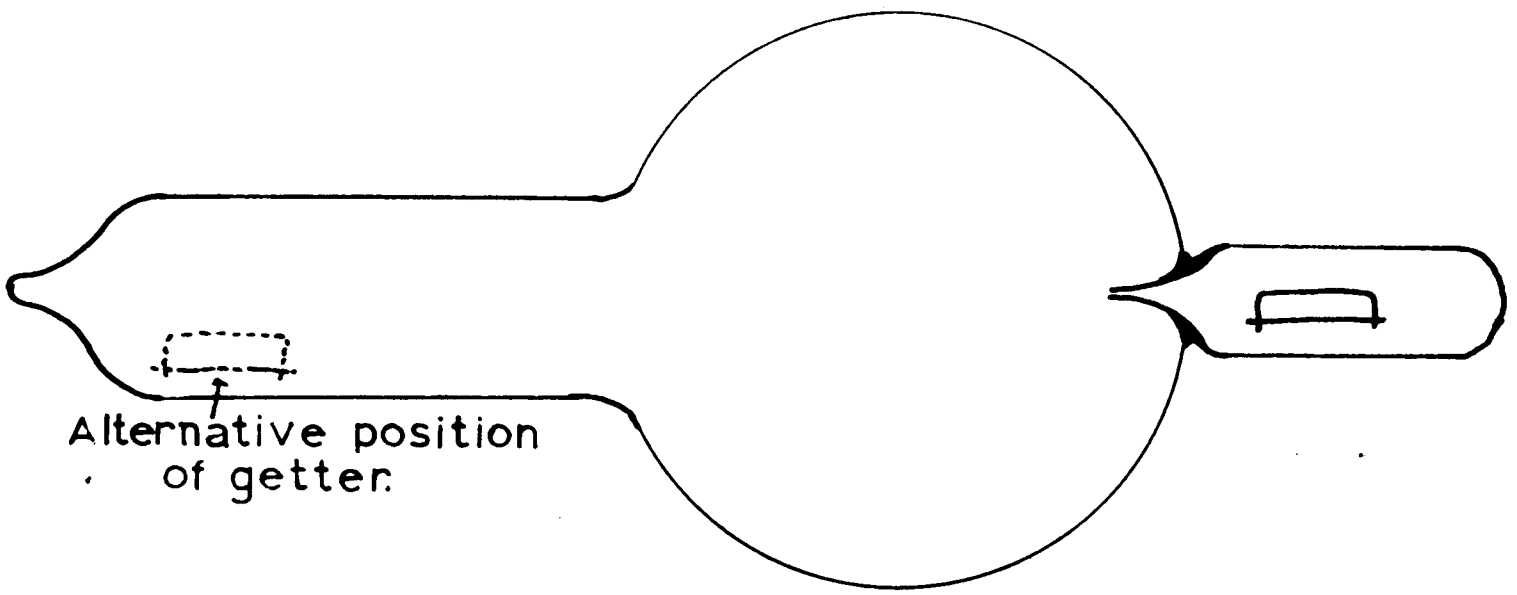


3abcd. INVERSION OF OPTICAL PUMPING SIGNALS

p 1.17 (Ref. 25)

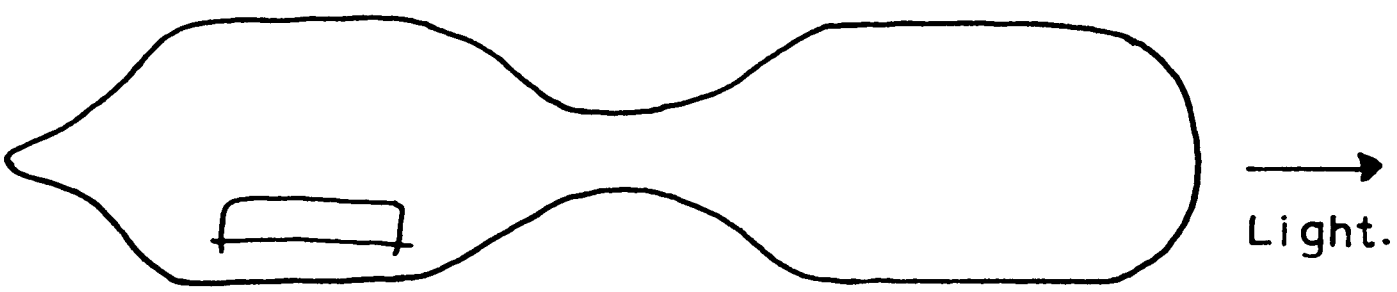


4 BLOCK DIAGRAM OF THE APPARATUS

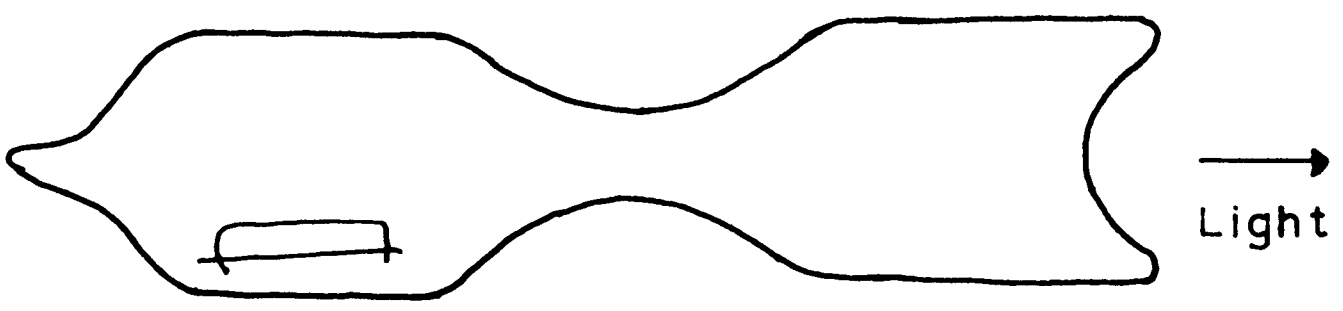


5 HE CELL WITH GETTER COMPARTMENT

p 2.5



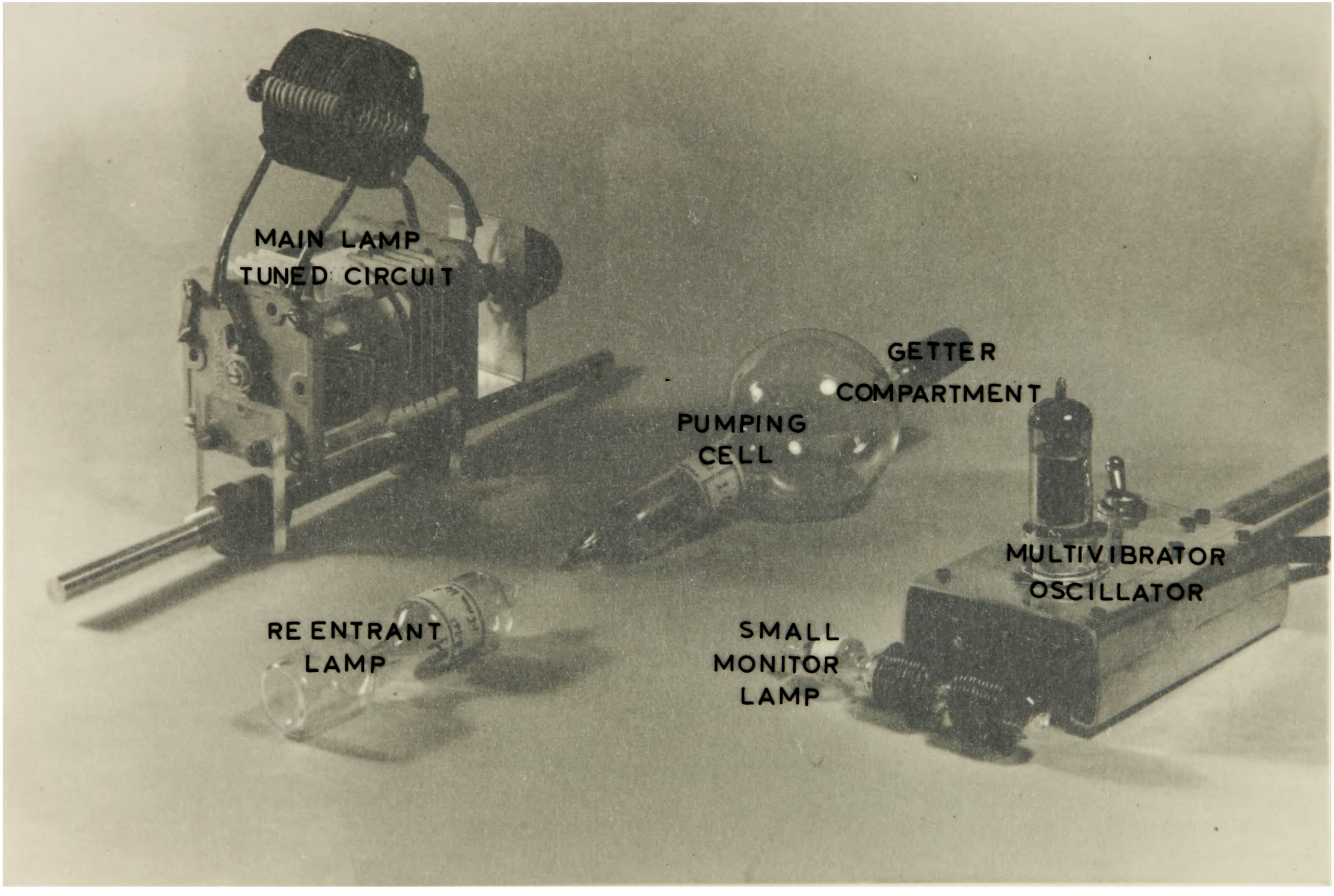
6a

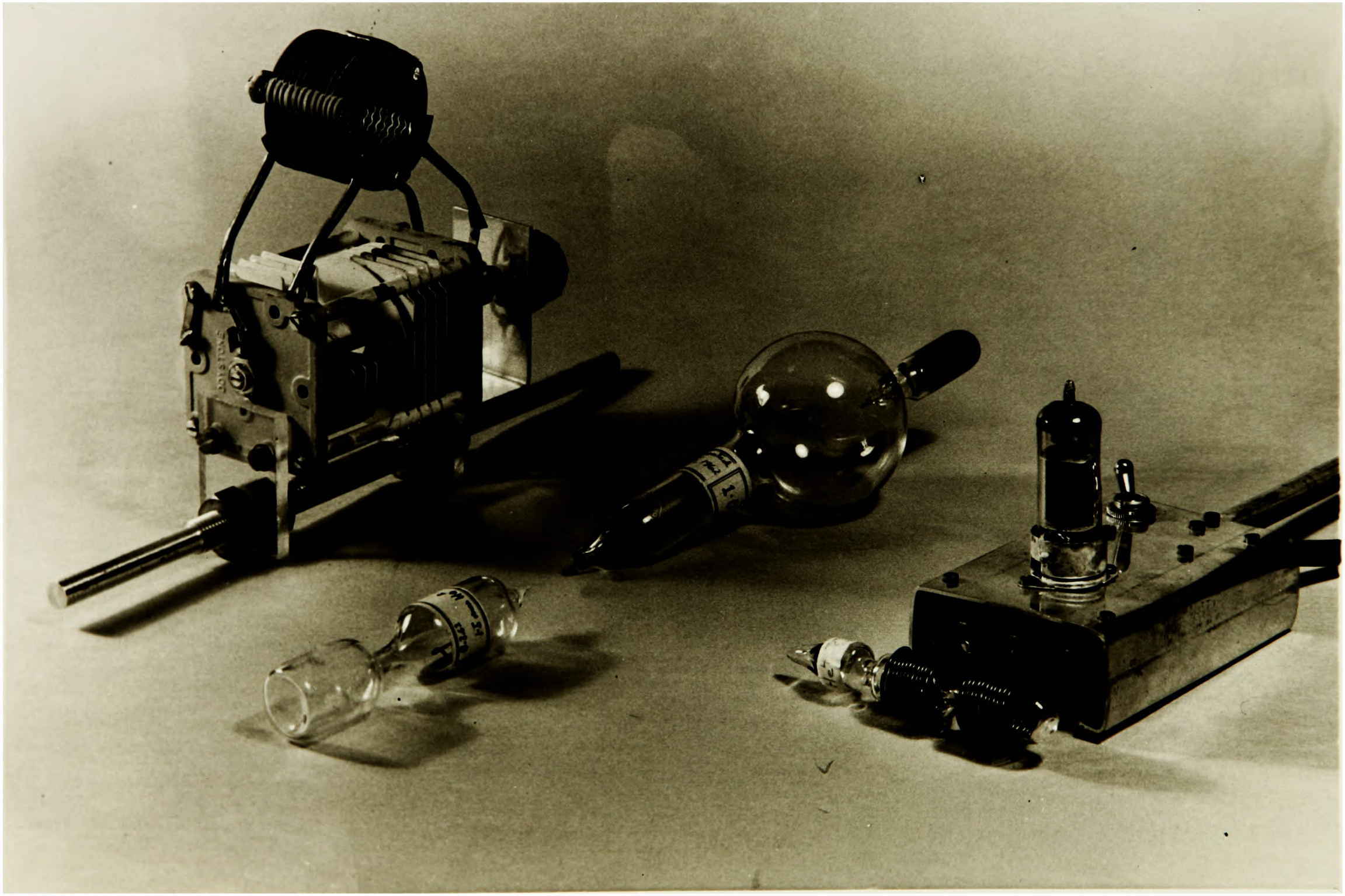


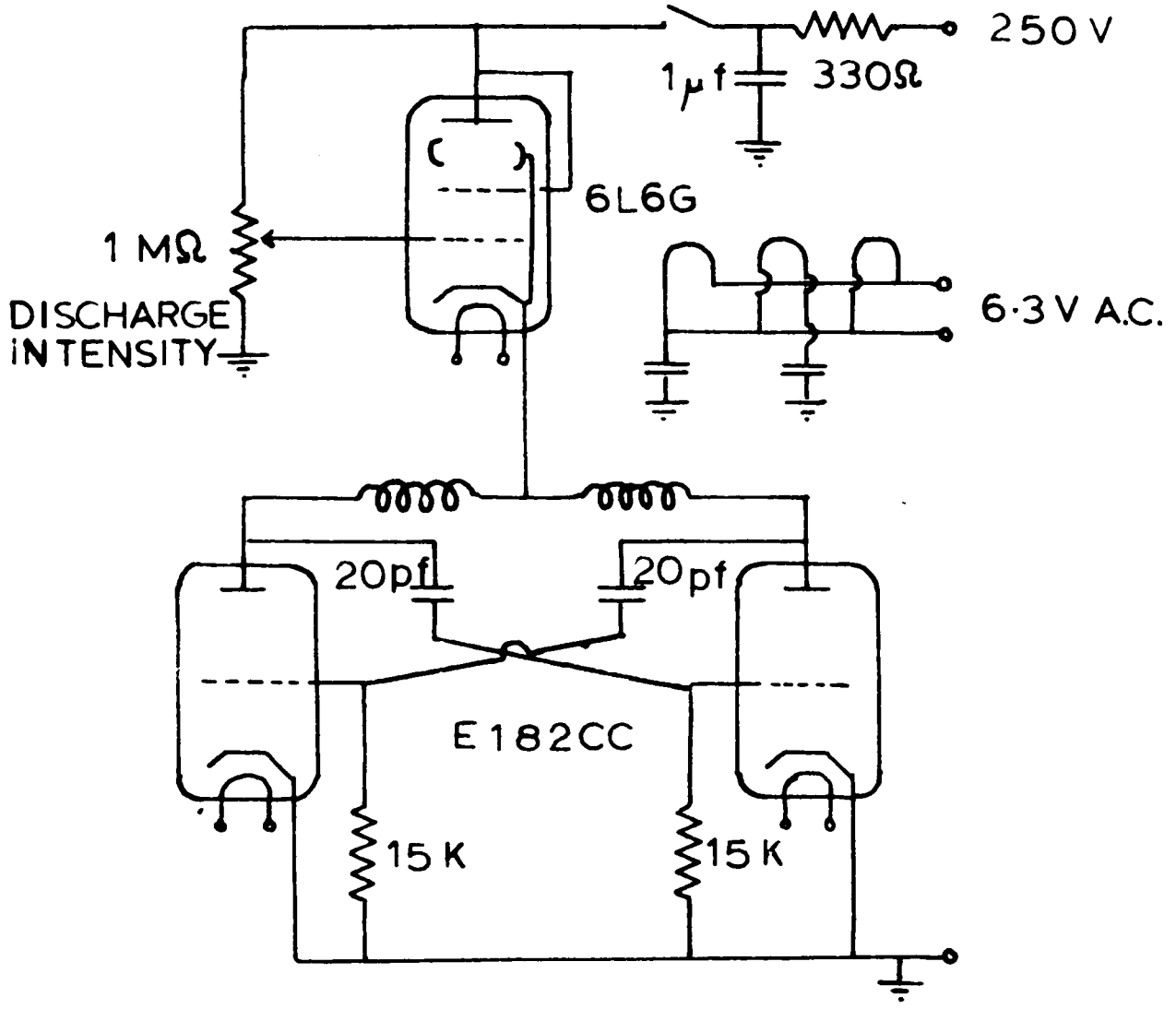
6b

6a b LAMP DESIGNS

p. 2.6

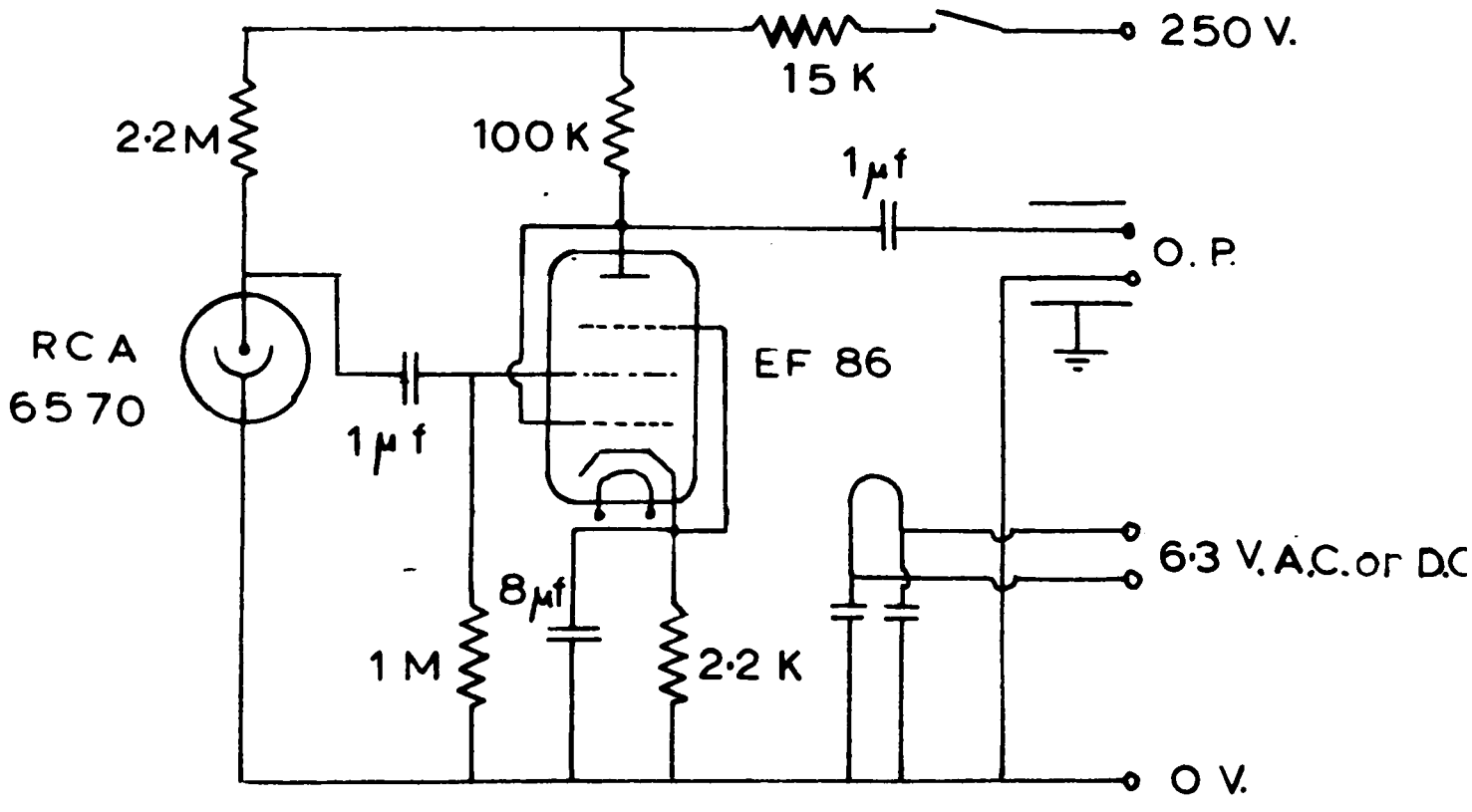

MAIN LAMP
TUNED CIRCUIT
GETTER
COMPARTMENT
PUMPING
CELL
MULTIVIBRATOR
OSCILLATOR
RE ENTRANT
LAMP
SMALL
MONITOR
LAMP





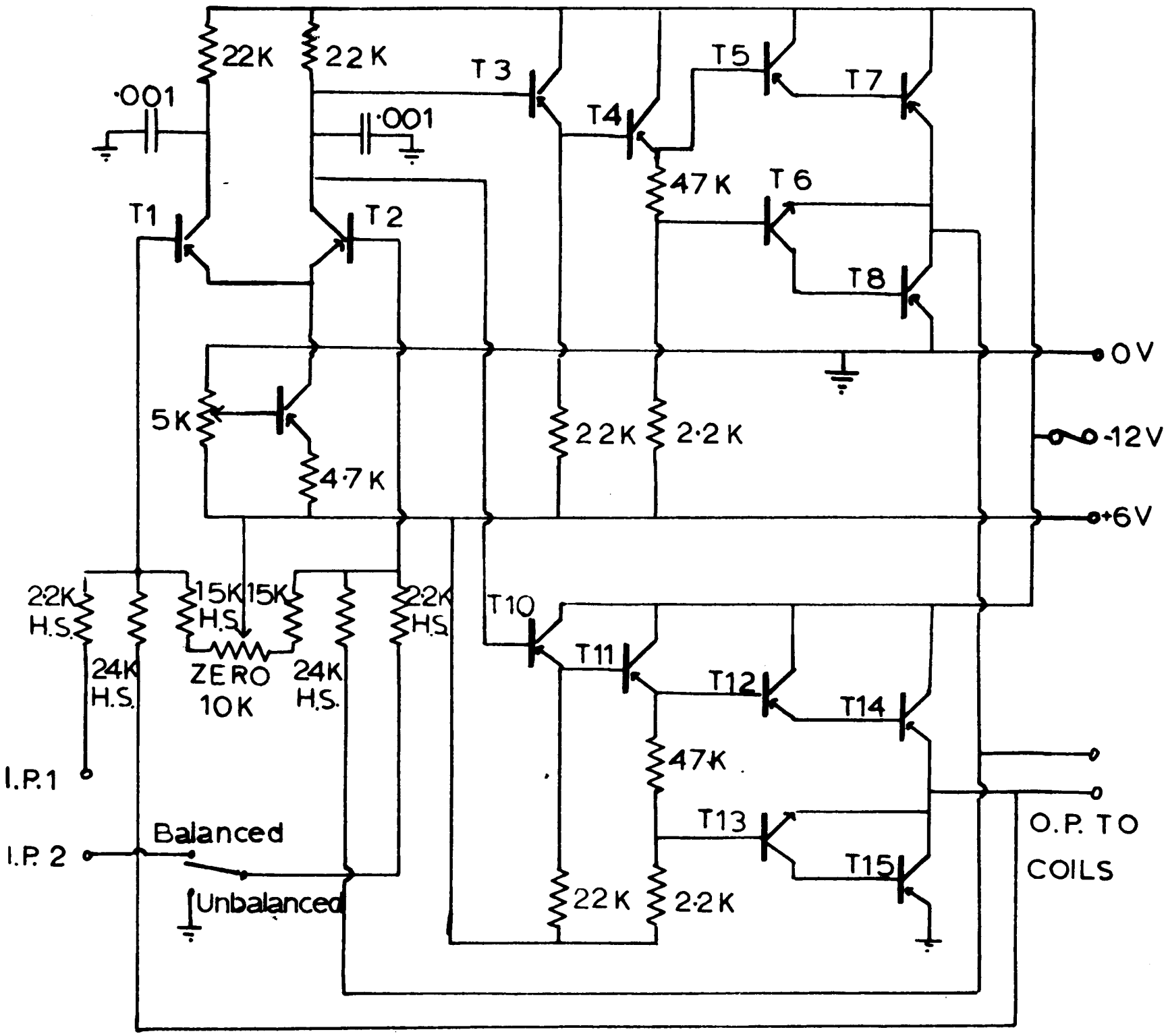
8 MULTIVIBRATOR USED FOR SMALL LAMP AND DISCHARGE

p. 2.8, 2.13



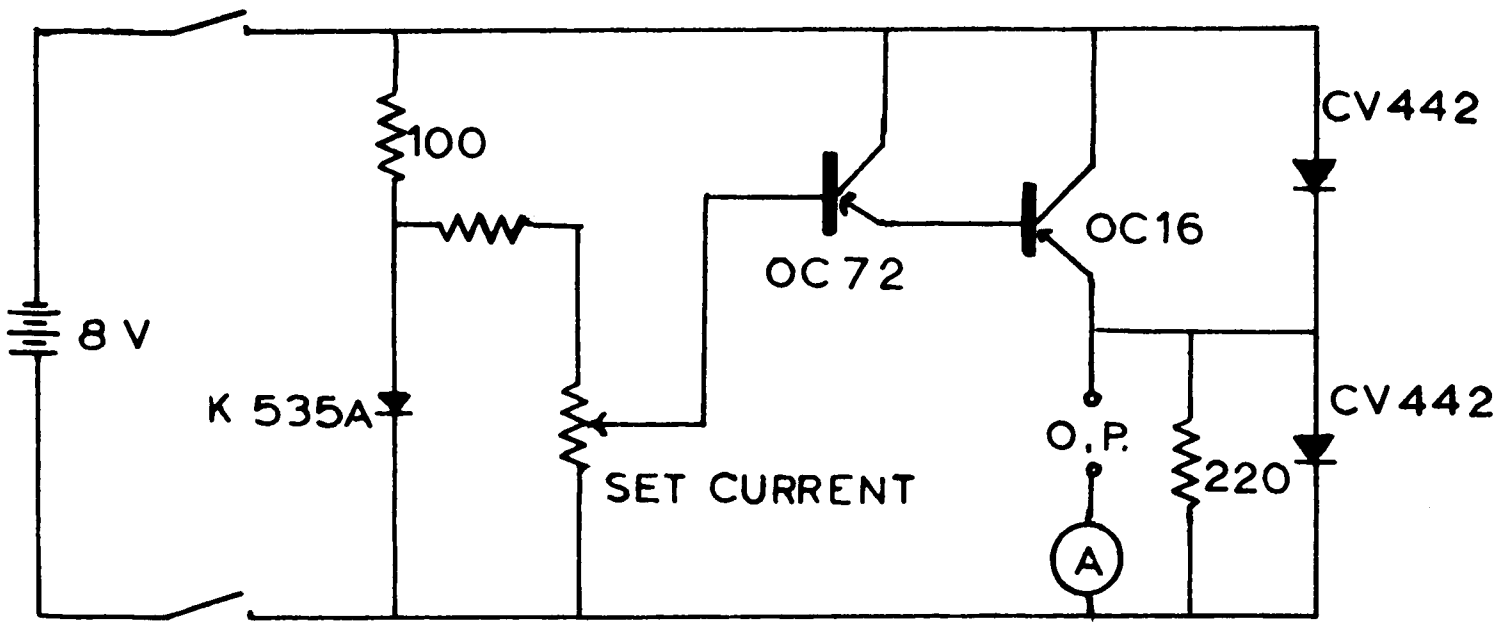
10 PHOTOCELL HEAD AMPLIFIER

p. 2.11



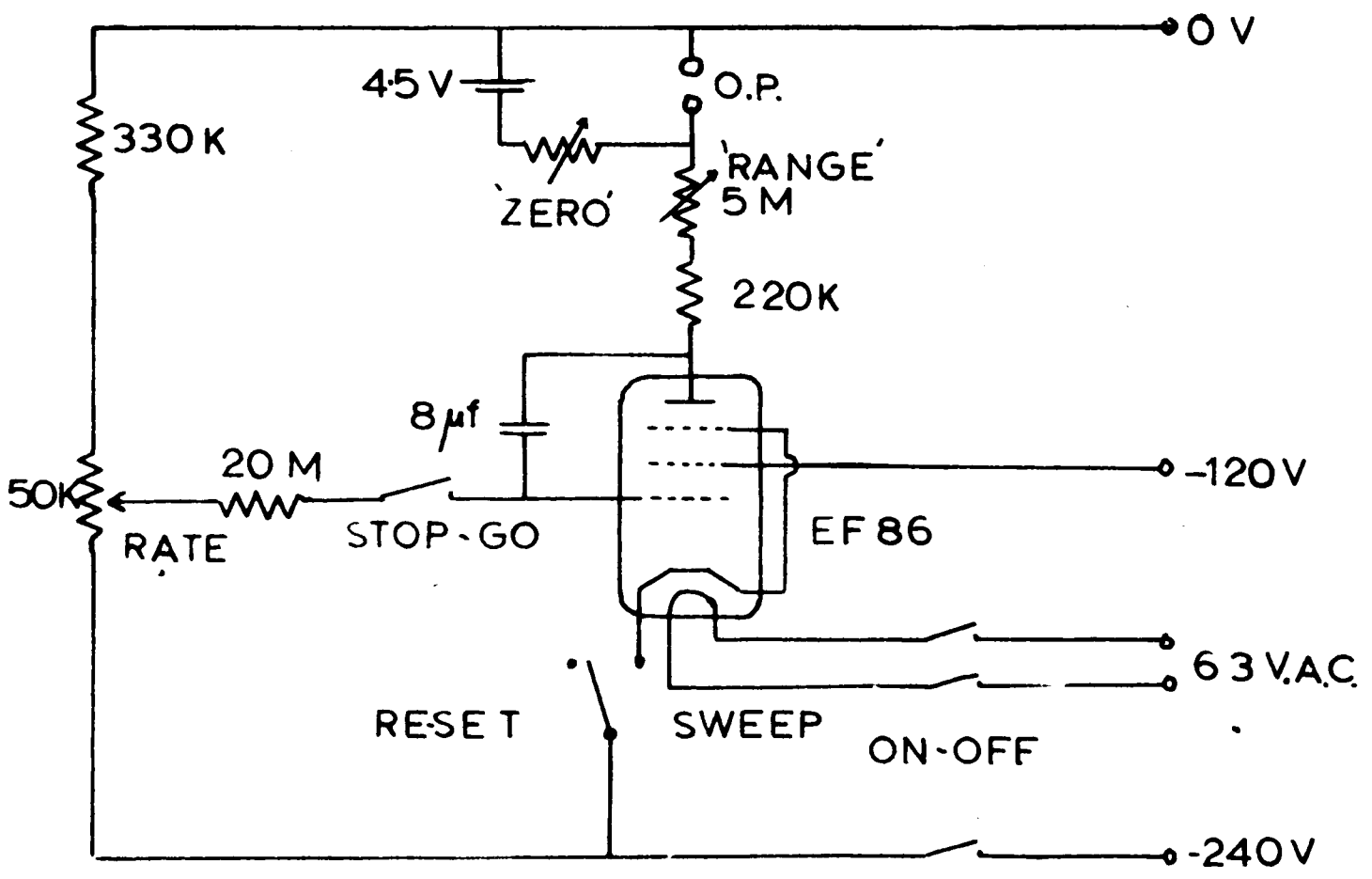
T 1,2,3,10	OC 71
T 4,11.	OC 72
T 5,12.	NKT 221
T 6,13	OC139
T 7,8,14,15.	NKT404

11 MAGNETIC FIELD CURRENT SUPPLY



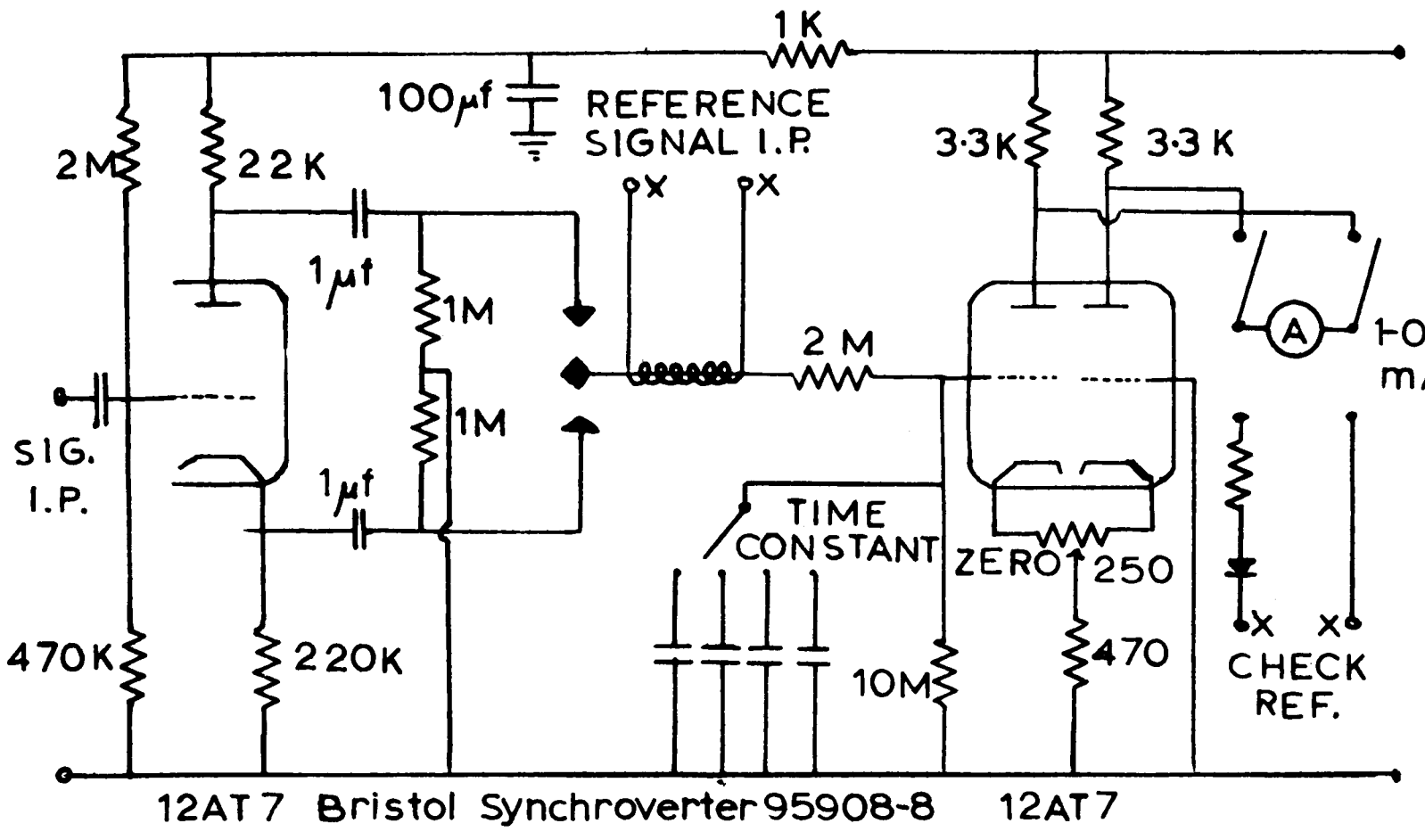
11b CURRENT CONTROLS FOR EARTH'S FIELD COMPENSATING COILS

p.2.14



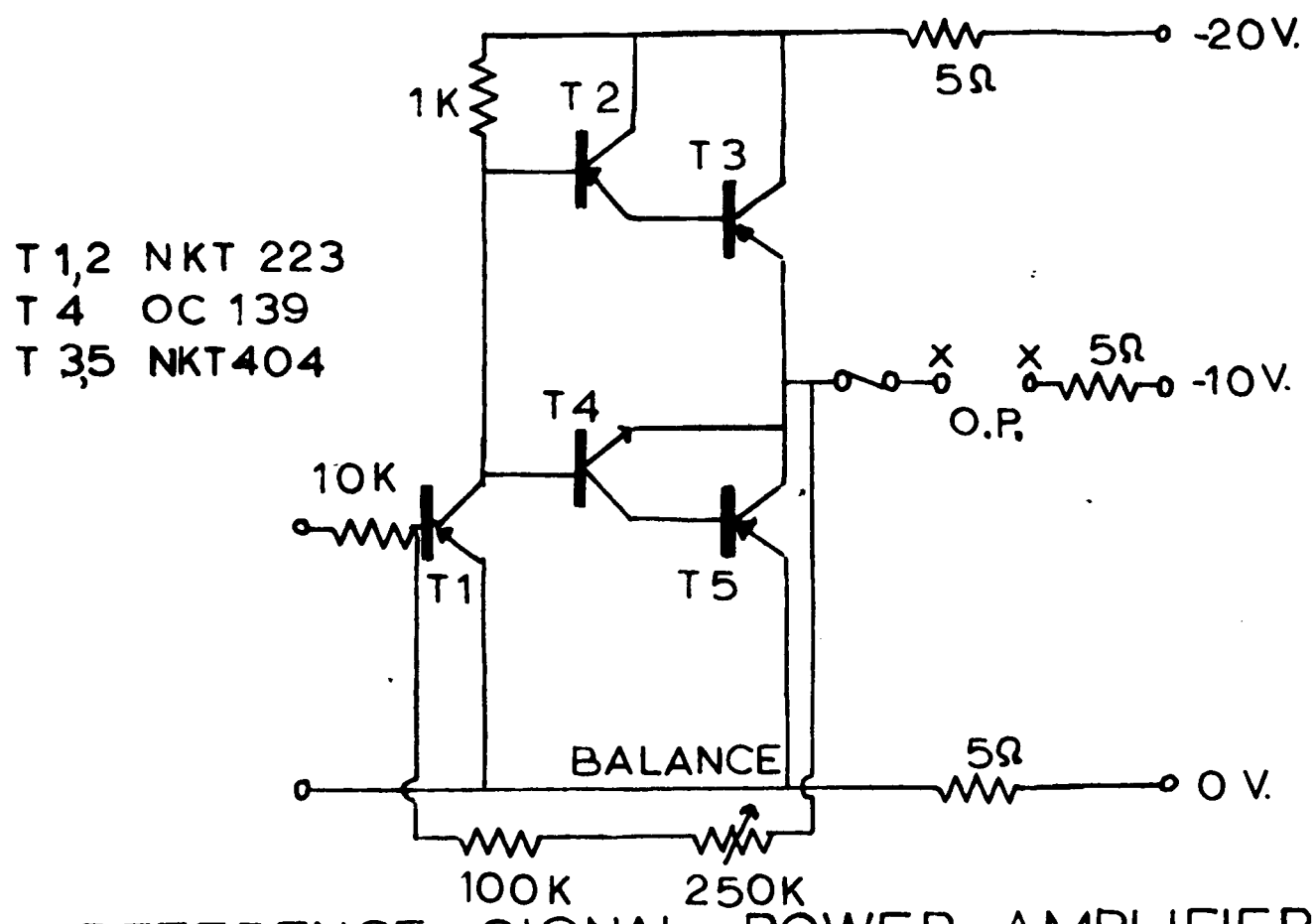
12 SWEEP CURRENT GENERATOR

p. 2.16



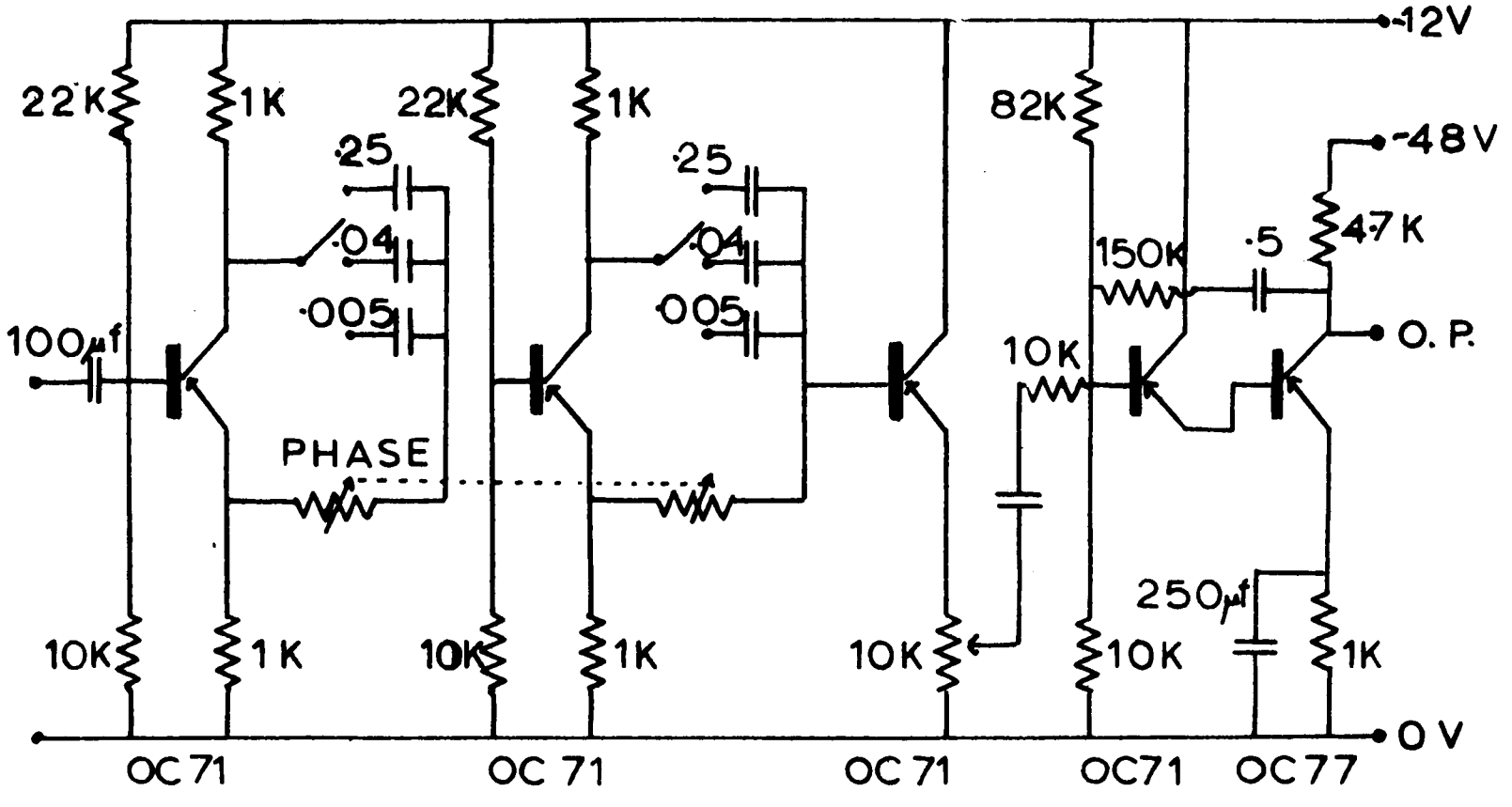
13a PHASE SENSITIVE DETECTOR

p. 2.16



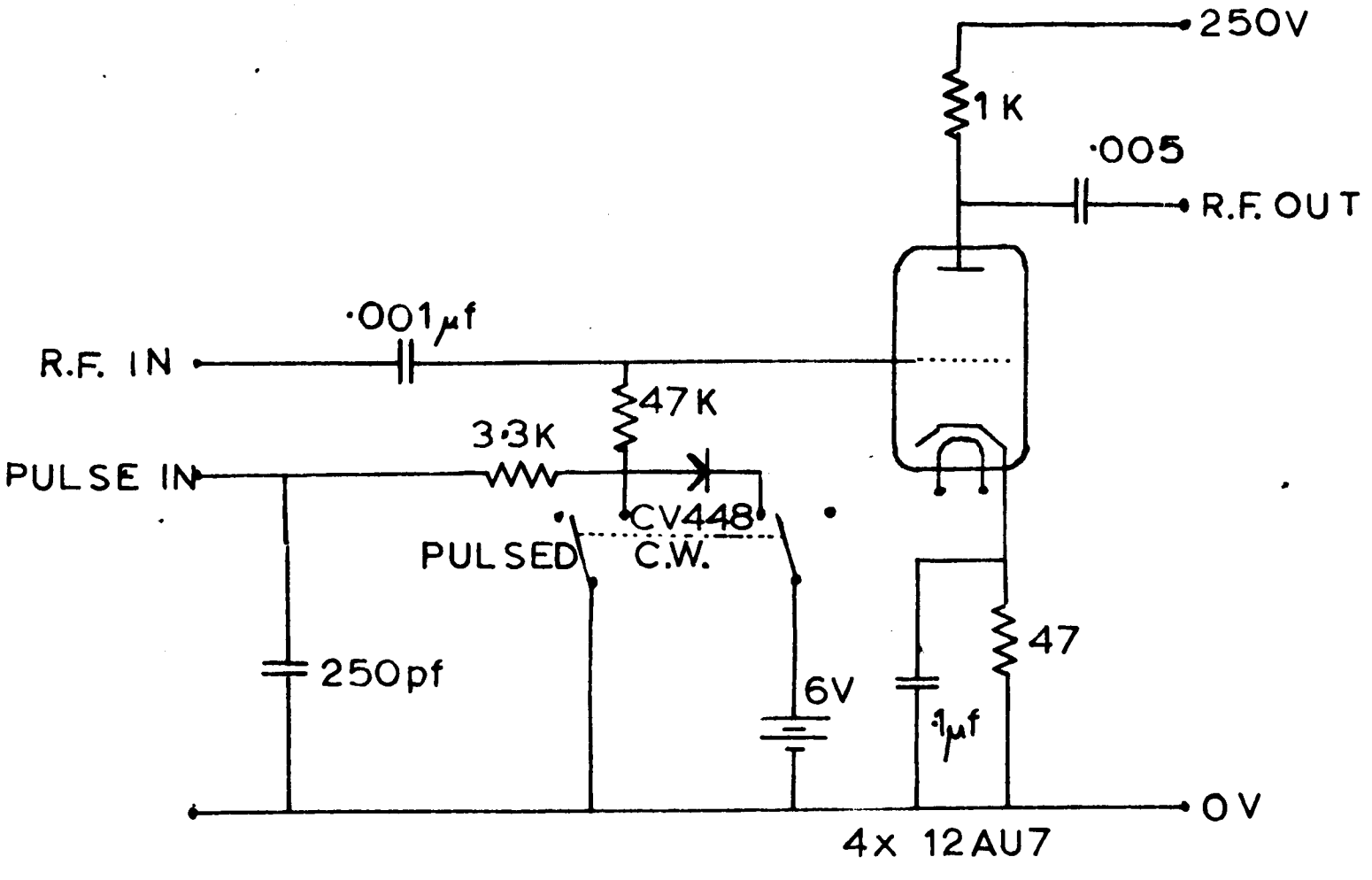
13b REFERENCE SIGNAL POWER AMPLIFIER

p. 2.16



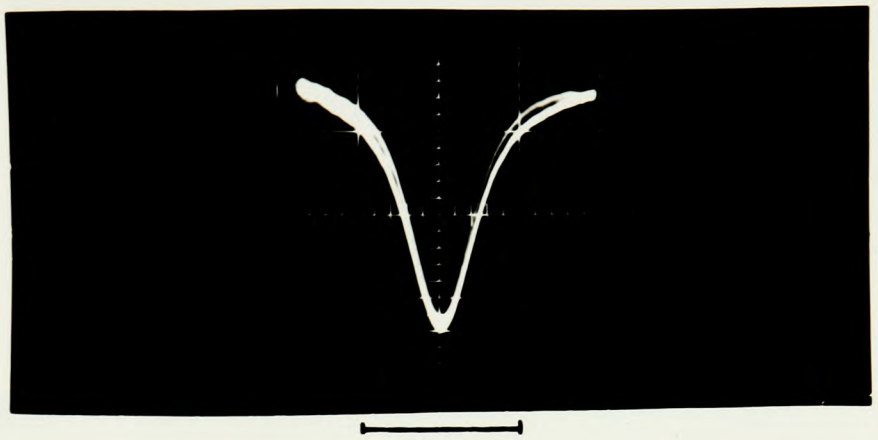
13c PHASE - SHIFTER

p. 2.16



14 R.F. POWER AMPLIFIER AND PULSER

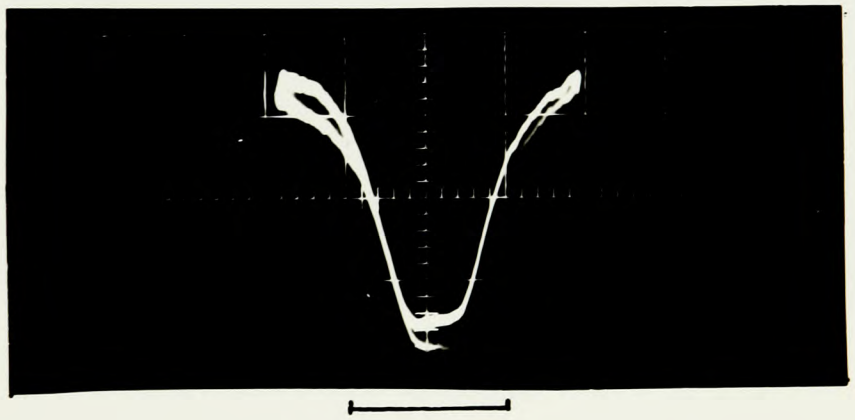
p. 2.17



15 mG.

15a Polarization Signal. $H_1 \sim 3$ mG.

·3 mm. Hg. Cell. 2 mm. Hg. Lamp.

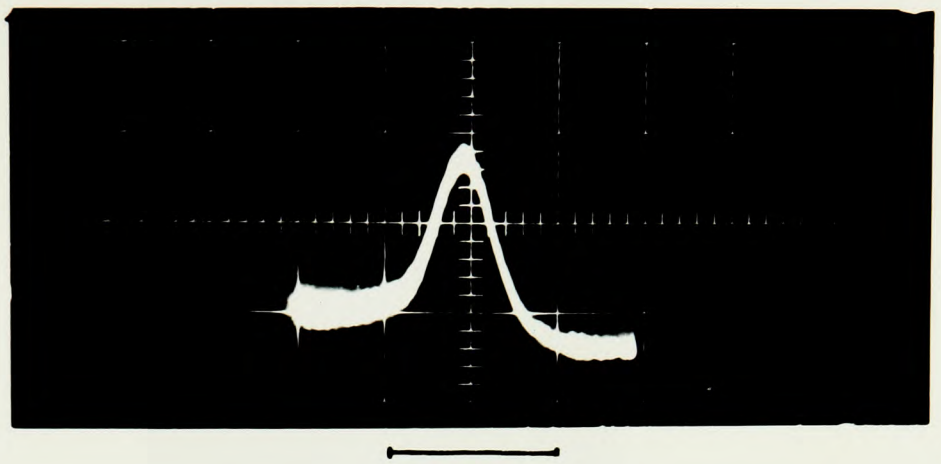


15 mG

15b Alignment Signal. $H_1 \sim 3$ mG.

·1 mm. Hg. Cell 5·5 mm Hg. Lamp.

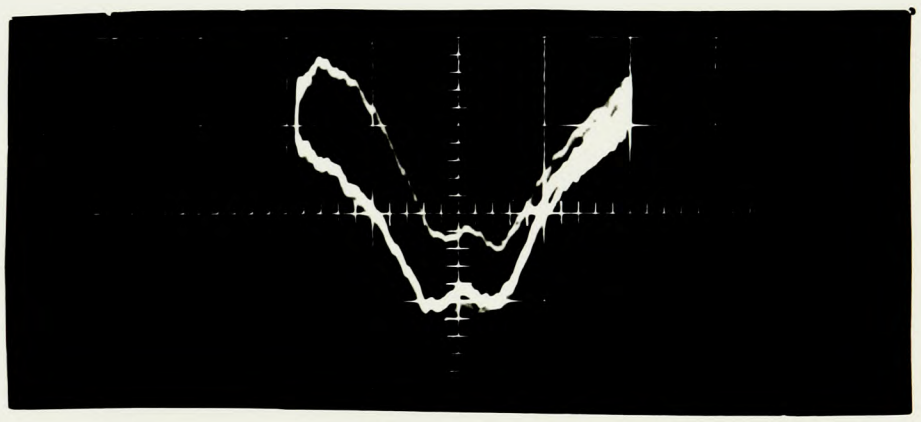
15a,b. RESONANCES IN He^4 $^3S_1$ METASTABLE LEVEL



14 mG.

16a. Polarization Signal. $H_1 \sim 4$ mG.

·1mm. Hg.Cell., 2mm. Hg. Lamp.

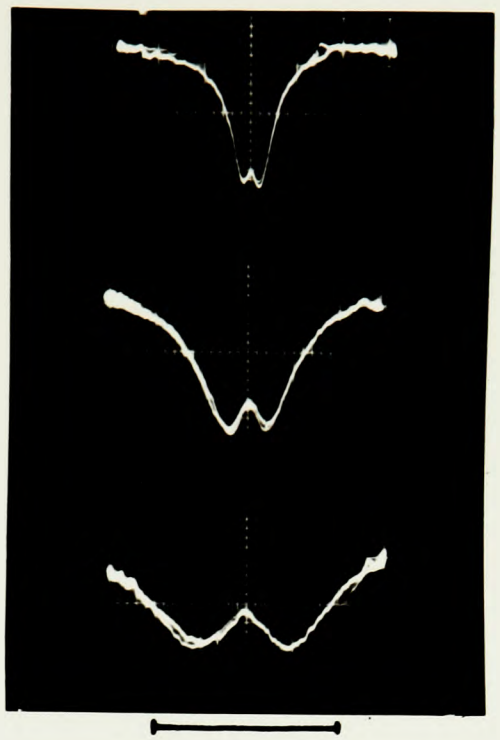


14 mG.

16b Alignment Signal. As above with polarizer removed.

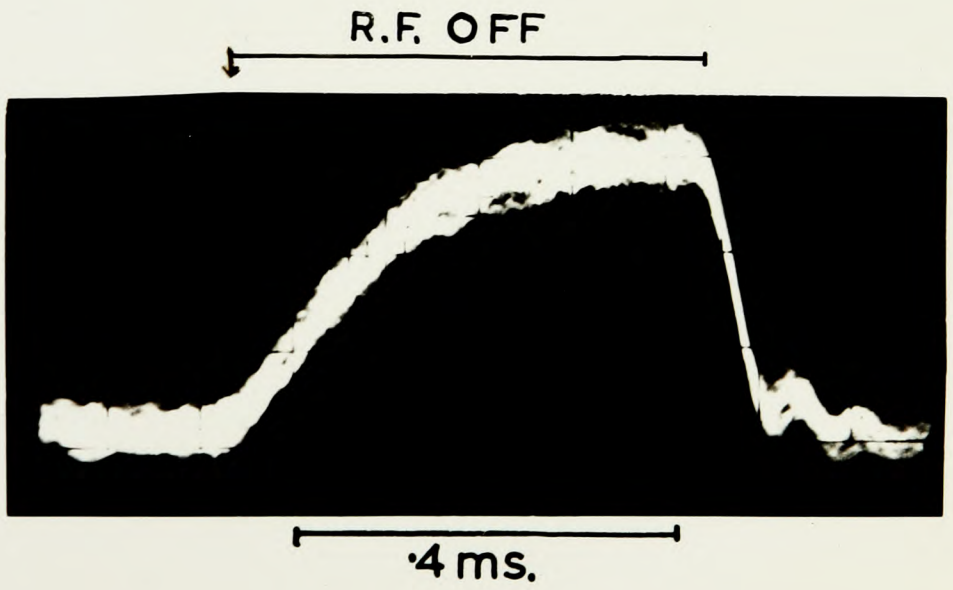
16a,b. RESONANCES IN He^4 $^3S_1$ METASTABLE LEVEL. (THIN SAMPLE.)

p. 3.3



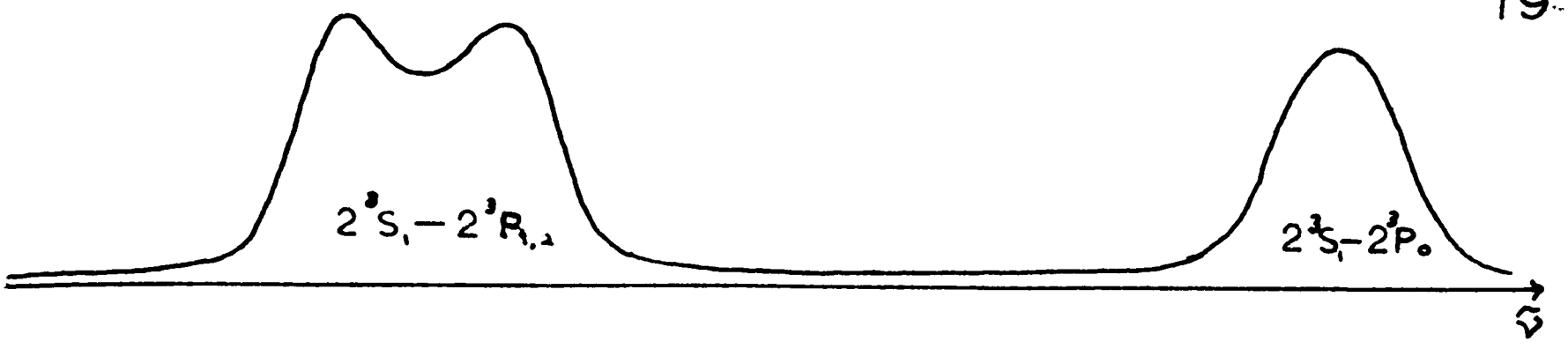
17. EFFECT OF H, O N He^4 ALIGNMENT SIGNAL

p. 3.7

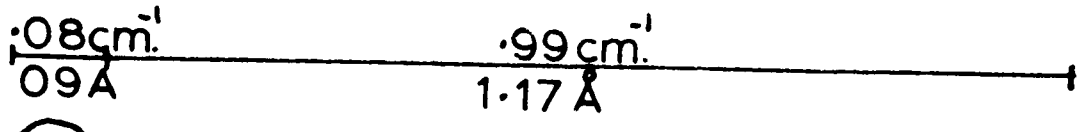


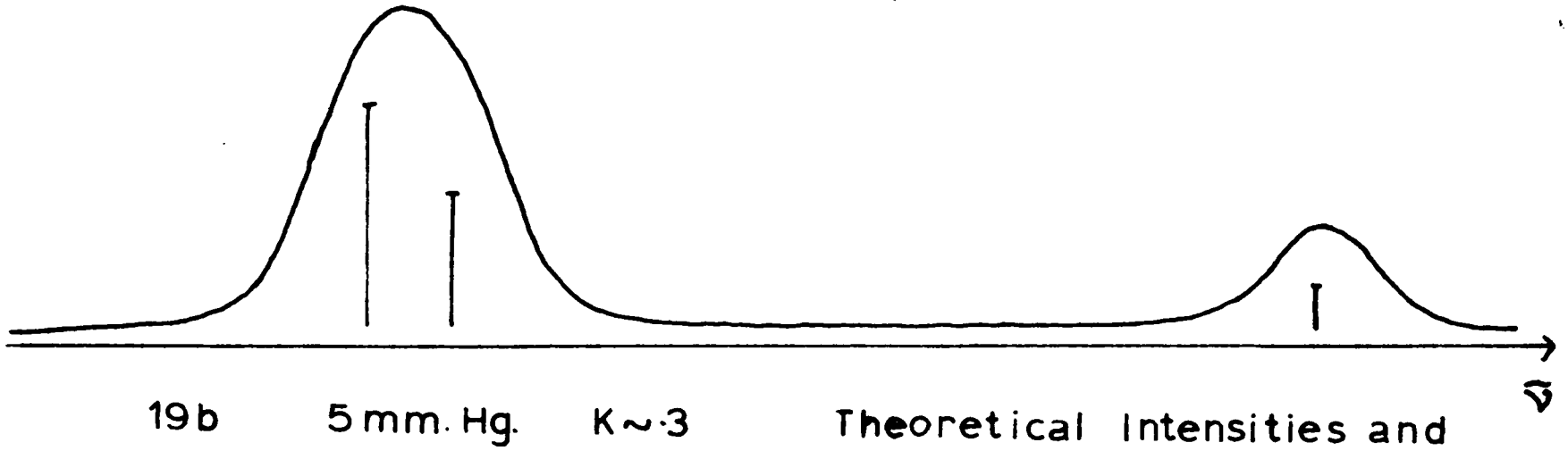
18. He^4 PUMPING TRANSIENT

p. 3.8



19a 1mm.Hg. SELF-REVERSED K>1

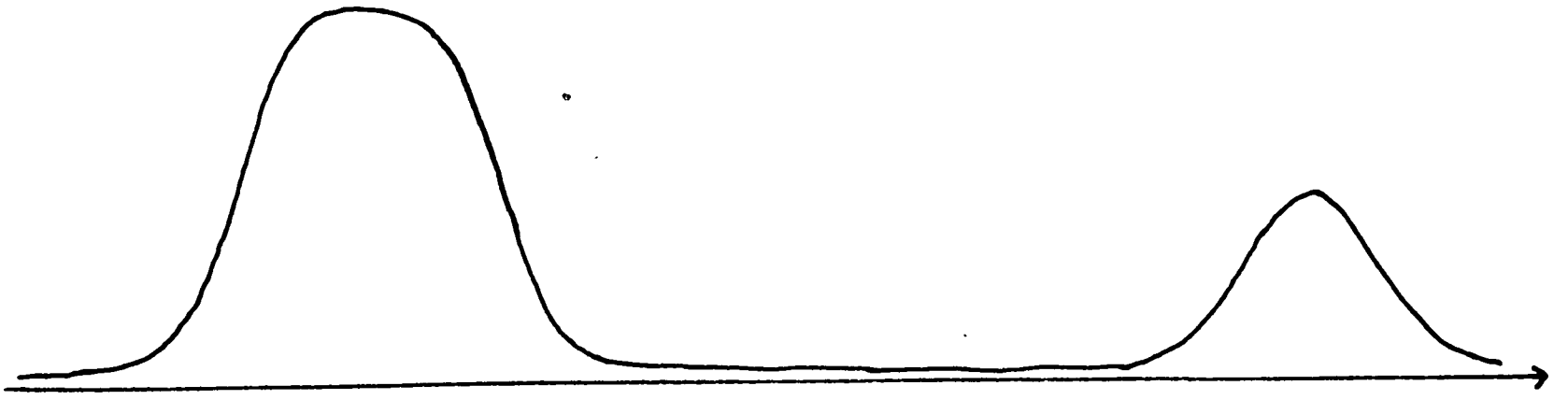




19b 5mm.Hg. K~·3 Theoretical Intensities and Positions Marked

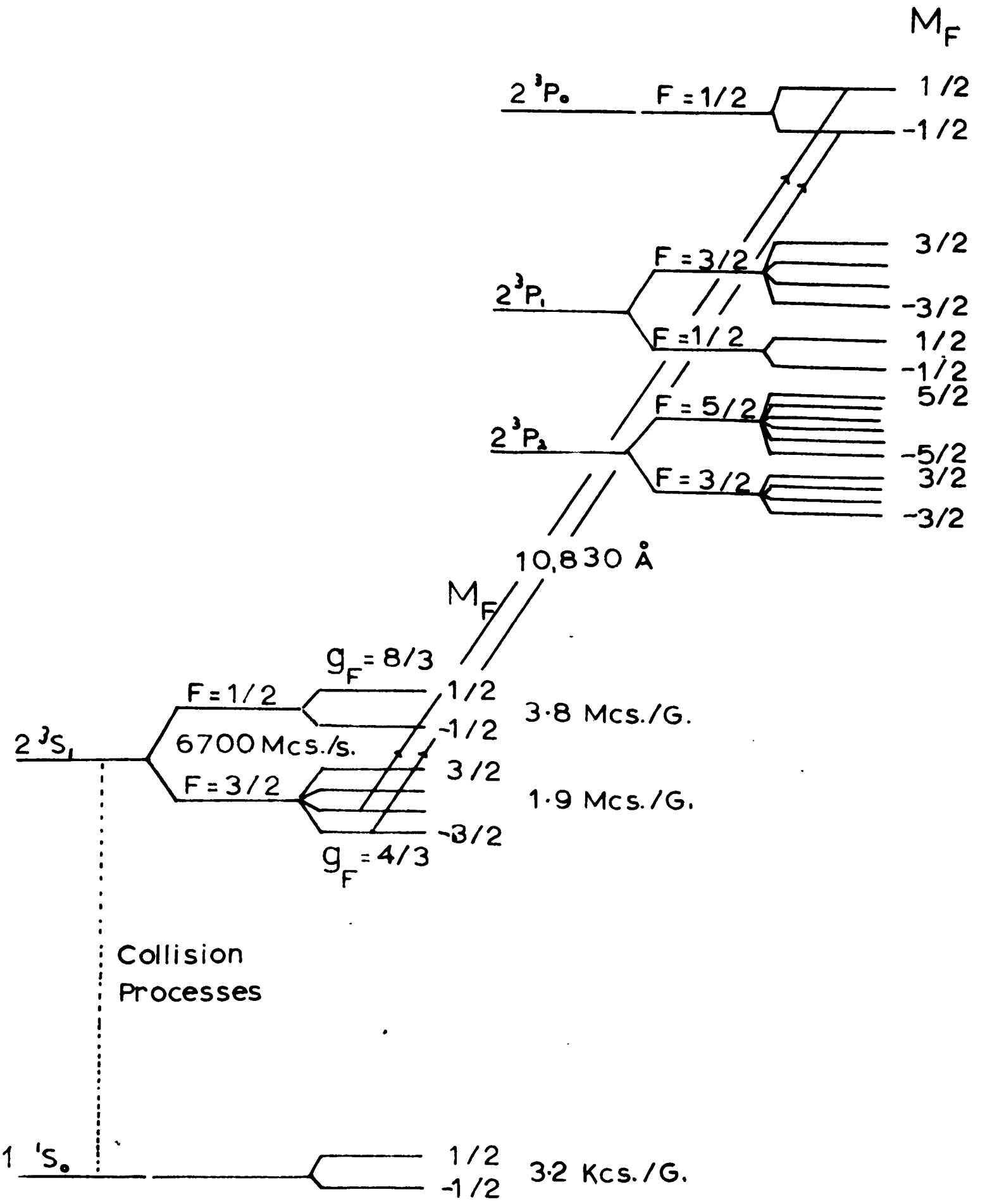


19c 1 mm.Hg. LAMP NOT RE-ENTRANT

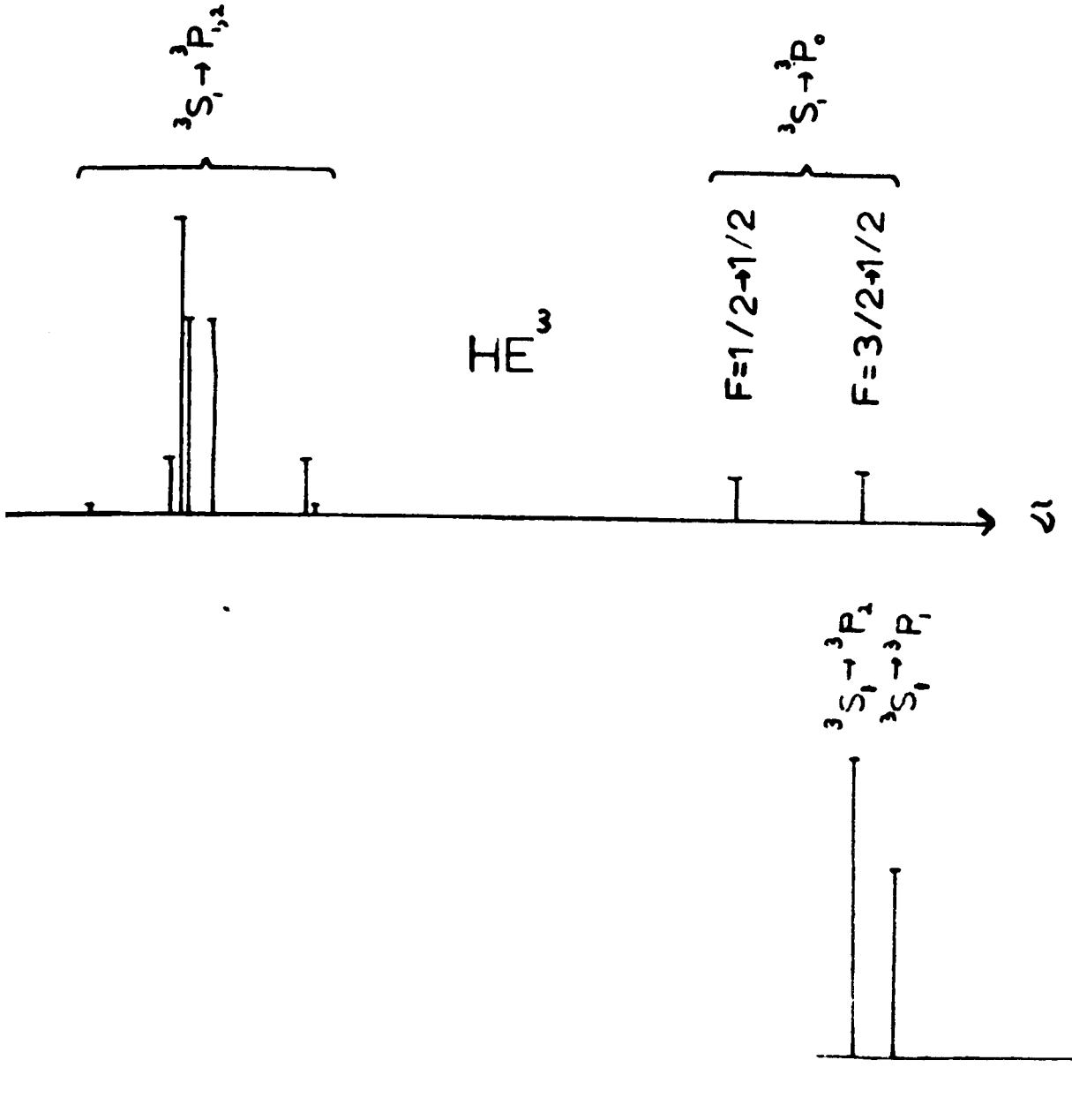


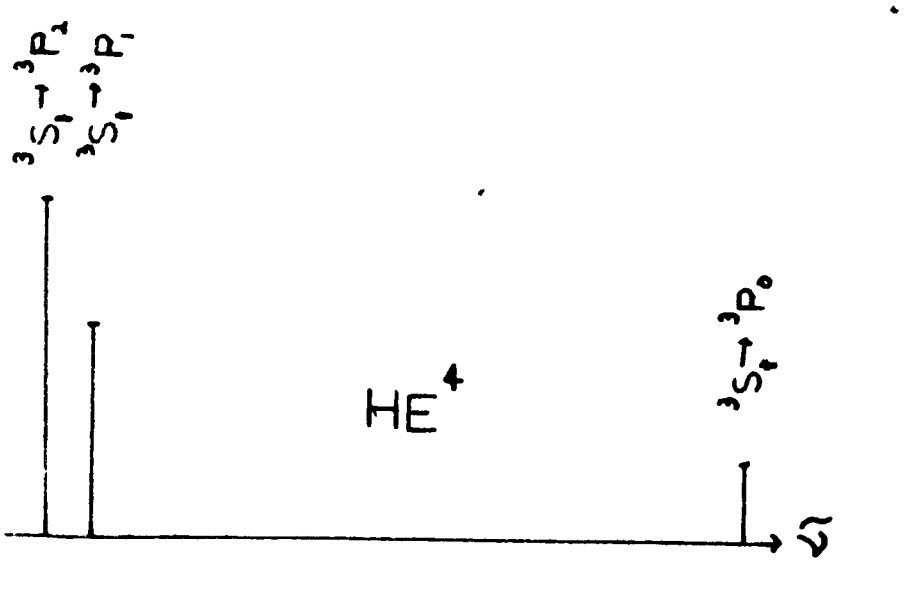
19d AS 19c BUT RE-ENTRANT LAMP

19 abcd. He^4 LAMP PROFILES. 10,830 Å

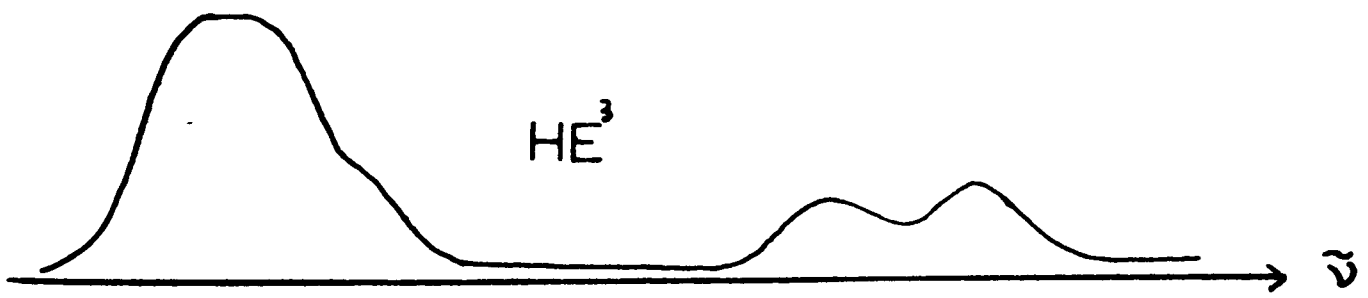


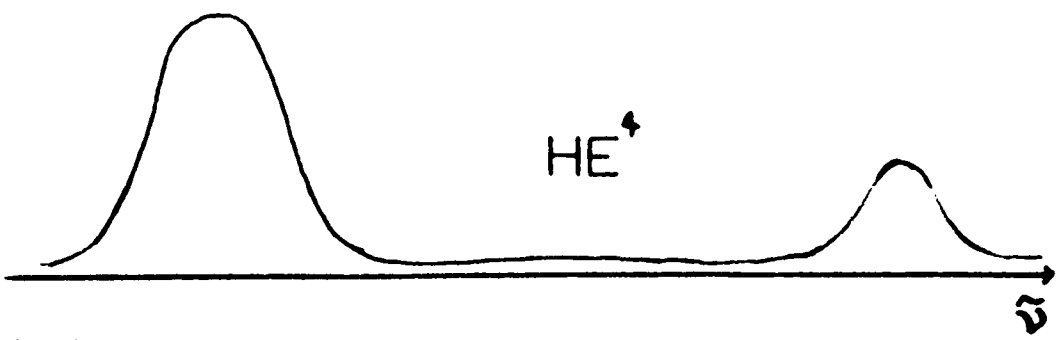
20 HE^3 TERM DIAGRAM





21a THEORETICAL





21b EXPERIMENTAL

21ab 10830 Å LINE STRUCTURE IN HE^3 & HE^4

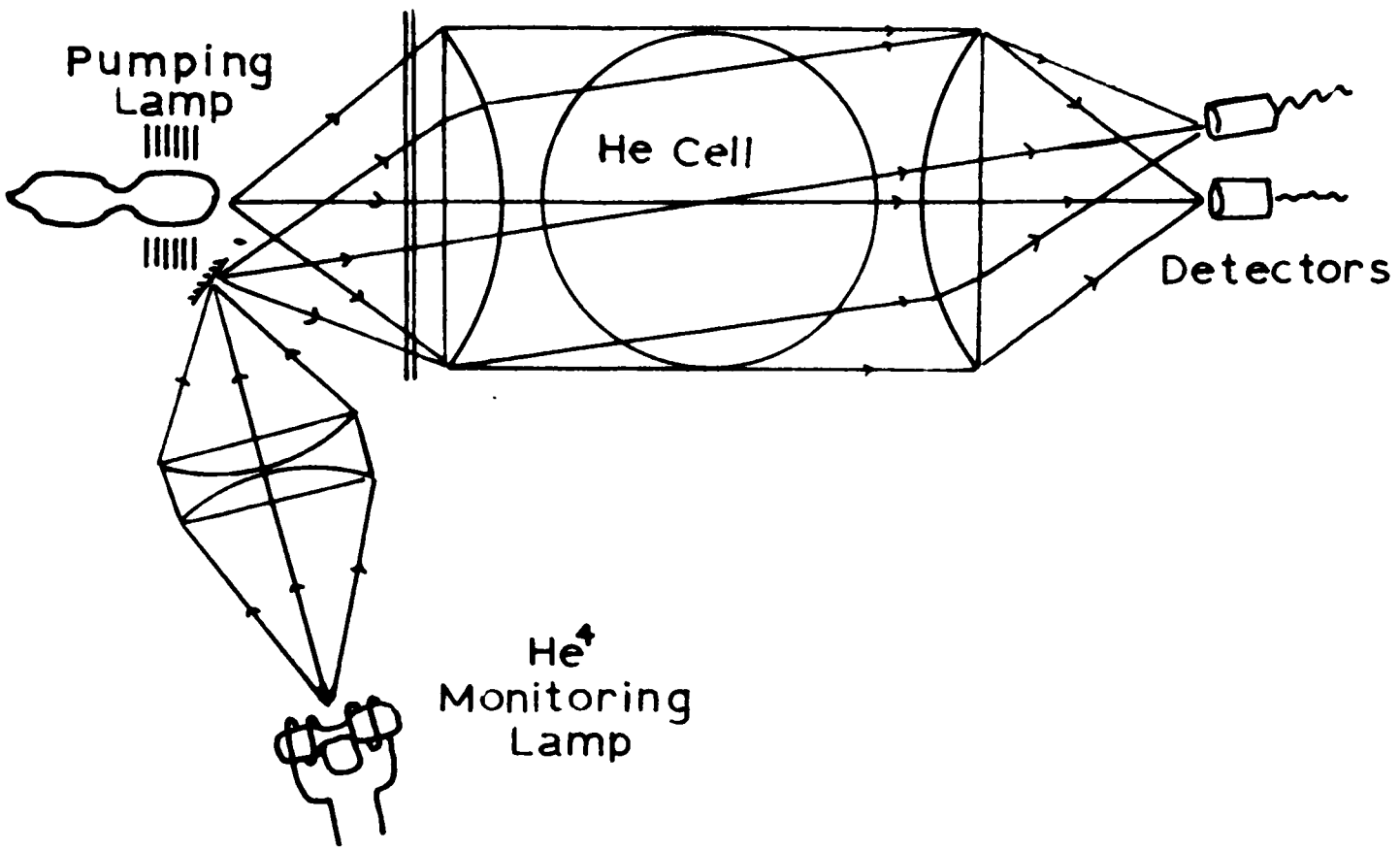
22a

		$^3P_0$		$^3P_1$		$^3P_2$	
	F	1/2	3/2	1/2	5/2	3/2	
$^3S_1$	1/2	15	65	19		2	
	3/2	19	2	19	100	65	

22b

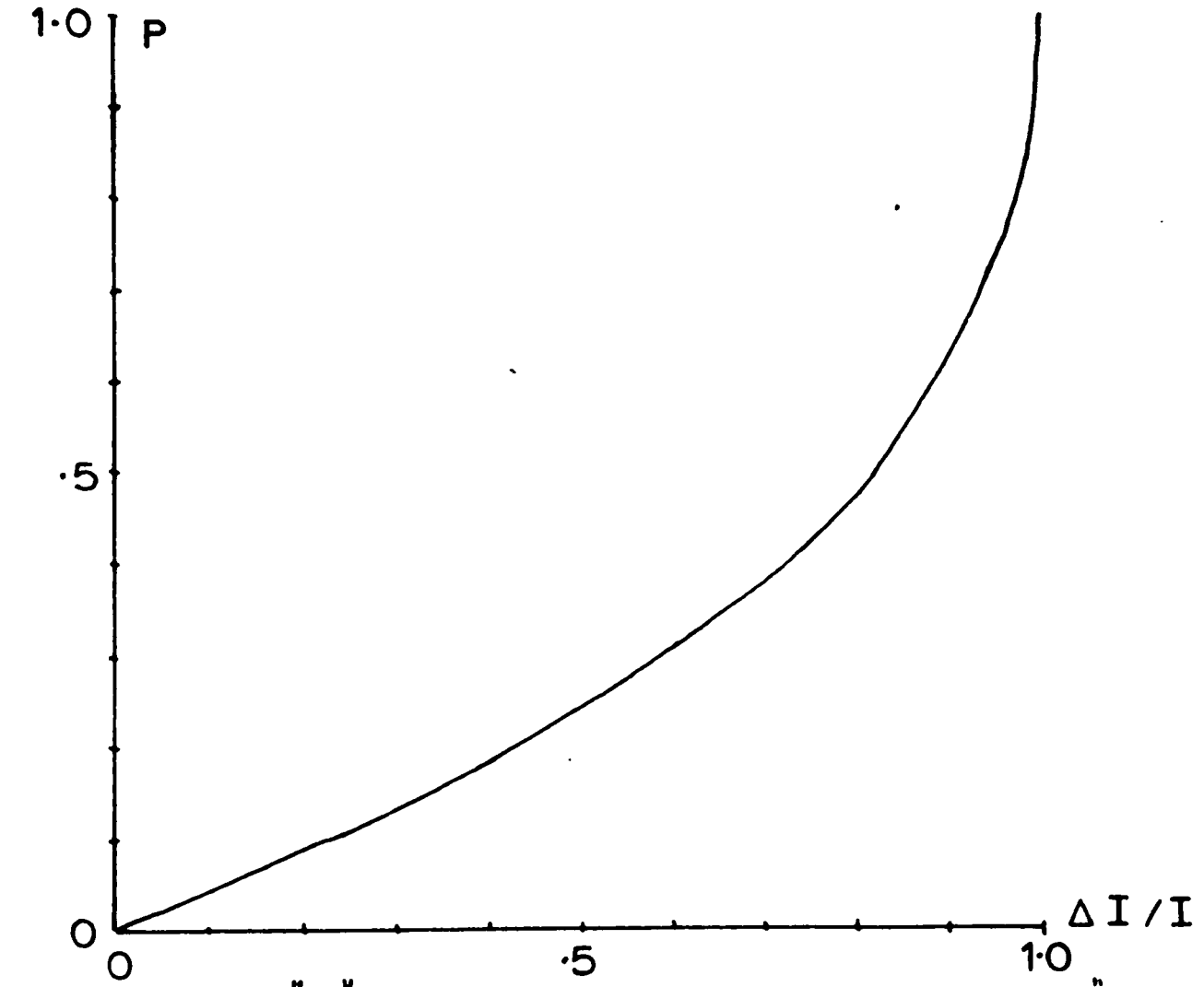
			$^3P_0$		$^3P_1$						$^3P_2$									
		F	1/2		3/2				1/2		5/2						3/2			
	F	M_F	1/2	-1/2	3/2	1/2	-1/2	-3/2	1/2	-1/2	5/2	3/2	1/2	-1/2	-3/2	-5/2	3/2	1/2	-1/2	-3/2
$^3S_1$	1/2	1/2	2·5	5	1625	10·8	5·4		3·17	6·33							·5	·33	·17	
		-1/2	5	2·5		5·4	10·8	1625	6·33	3·17								·17	·33	·5
	3/2	3/2	4·75		·3	·2			4·75		1·67	6·67	1·67				9·75	6·5		
		1/2	3·17	1·58	·2	·03	·27		3·17	1·58		10	10	5				6 5	1·1	8·7
		-1/2	1·58	3·17		·27	·03	·2	1·58	3·17			5	10	10			8·7	1·1	6·5
		-3/2		4·75			·2	·3		4·75				1·67	6·67	16·7			6·5	9·75

PERTURBED RELATIVE TRANSITION PROBABILITIES IN HE^3



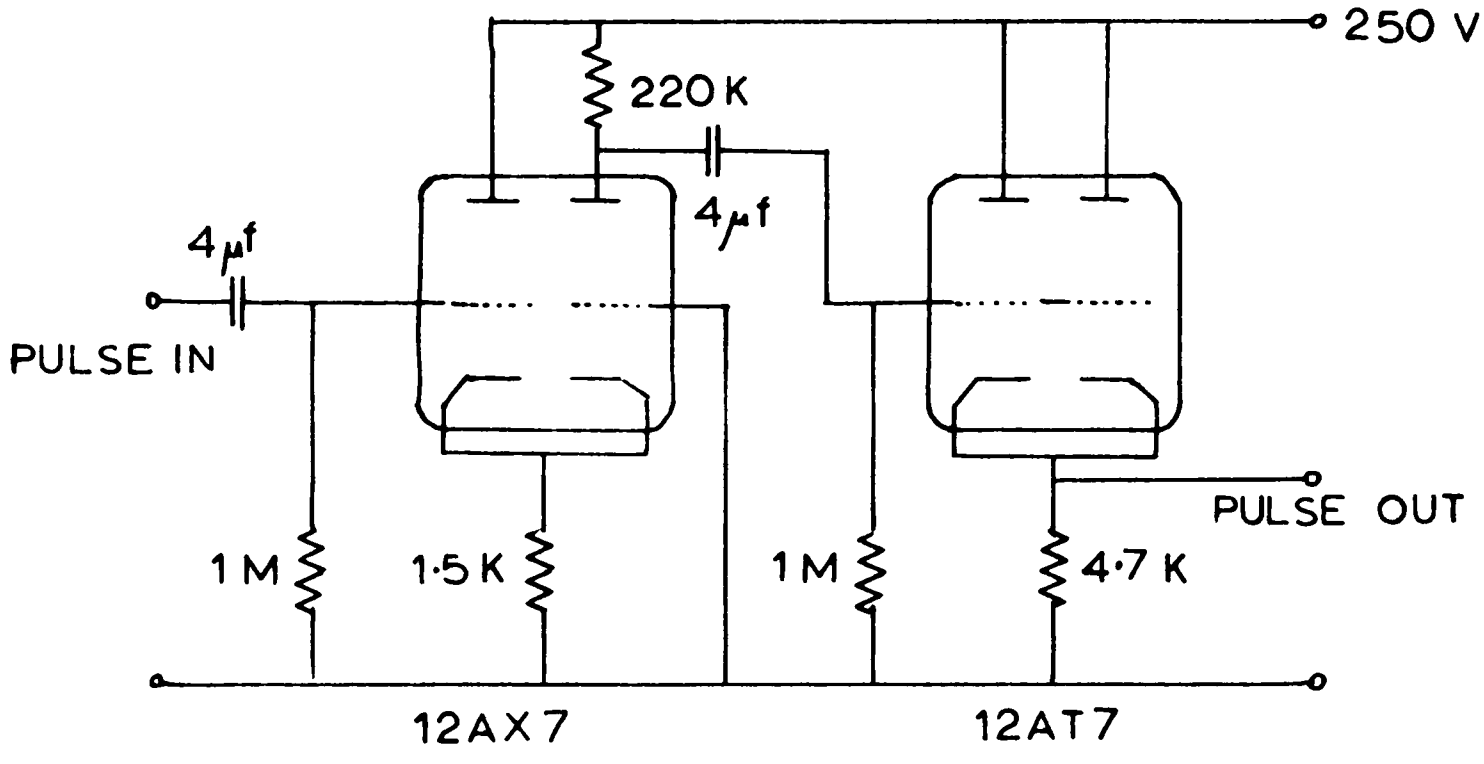
23b. APPARATUS WITH SUBSIDIARY LAMP

p. 5.4



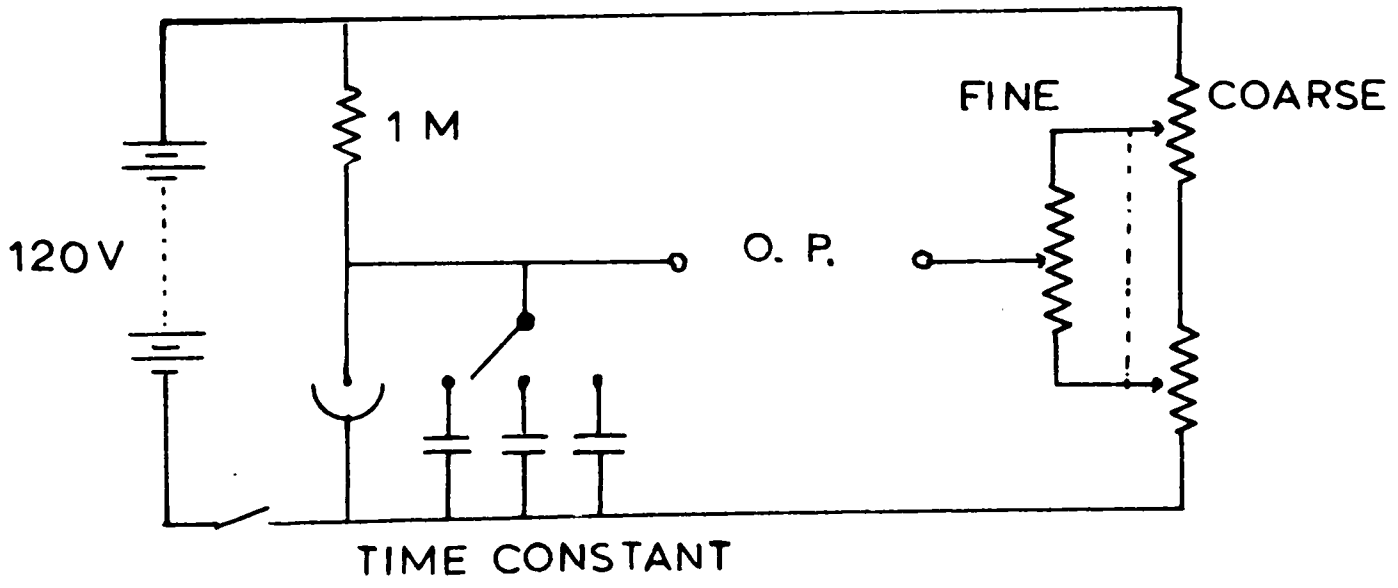
23a "P" AS A FUNCTION OF "ΔI/I"

p.4.14



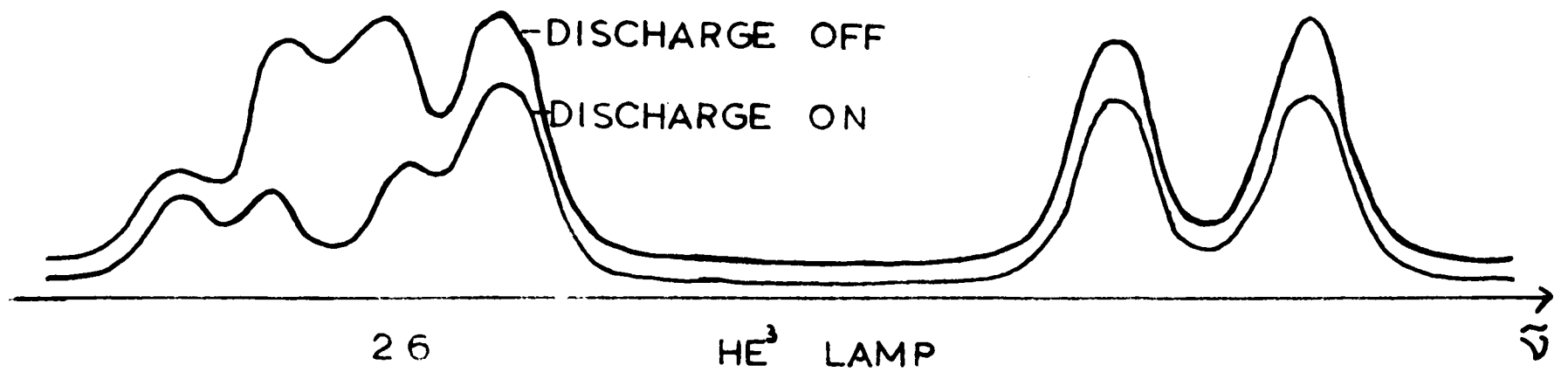
24 PULSE AMPLIFIER

p. 5.9

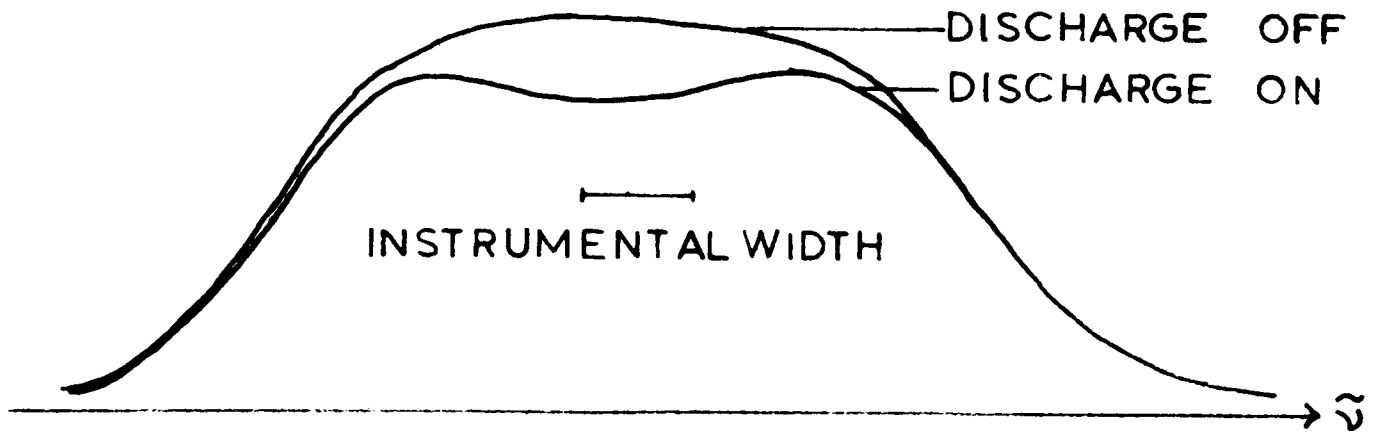


25 D.C. PHOTOCELL CIRCUIT

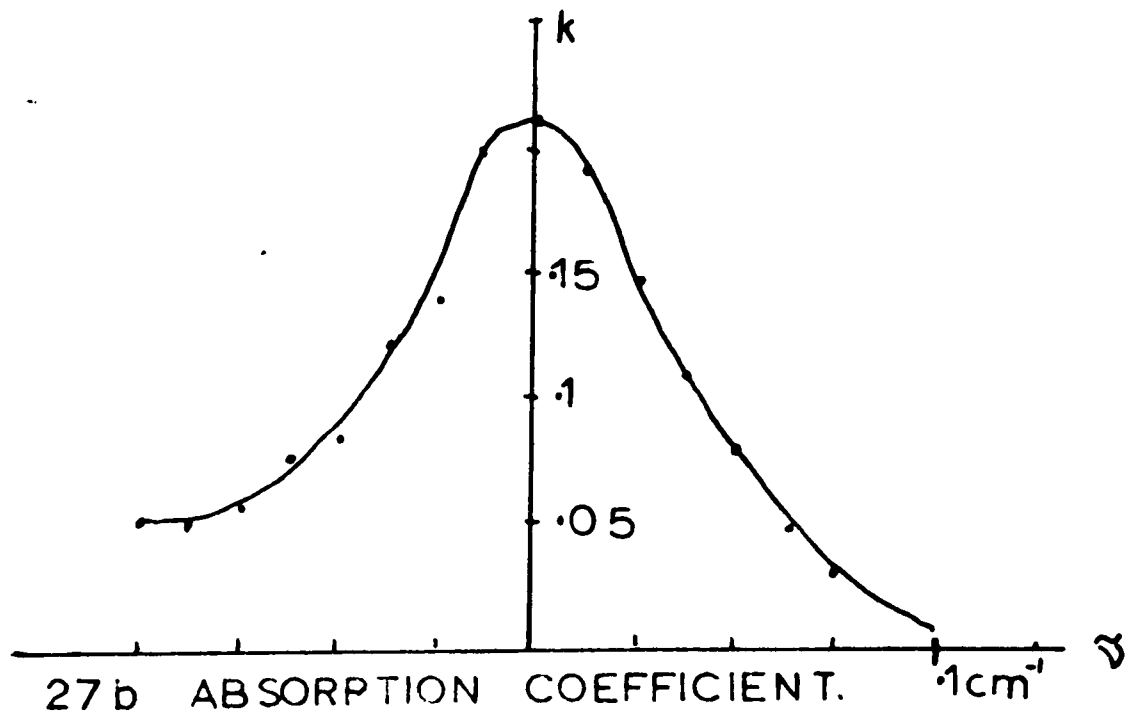
p. 5.9



26 HE^3 LAMP

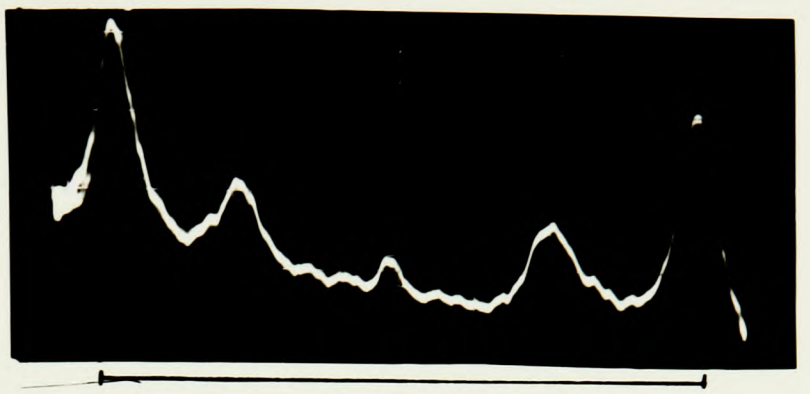


27a HE^4 LAMP



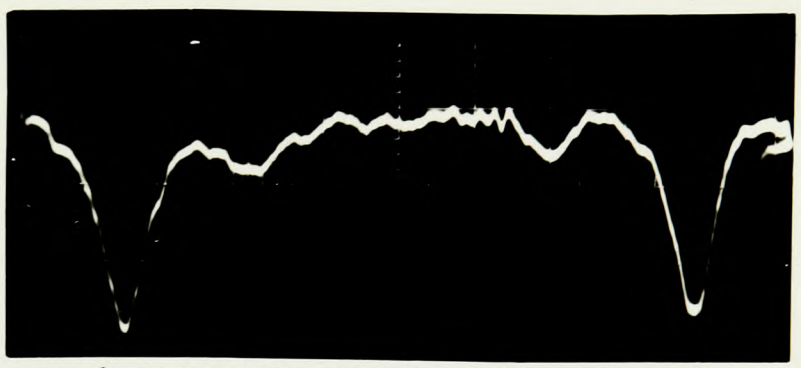
27b ABSORPTION COEFFICIENT.

26, 27a,b ABSORPTION IN HE^3 DISCHARGE



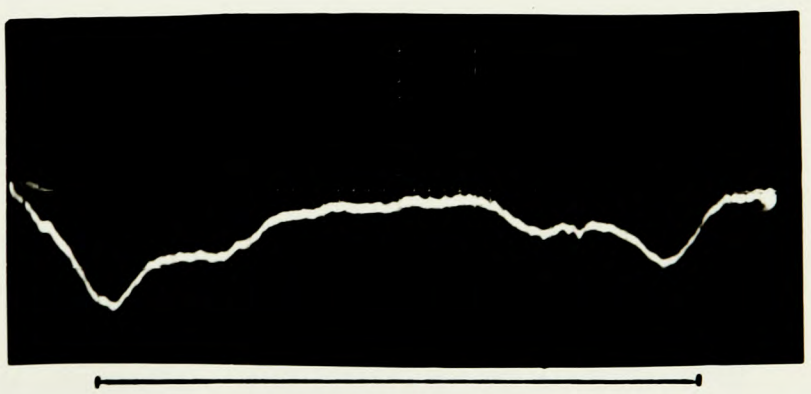
1 G.

28 ·1 mm. Hg. Cell.
1·5mm. Hg. He^3 Lamp.



1 G

29 ·1mm. Hg. Cell.
2 mm. Hg. He^4 Lamp.

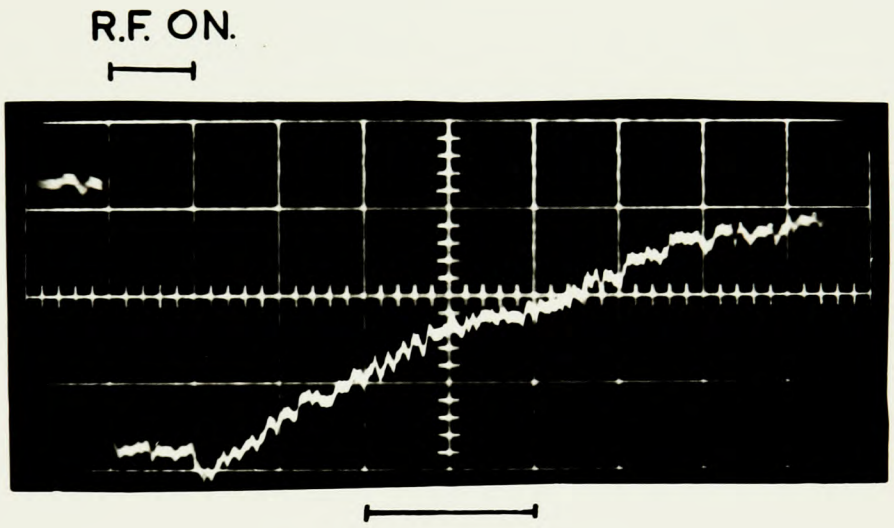


1 G

30 ·33mm. Hg. Cell.
2mm Hg. Cell He^4 Lamp.

28.29.30. RESONANCES IN He^3 $^3S_1$ METASTABLE LEVEL

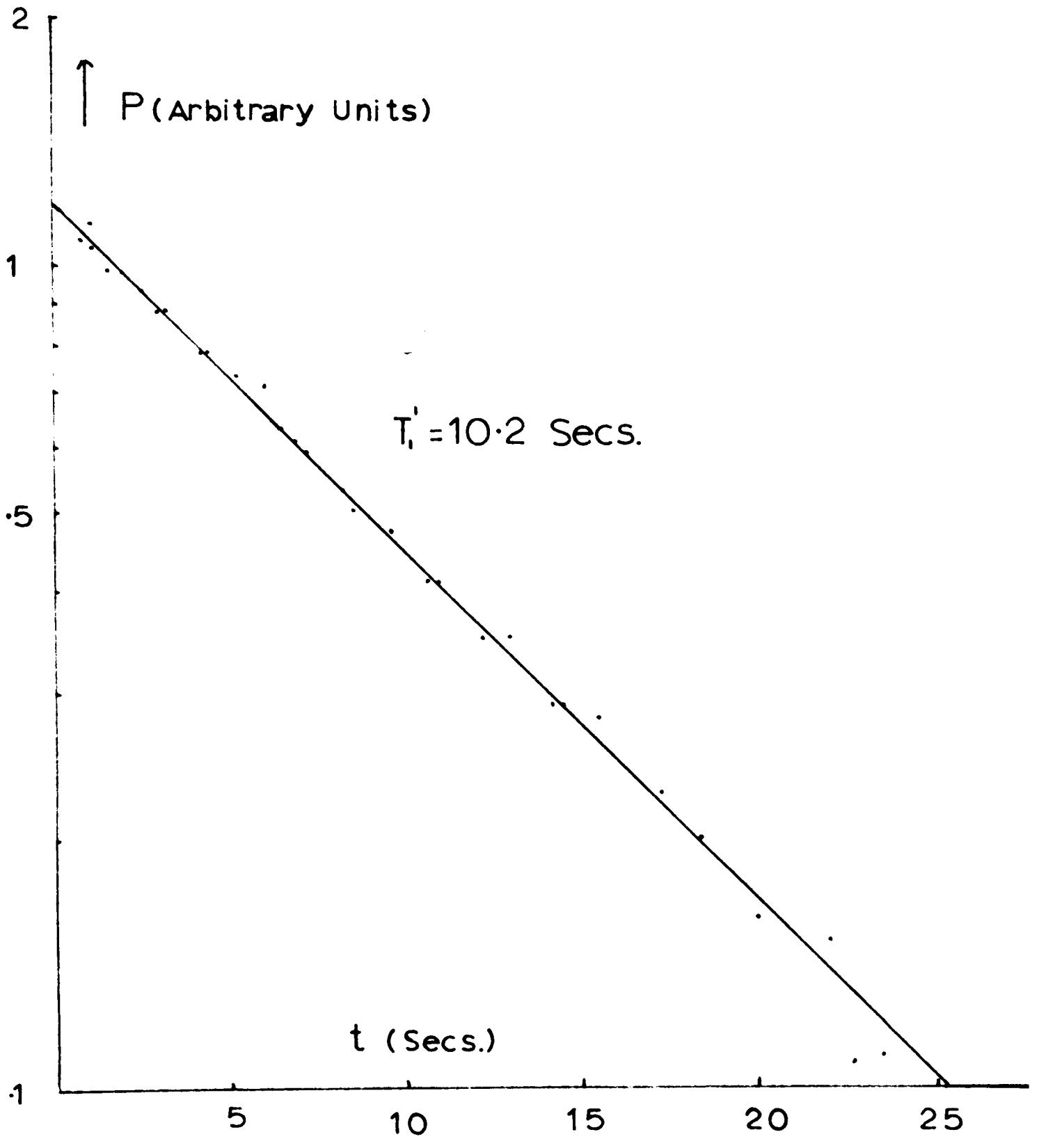
$H_1 \sim 25$ mG.



31 PUMPING TRANSIENT IN He^3

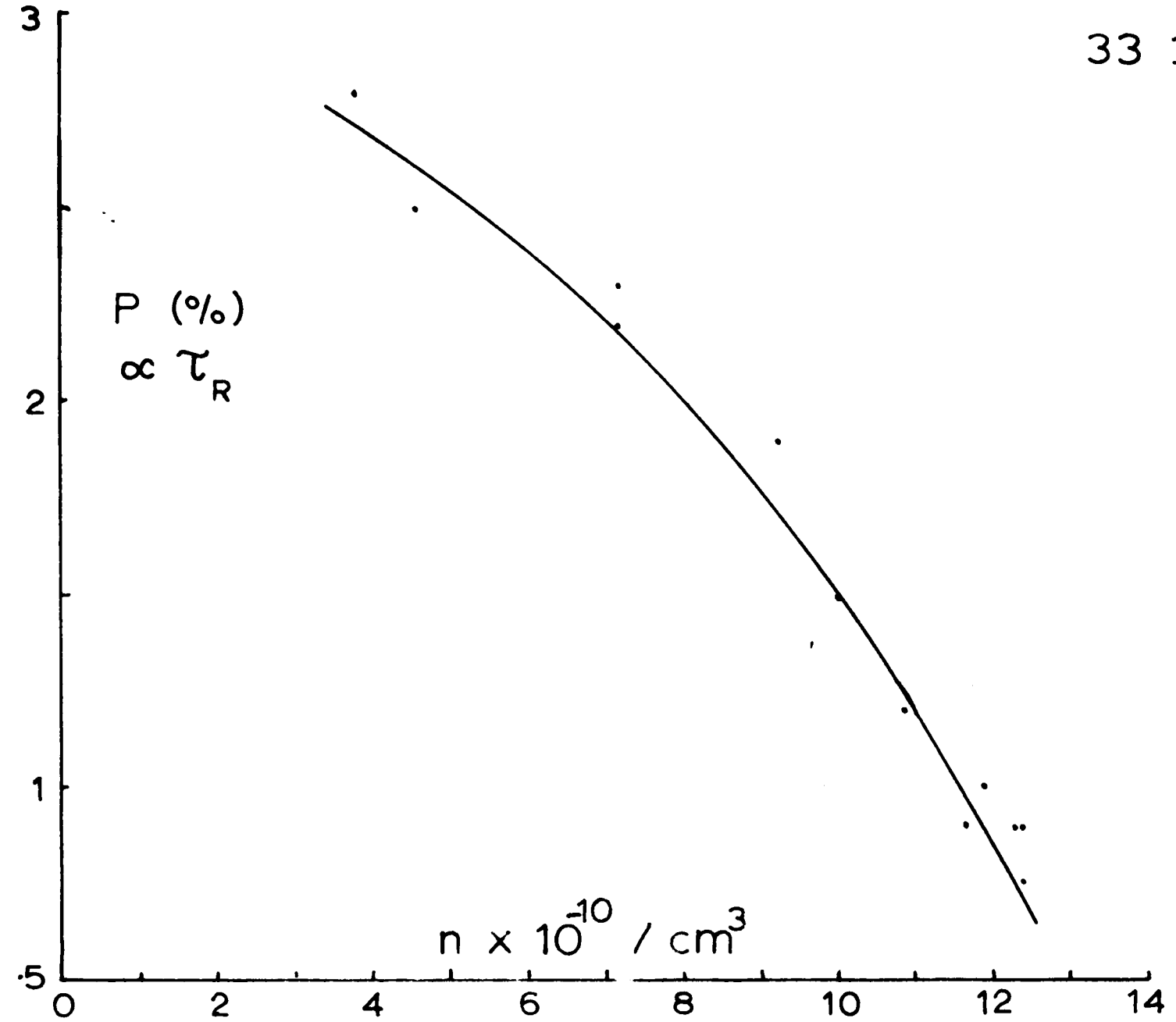
1mm. Hg. Cell. $n \sim 9 \times 10^{16}/cm^3$.

p. 6.7



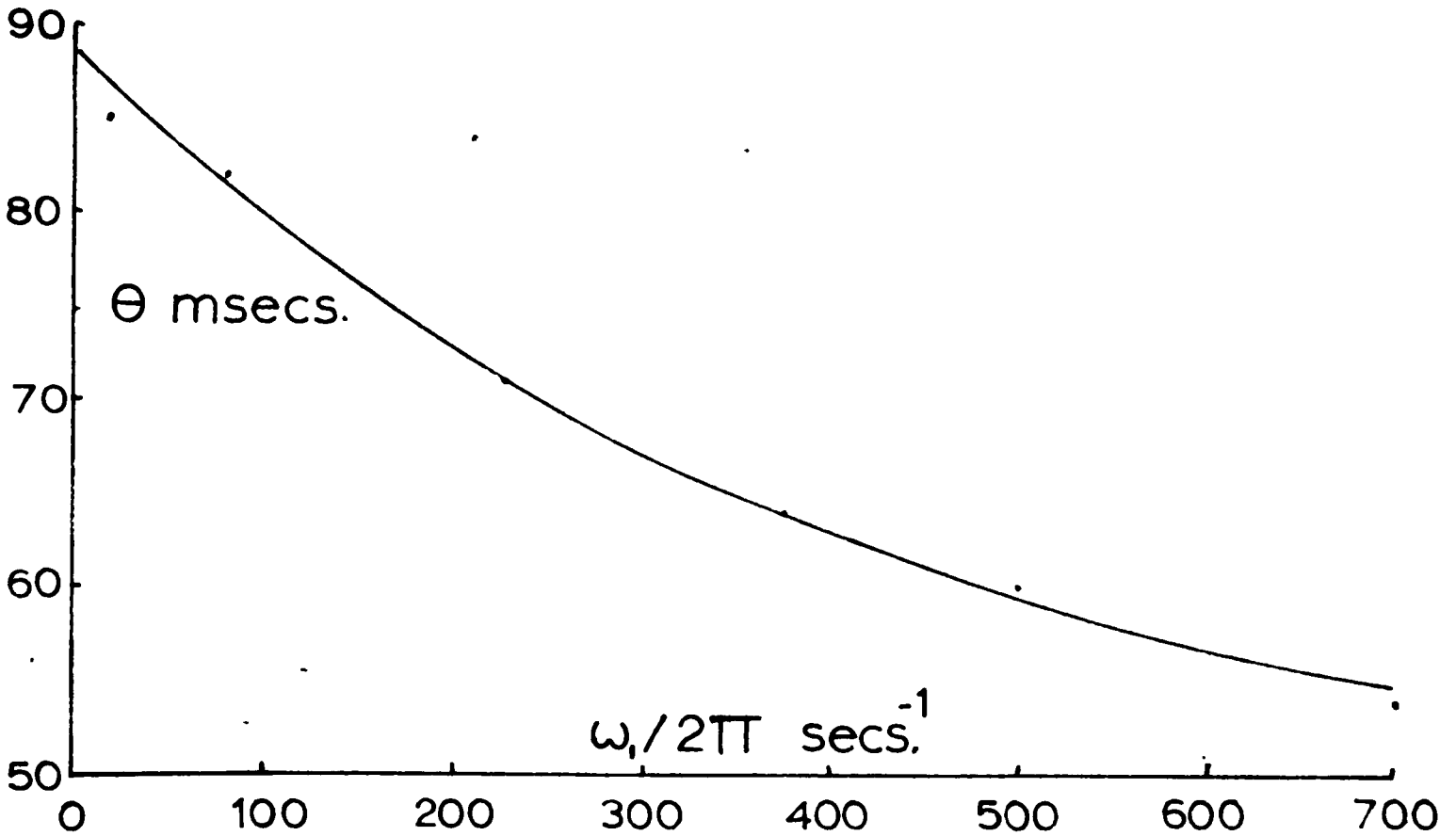
32 DECAY OF POLARIZATION
WITH DISCHARGE ON ($n \sim 10^{11}$)
1mm Hg Cell

33 35



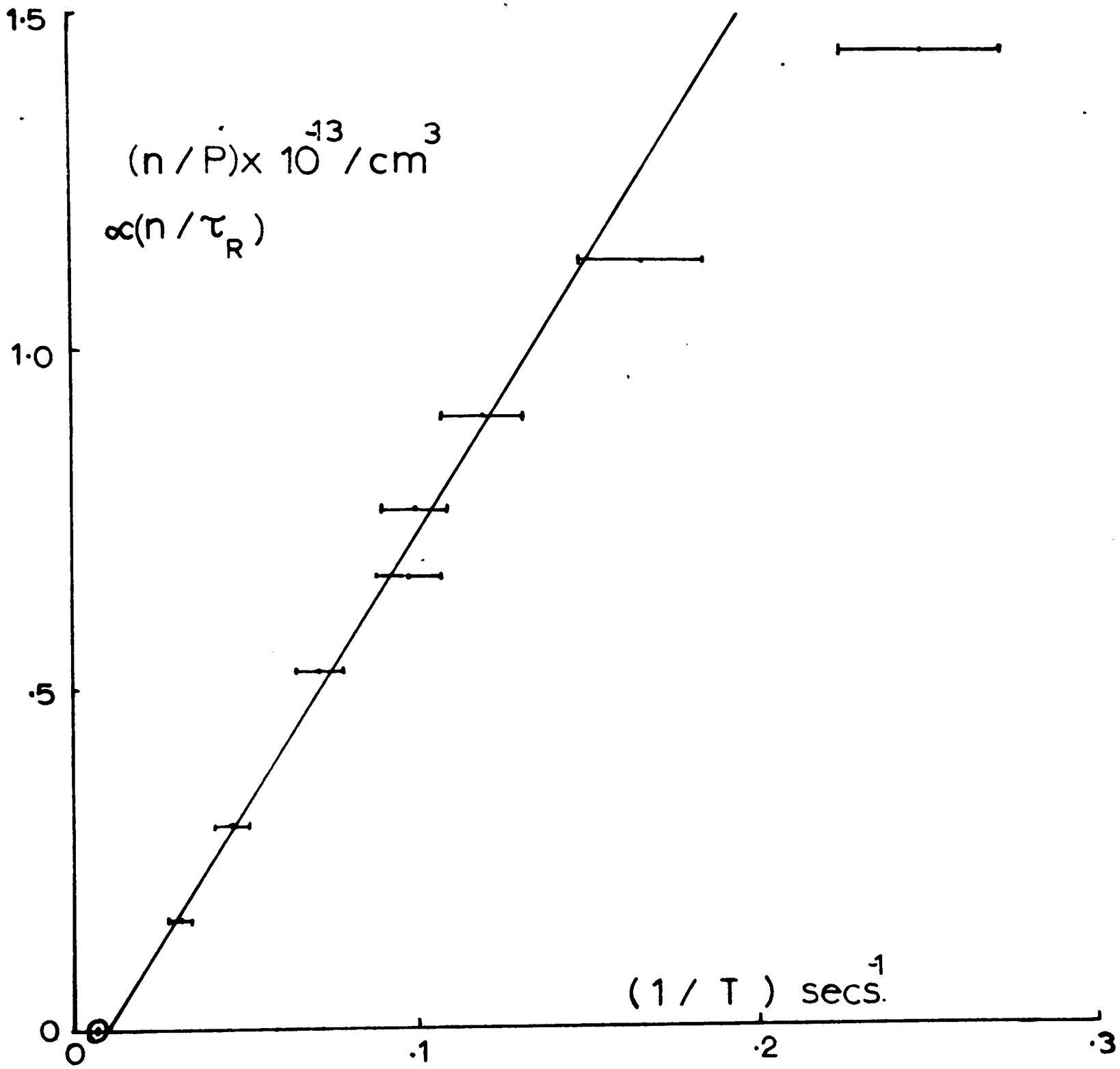
33. VARIATION OF POLARIZATION (AND HENCE τ_R) WITH METASTABLE DENSITY

p. 6.11

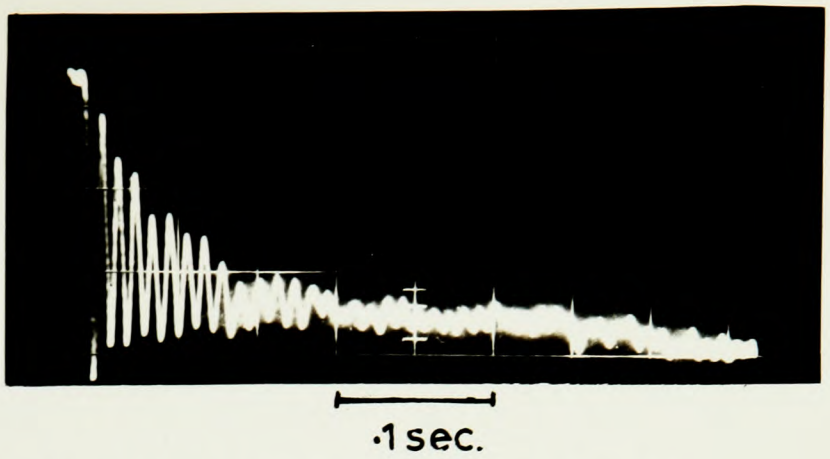


35 VARIATION OF θ WITH NUTATION FREQUENCY

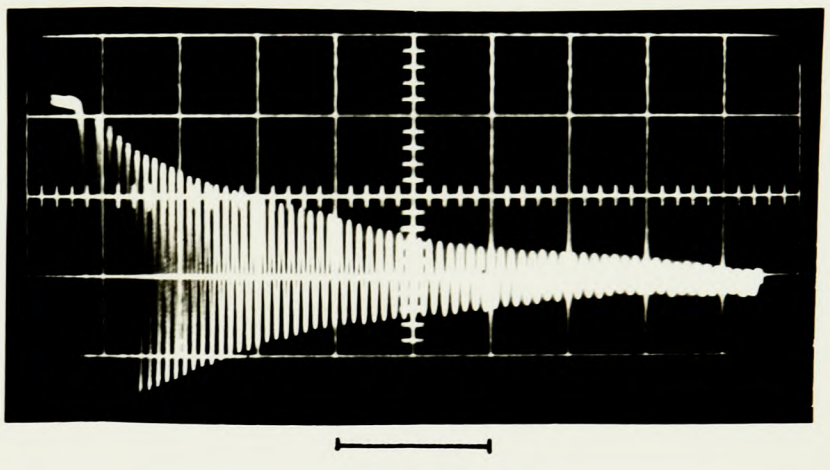
p.6.16



34 VARIATION OF T WITH METASTABLE DENSITY

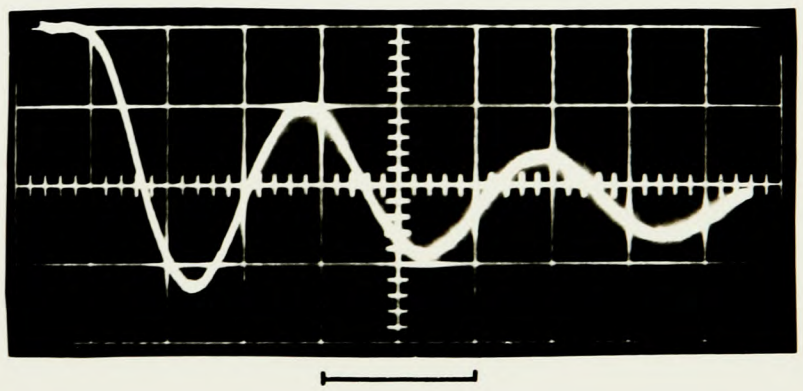


36a OFF-RESONANCE NUTATION



36b NUTATION AT RESONANCE

$\omega_1/2\pi$ = 375 c/sec. θ = 64 msecs.



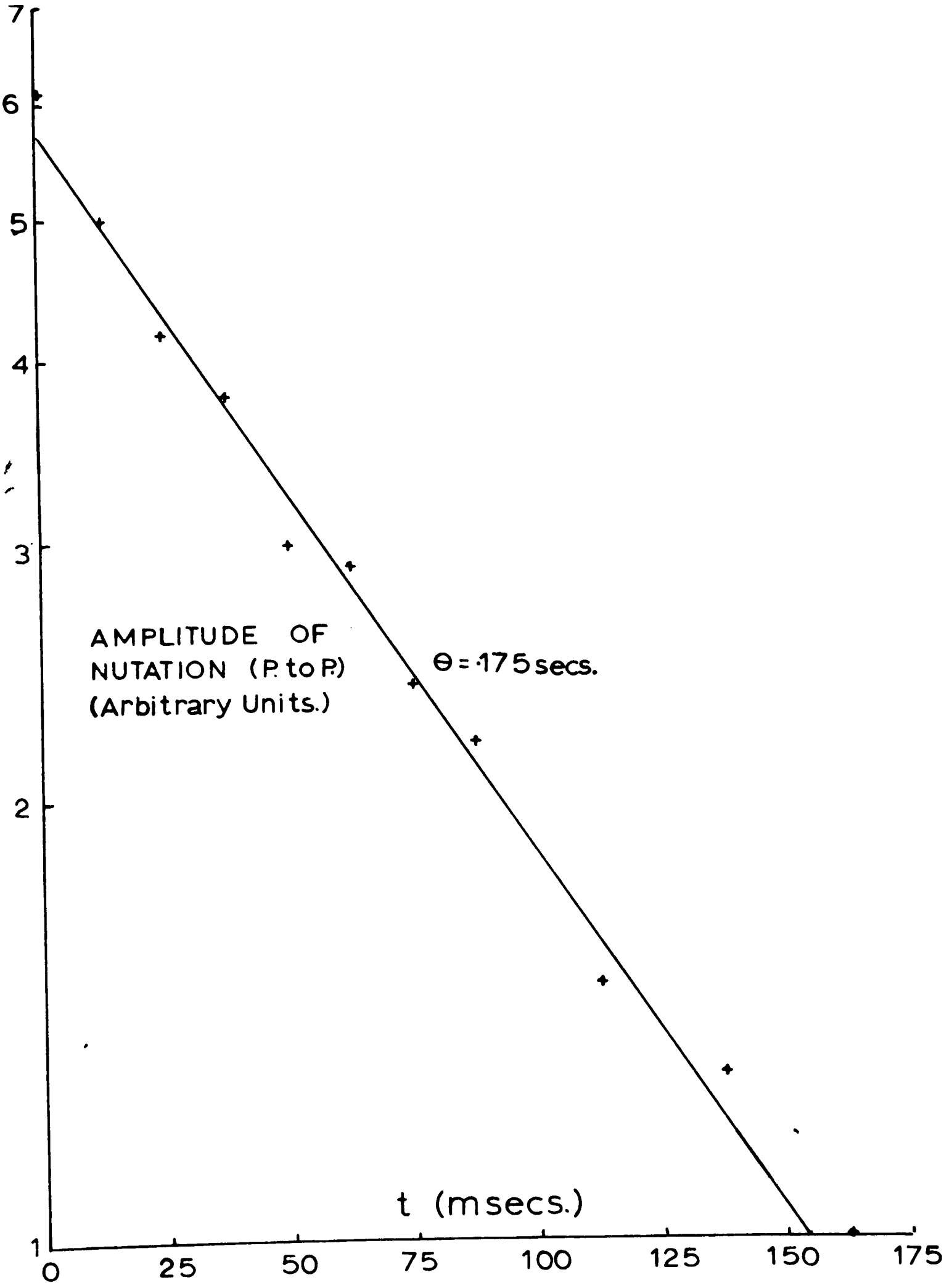
36c NUTATION AT RESONANCE

$\omega_1/2\pi$ = 17 c/sec. θ = 85 msecs.

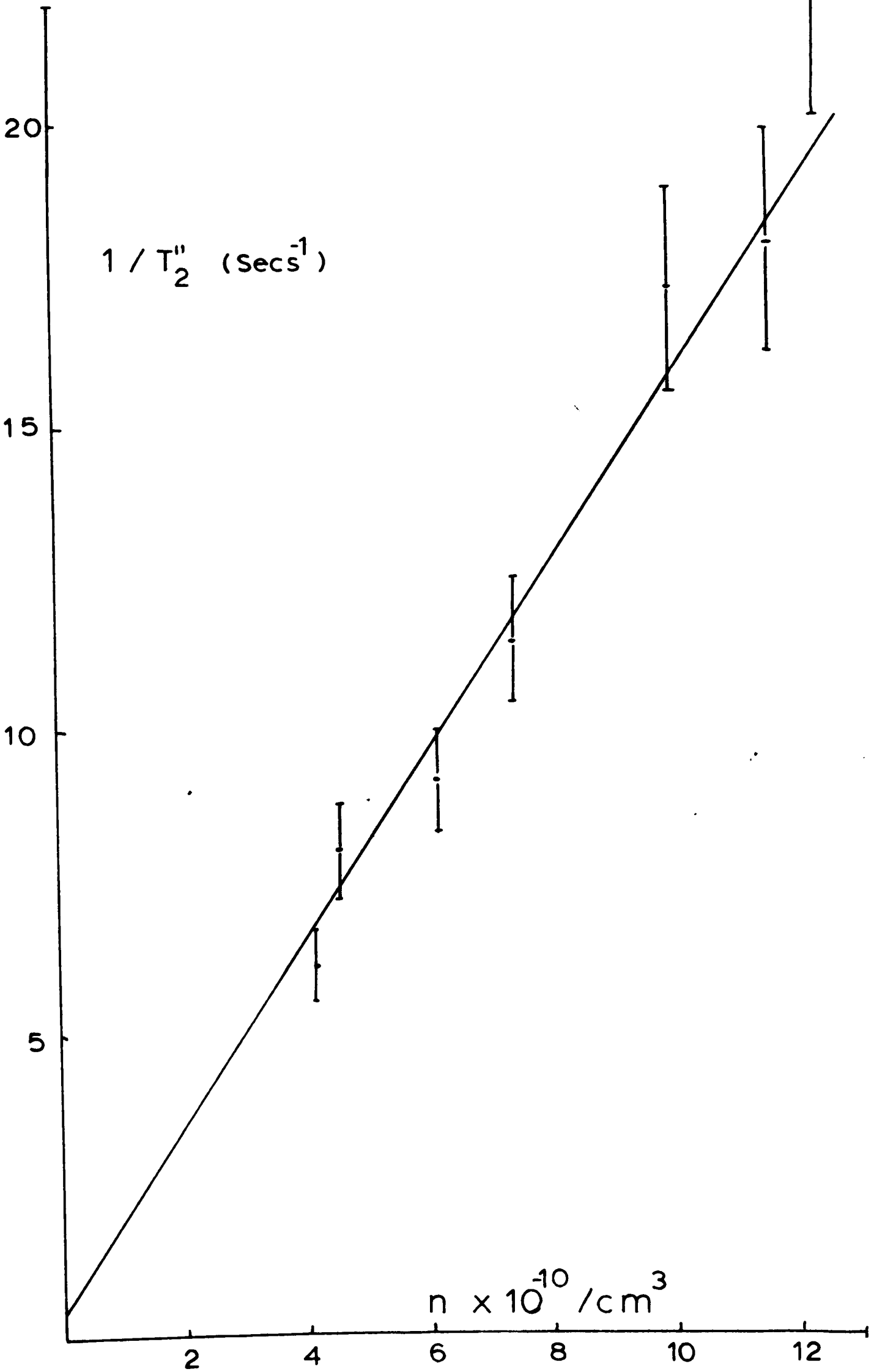
36 abc $1\,{}^1S_0$ NUTATION TRANSIENTS IN He^3

1mm. Hg. Cell $n \simeq 9 \times 10^{10}$ /cm^3

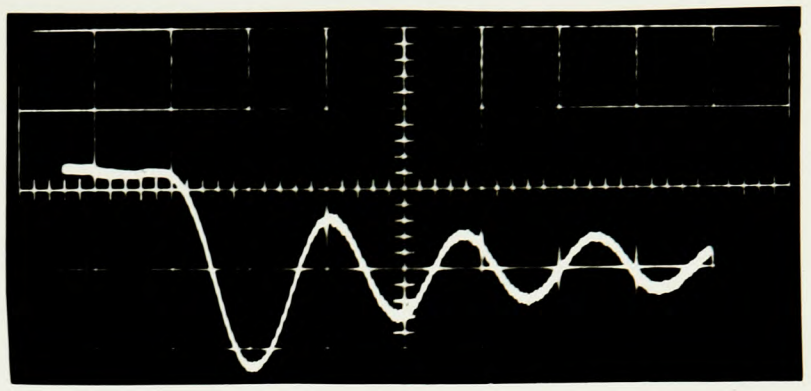
p. 6.16



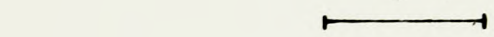
37 DECAY OF NUCLEAR NUTATION
WITH DISCHARGE ON
1 mm. Hg. Cell $n \simeq 7{\cdot}4 \times 10^{10}\ cm^{-3}$
p 6.16



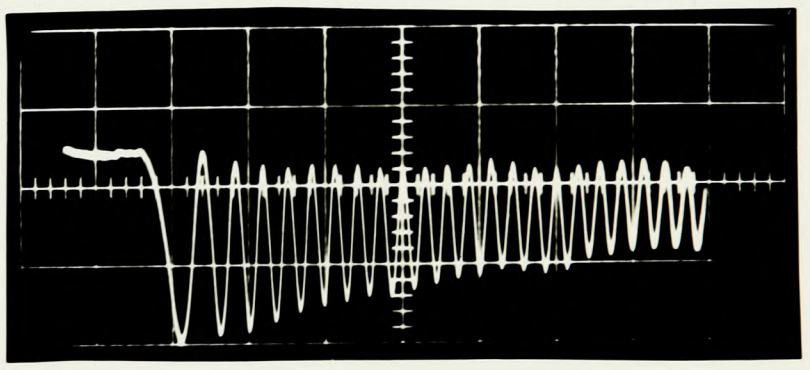
38 VARIATION OF T_2'' WITH METASTABLE DENSITY



39a $\omega = \omega_0/3$ $H_1 \simeq .22$ G



10 msecs.

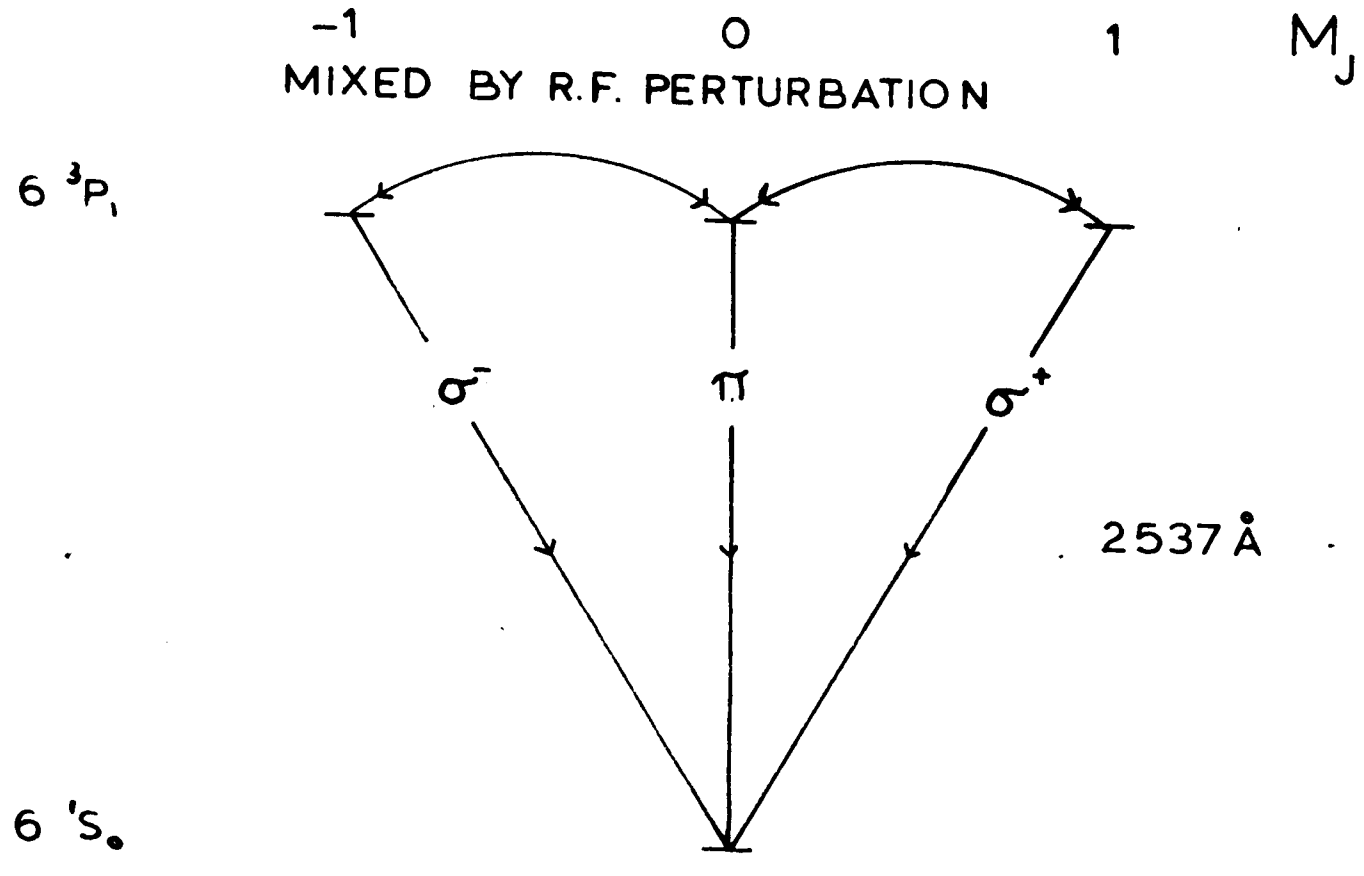


39 b $\omega = \omega_0$ $H_1 \simeq .22$ G

39ab He^3 1^1S_0 TRIPLE QUANTUM TRANSITION

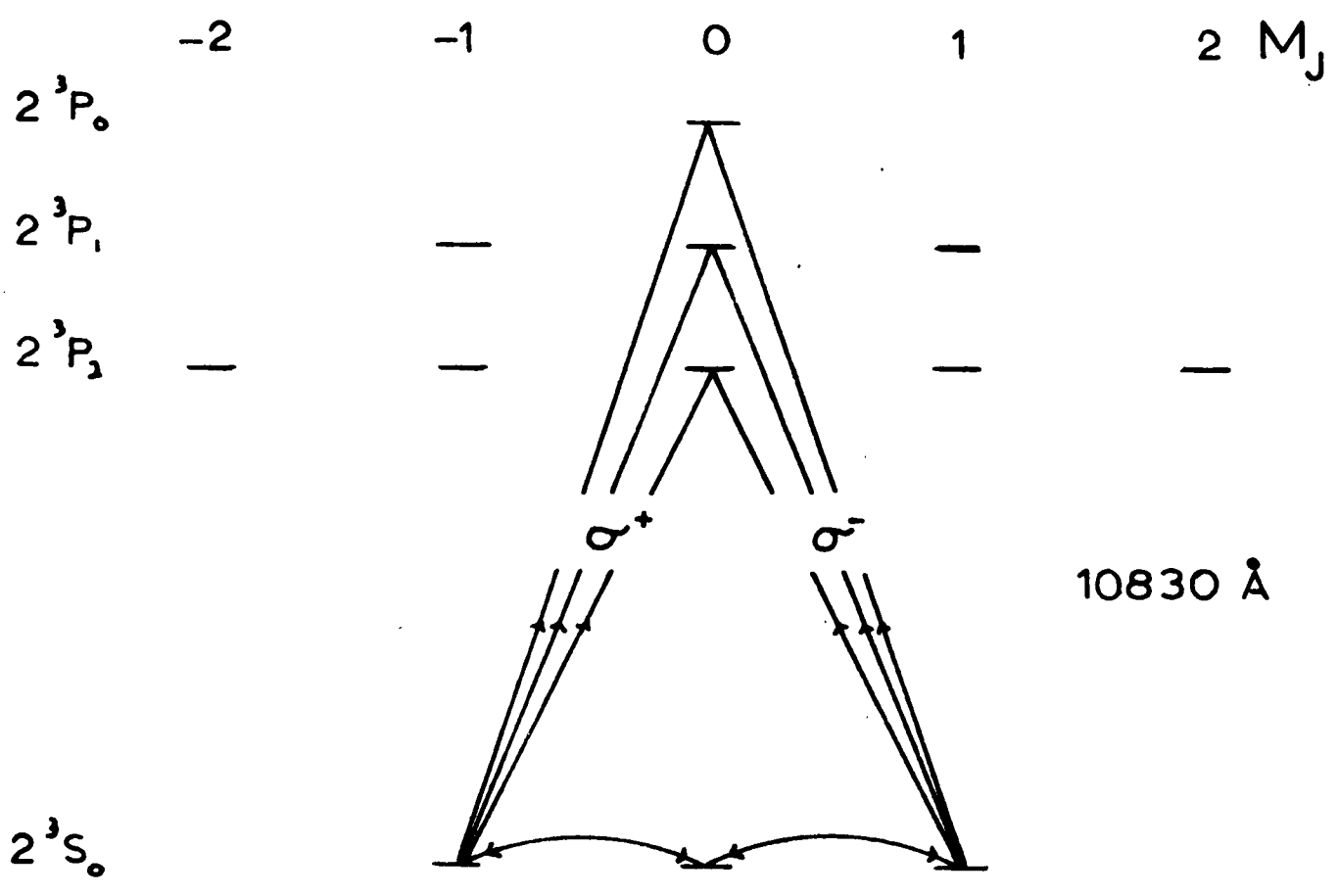
1 mm. Hg. Cell. ω = 1·6 kcs./sec.

p. 6,20



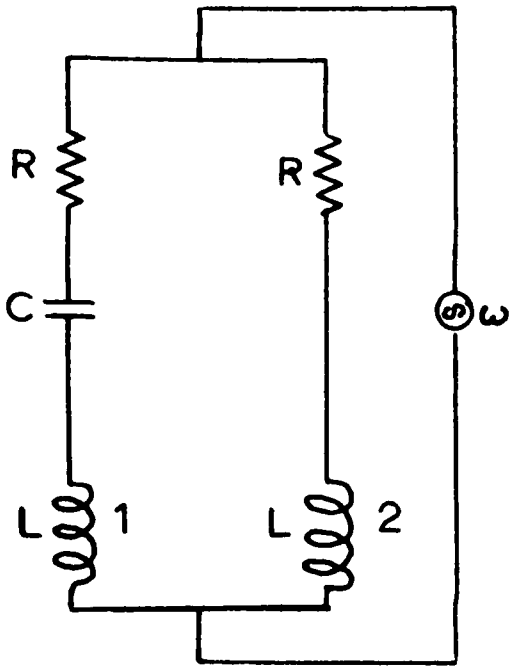
40 MODULATION OF HG. FLUORESCENCE

p.7.1

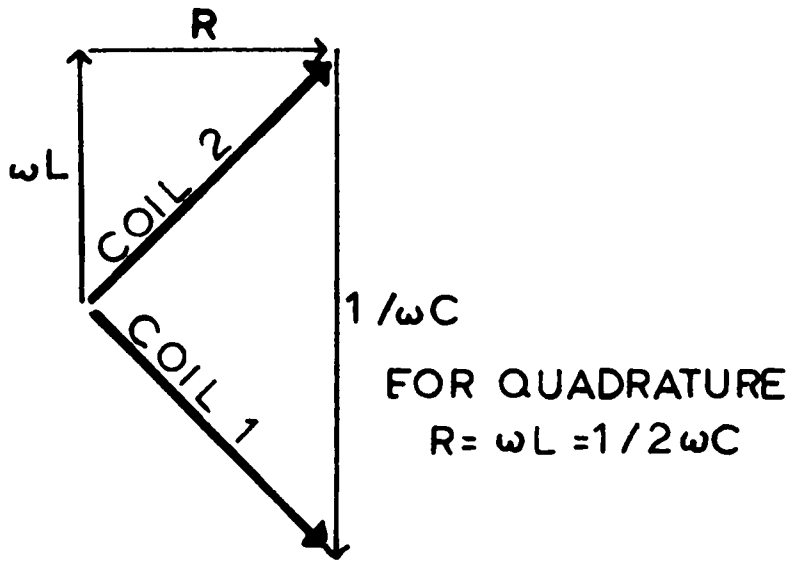


41 MODULATION OF HE^4 ABSORPTION

p.7.2



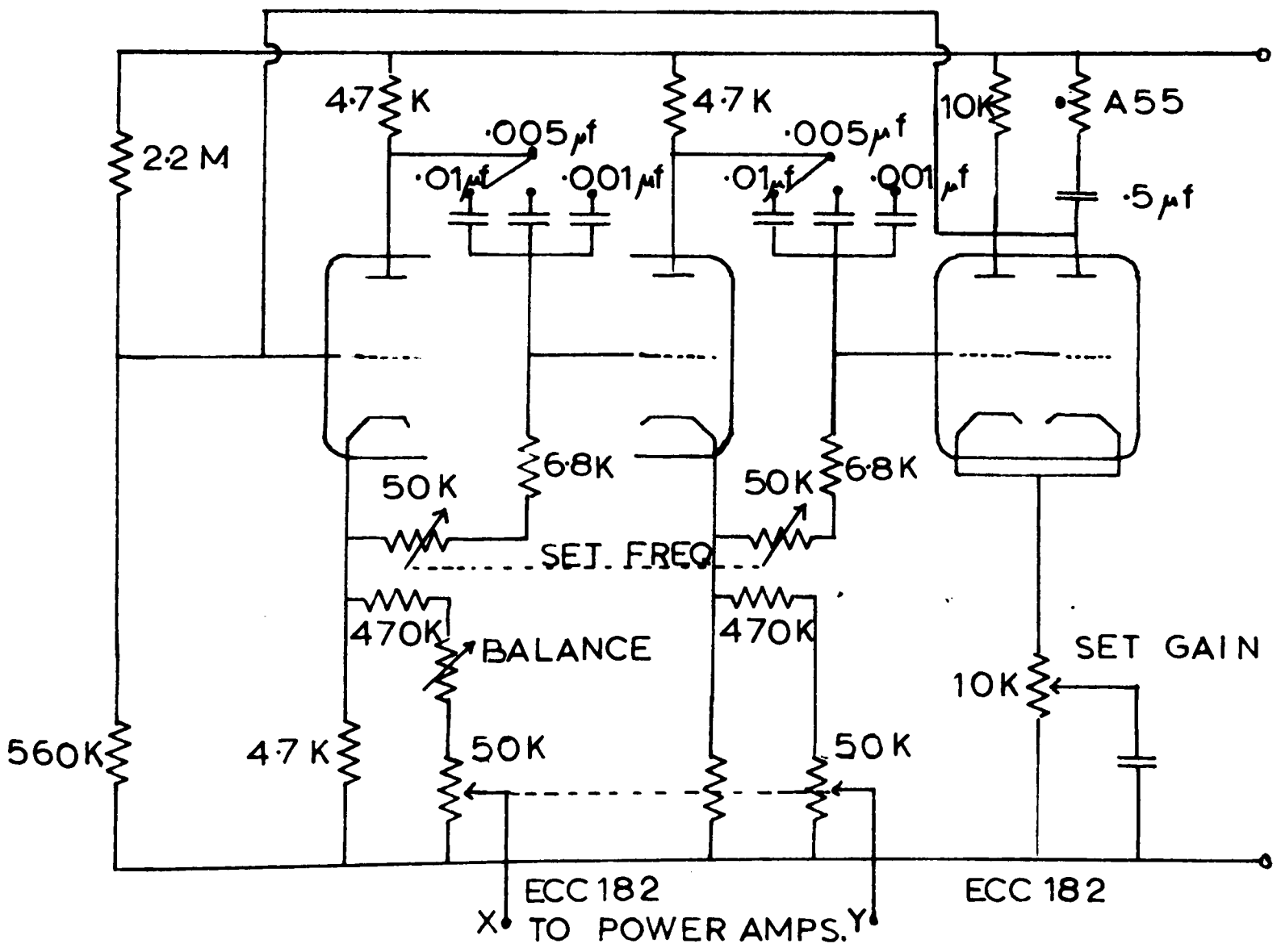
CIRCUIT



PHASE DIAGRAM

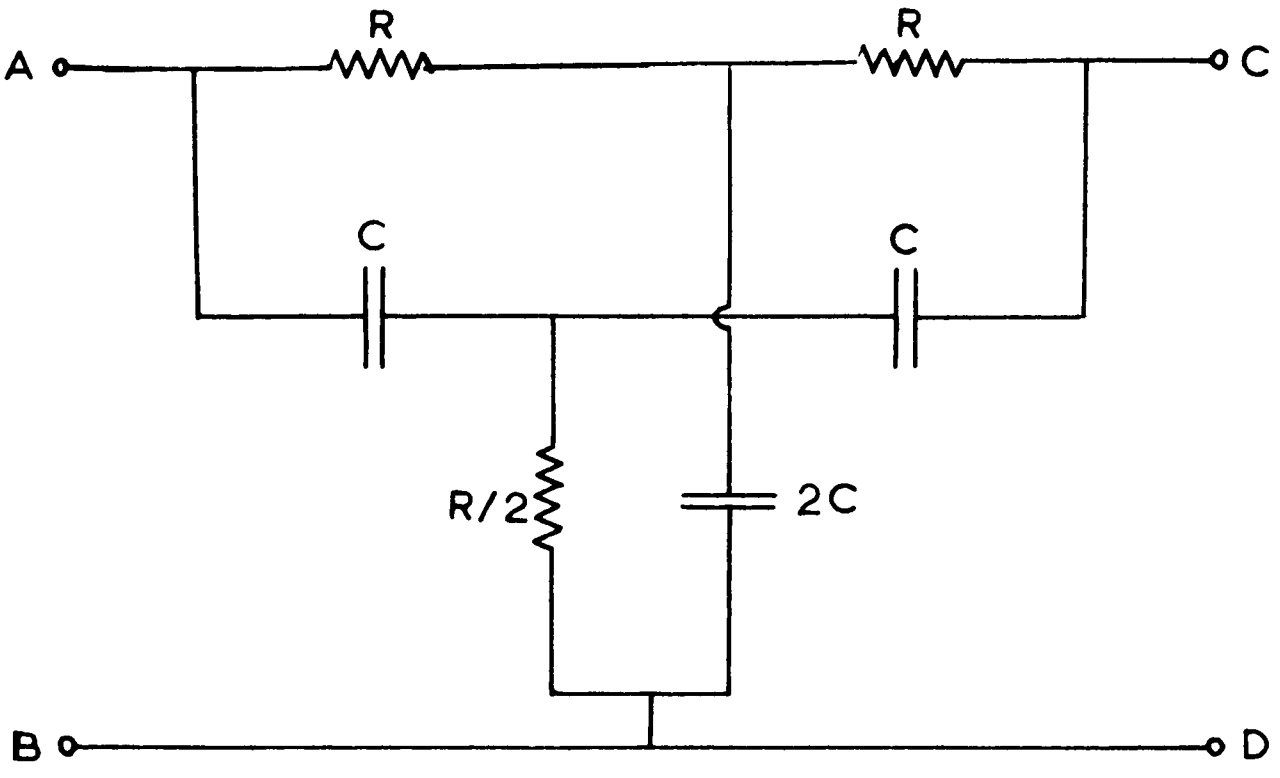
42 a PASSIVE NETWORK FOR ROTATING FIELD

p. 8.4



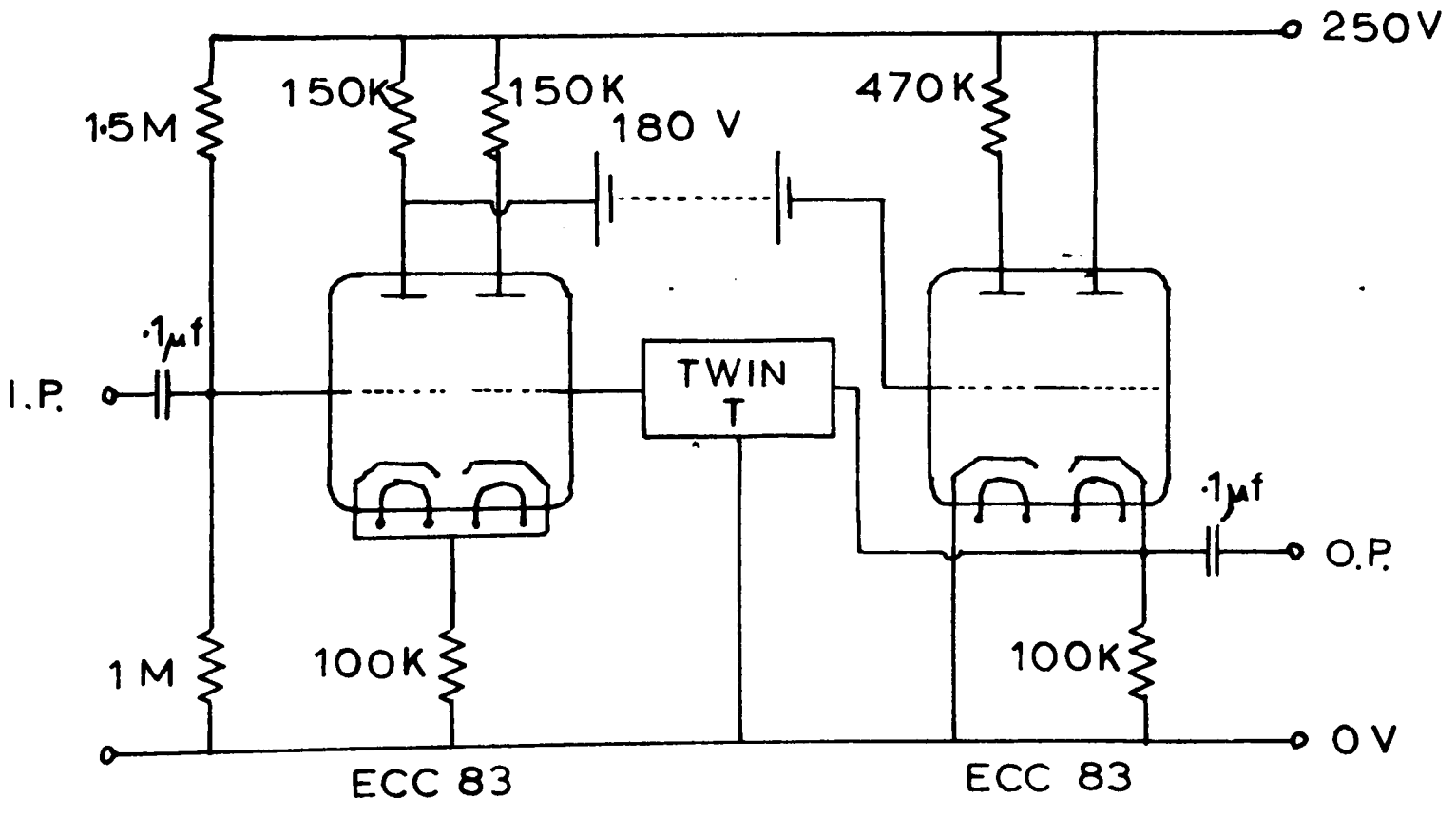
42b TWO PHASE OSCILLATOR

p. 8.4



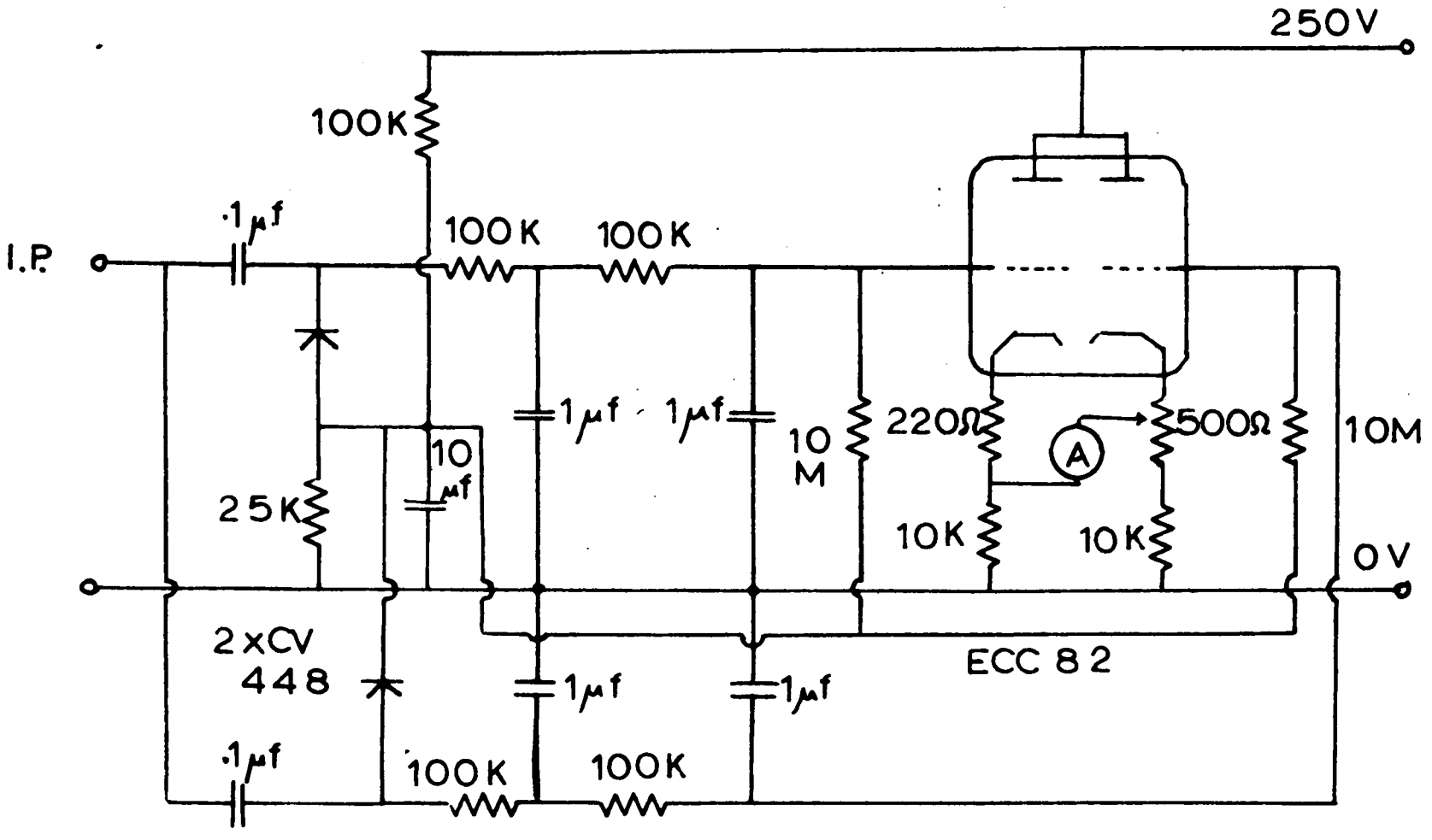
43a TWIN T NETWORK

p.8.5



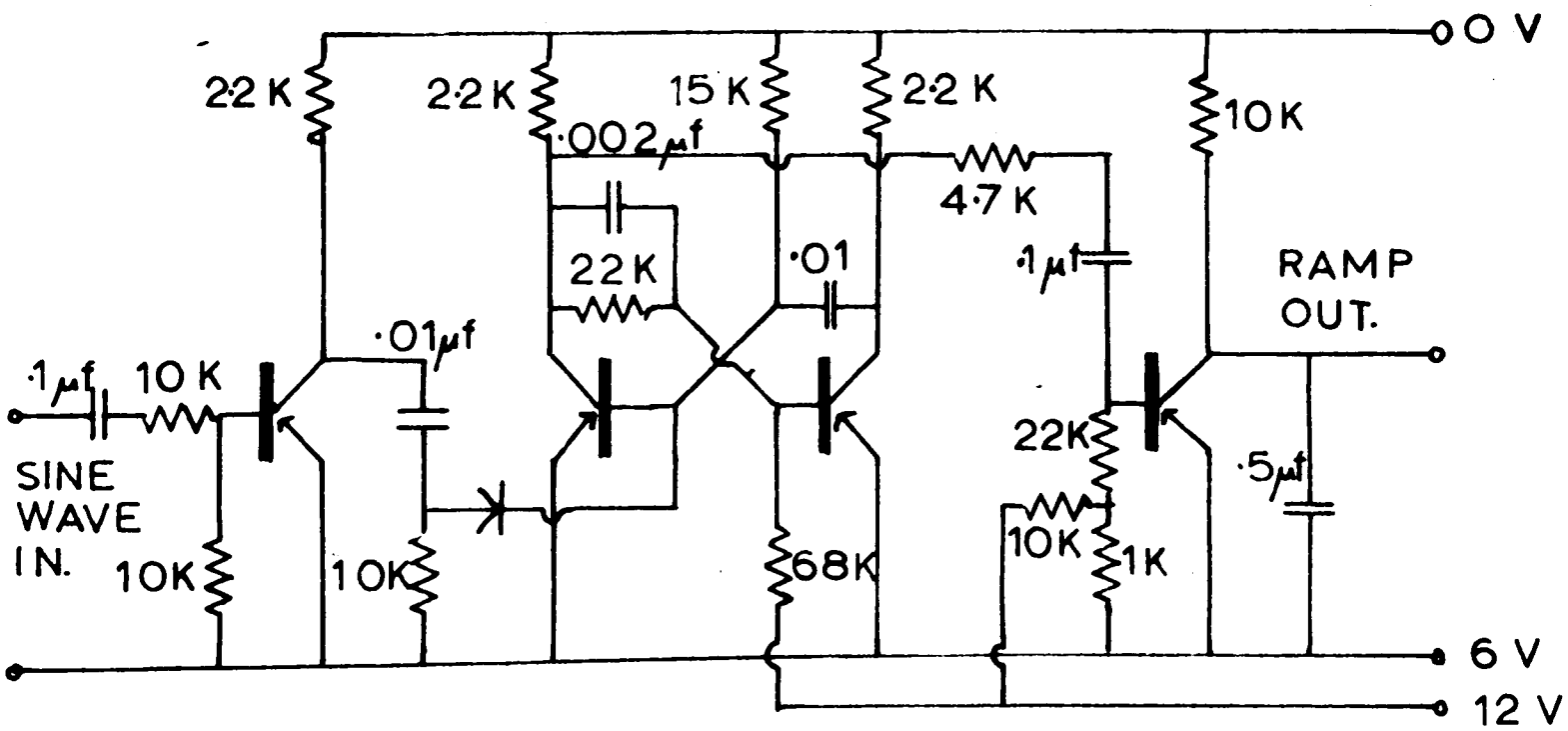
43b TWIN T NARROW BAND AMPLIFIER

p.8.5



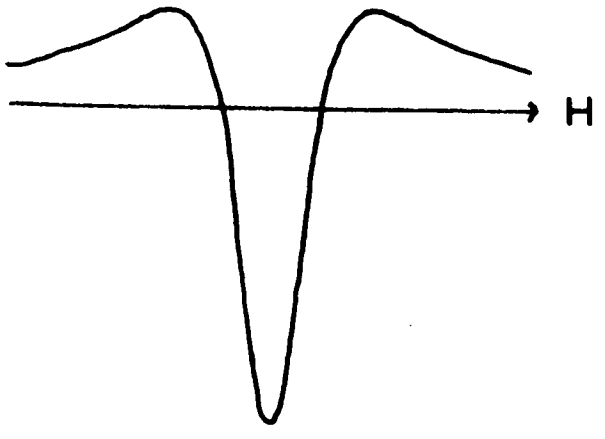
44 DETECTOR

p. 8.6



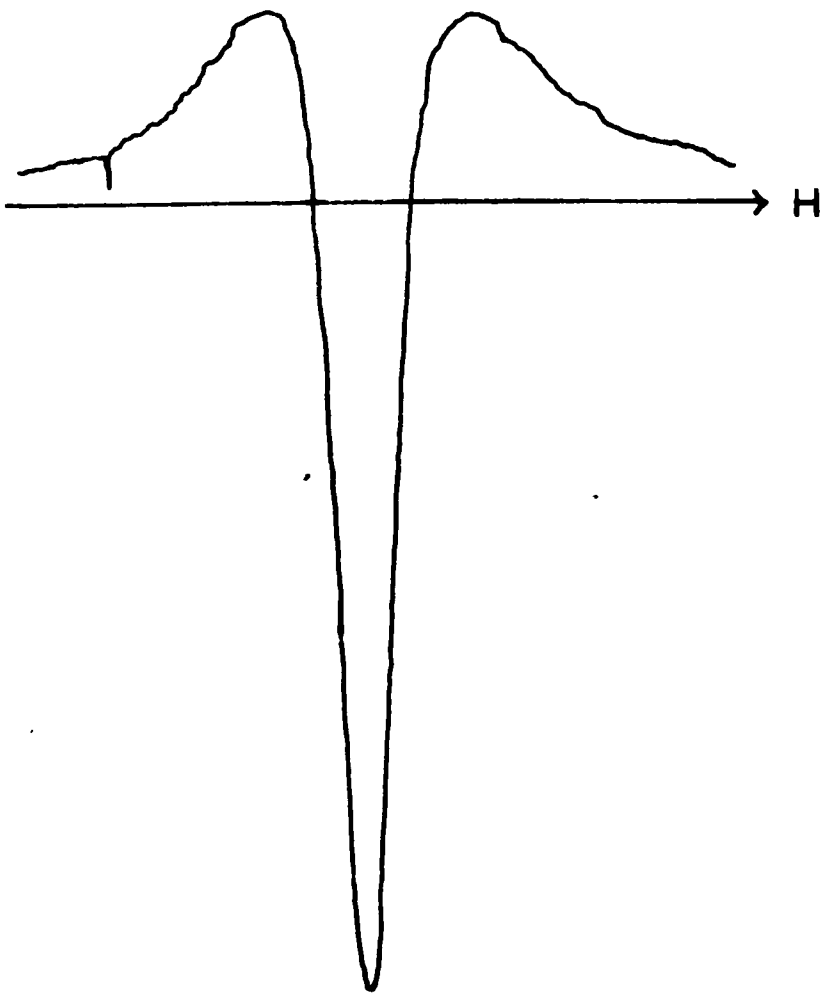
45 RAMP WAVE-FORM GENERATOR

p. 6.7



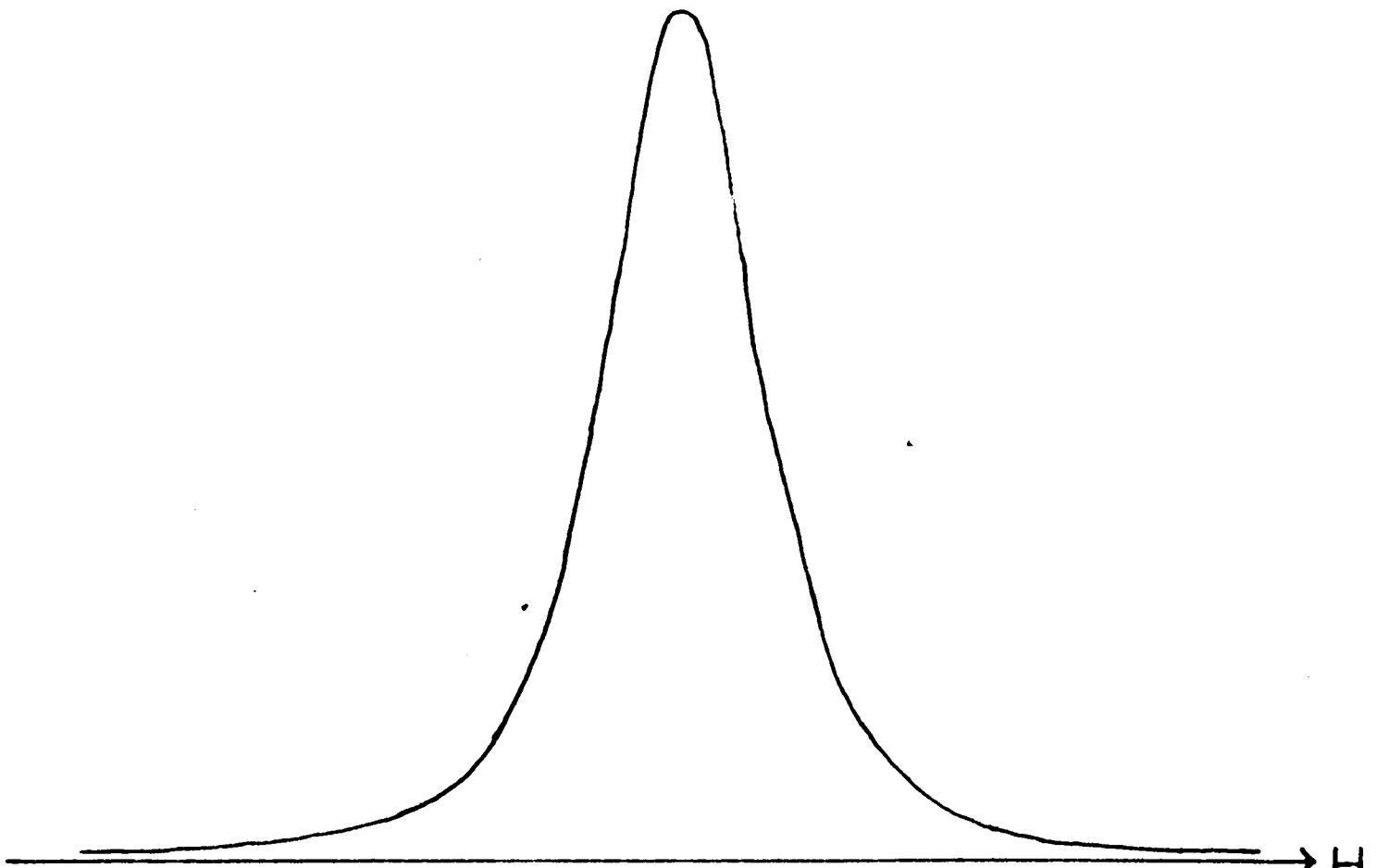
46a THEORETICAL CURVE 'D'

p. 7.7



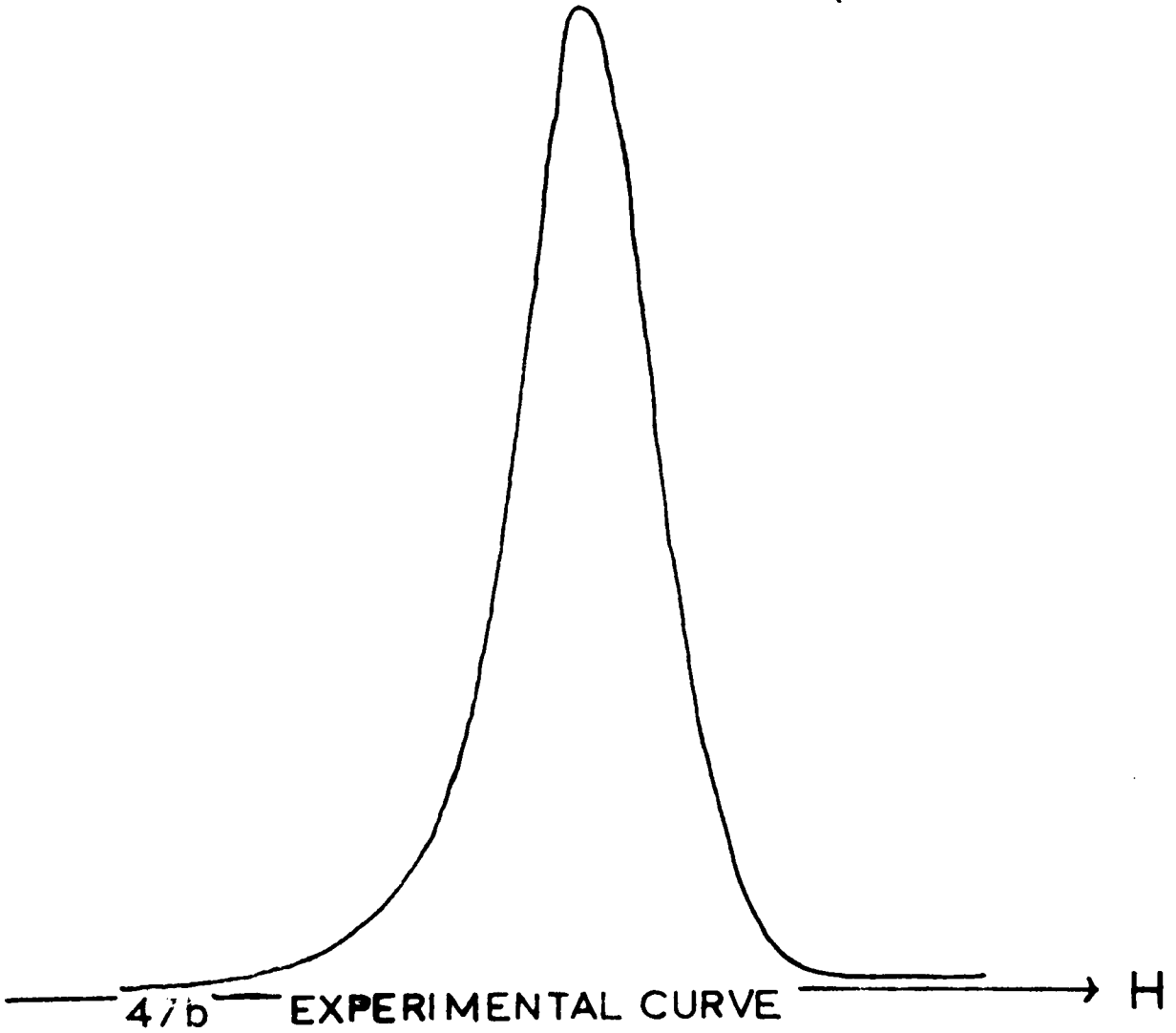
46b EXPERIMENTAL CURVE
P.S.D. Trace of modulation amplitude.

46ab MODULATION AT $2\omega_0$ p. 9.2



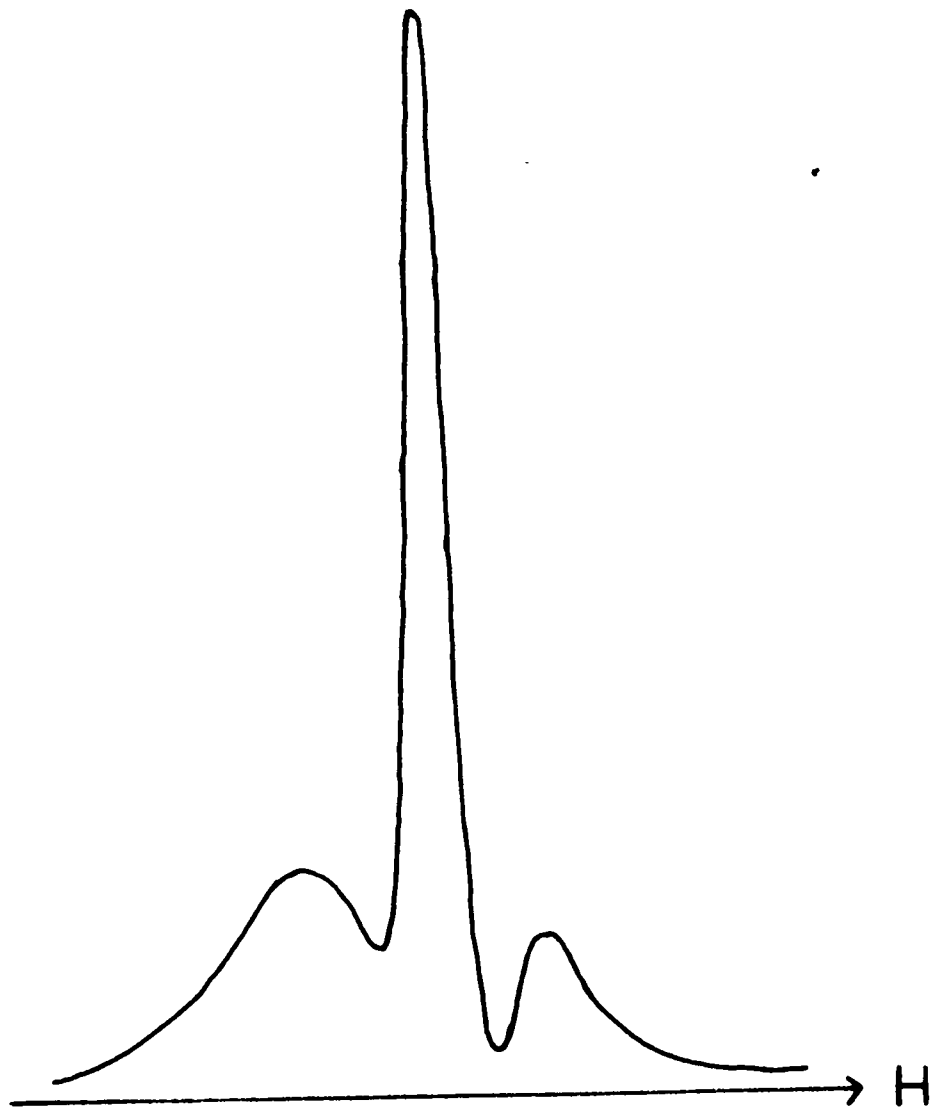
47a THEORETICAL CURVE 'F'

p.7.9



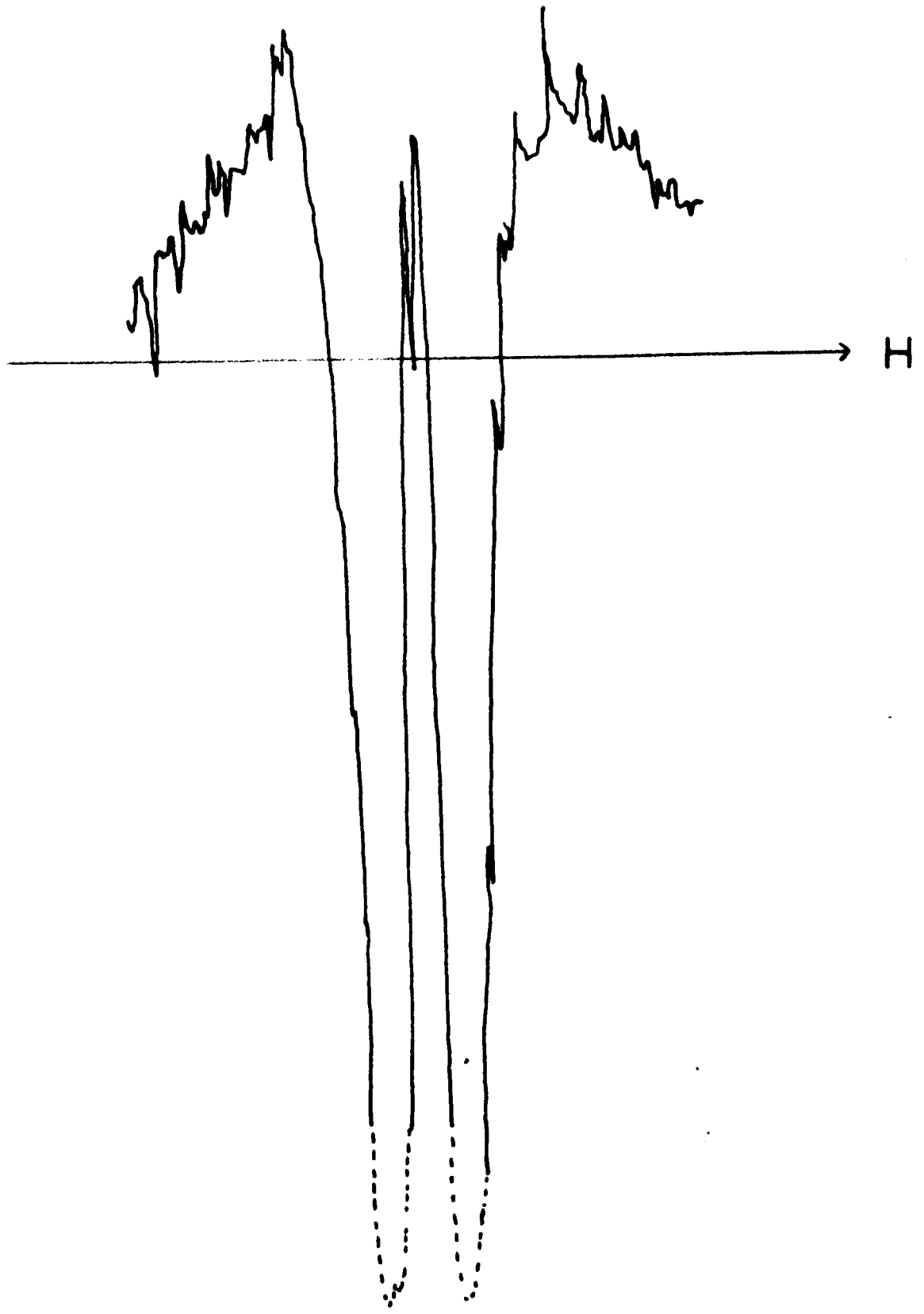
47ab MODULATION AT $4\omega_o$

p. 9.3



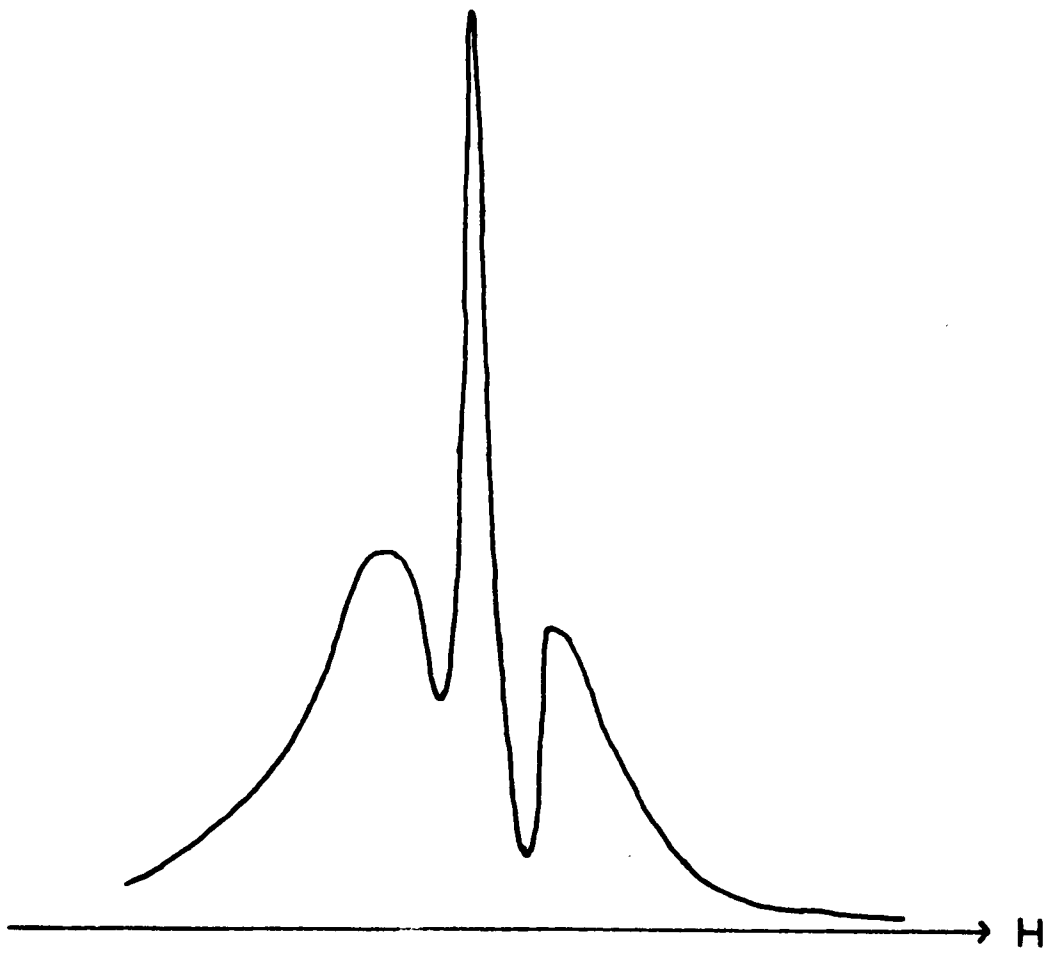
47c MODULATION AT $4\omega_o$

AS 47b BUT LINEAR POLARIZER
REPLACED BY LINEAR ANALYSER.



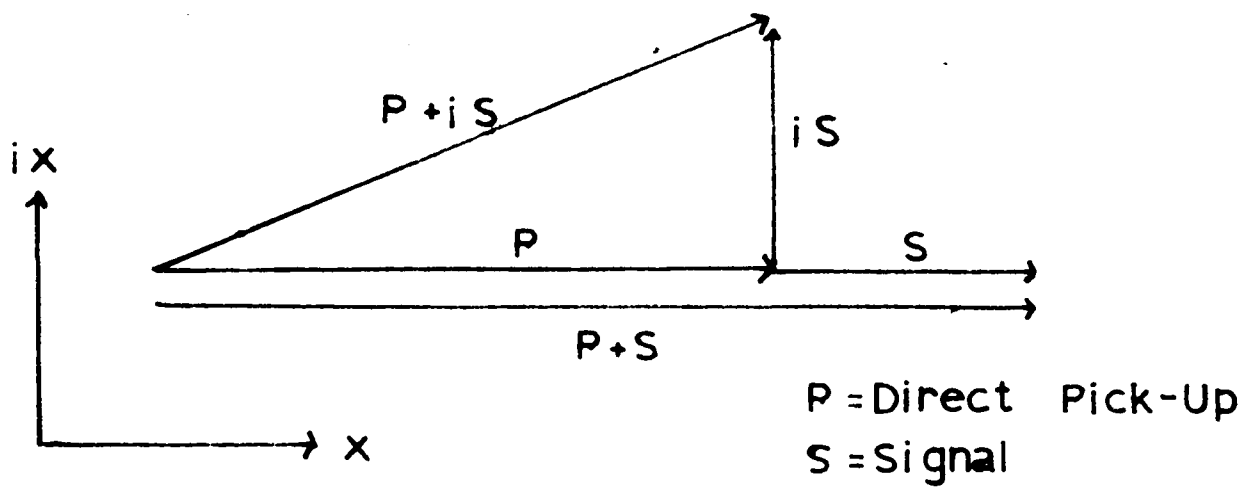
48. MODULATION AT $4\omega_0$

NO POLARIZER OR ANALYSER
EARTHS FIELD COMPENSATION MISALIGNED



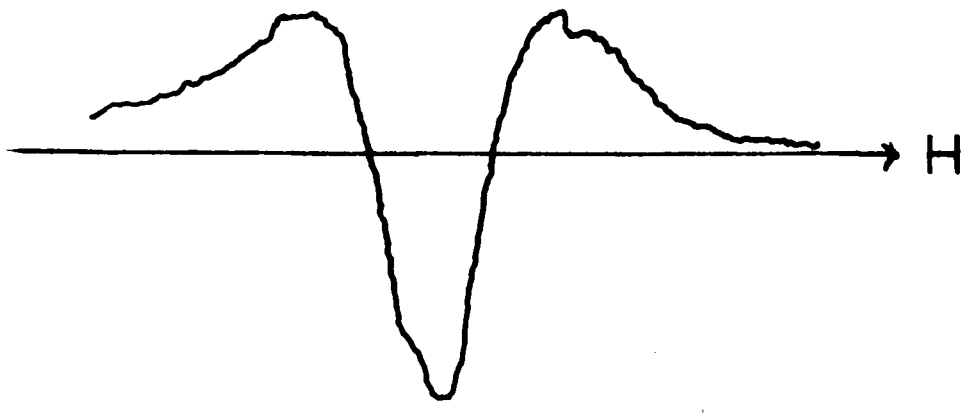
49. ENVELOPE OF MODULATION AT ω_o

p. 9.4

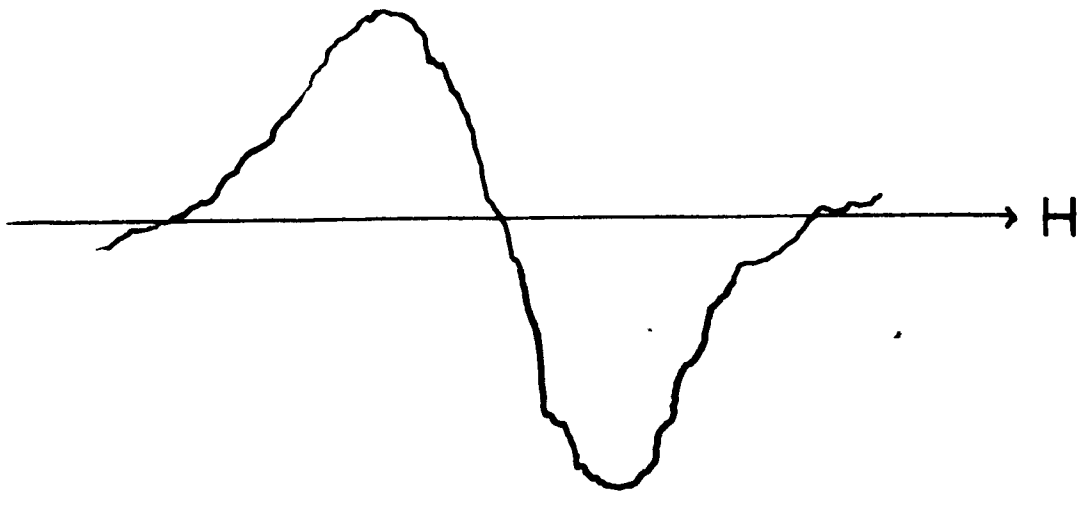


50. ILLUSTRATING THE EFFECT OF DIRECT PICK-UP ON DETECTOR

p. 9.4

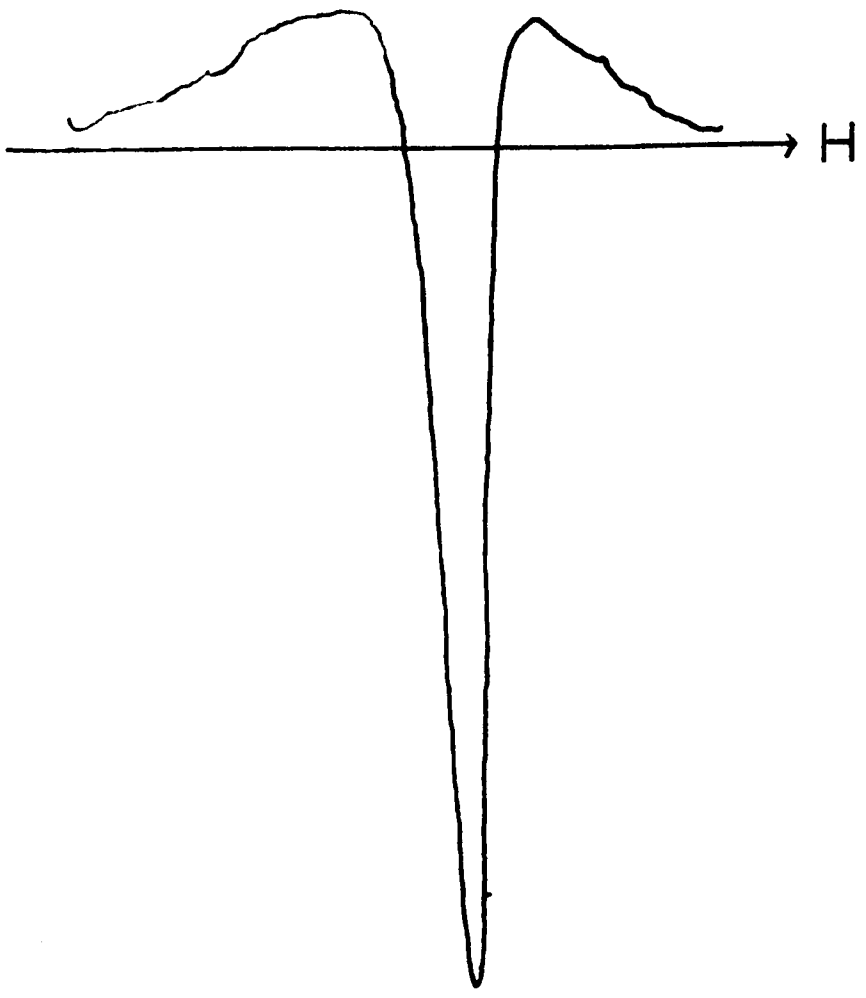


51a



51b

51a b ENVELOPES OF MODULATION AT $3\omega_0$

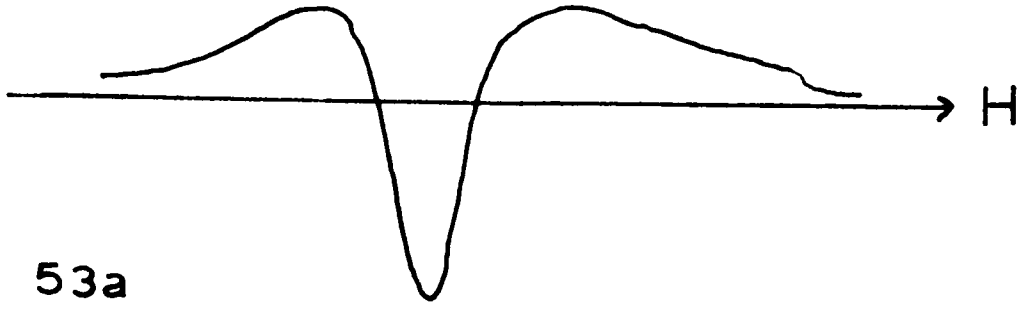


52 a

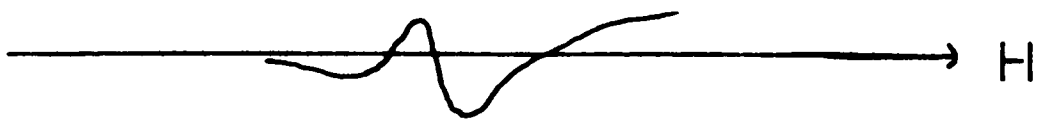


52 b

52ab ENVELOPES OF MODULATION AT ω_o IN X-BEAM



53a



53b

53ab ENVELOPES OF MODULATION AT ω_o
IN LIGHT SCATTERED IN .X-DIRECTION

APPENDIX

It is required to solve the equations 65 and 66 (p.4.7) making approximations consistent with the orders of magnitude given on p.4.5 for the various parameters.

We have :-

$$\frac{dP}{dt} = \frac{1}{\tau_p} - \left(\frac{1}{\tau_p} + \frac{1}{\tau_a} + \frac{1}{2\tau_2}\right) + \frac{1}{2\tau_2} P \qquad (a)$$

$$\frac{dP}{dt} = -\left(\frac{1}{T_1} + \frac{n}{N\tau_a} + \frac{1}{2T_2'}\right)P + \frac{n}{2N\tau_2} P \qquad (b)$$

For convenience, we introduce :-

$$\alpha = \left(\frac{1}{\tau_p} + \frac{1}{\tau_a} + \frac{1}{2\tau_2}\right) \quad \beta = \frac{1}{2\tau_2} \quad \gamma = \frac{1}{\tau_p}$$

$$\delta = \left(\frac{1}{T_1} + \frac{n}{N\tau_a} + \frac{1}{2T_2'}\right) \quad \varepsilon = \frac{n}{2N\tau_2} = \frac{1}{2T_2'} \quad D = d/dt$$

(a) and (b) then become :-

$$(D+\alpha)p = \beta P + \gamma \qquad (c)$$

$$(D+\delta)P = \varepsilon p \qquad (d)$$

Eliminating P, $D^2p + (\delta+\alpha)Dp + (\alpha\delta - \beta\varepsilon)p = \gamma\delta$ (e)

(e) is of the form :-

$$D^2p + \lambda Dp + \mu p \qquad (f)$$

and has the solution containing the two exponentials,

$$\exp \tfrac{1}{2}\left[-\lambda \pm \sqrt{\lambda^2 - 4\mu}\right]t$$

Substituting the numerical values of the parameters from p.4.5 we find :- $\lambda^2 \simeq 5 \times 10^{11}$ sec.$^{-1}$ $\quad 4\mu \simeq 10^5$ sec.$^{-1}$

Therefore $\lambda^2 \gg 4\mu$ (g)

Expanding the index of the above exponentials binomially,

we have :- $\frac{1}{2}\left[-\lambda \pm \lambda\left(1-\frac{1}{2}\frac{4\mu}{\lambda^2}+\cdots\right)\right]$

$$= -\frac{\mu}{\lambda} \quad \text{or} \quad -\lambda$$

Hence the solution of (f) is

$$P = A e^{-\lambda t} + B e^{-\frac{\mu}{\lambda} t} + \frac{k}{\mu}$$

Similarly $$P = C e^{-\lambda t} + D e^{-\frac{\mu}{\lambda} t} + \frac{K}{\mu}$$

The initial conditions are p=P=0 at t=0 , and hence, from

(c) and (d) $\frac{dp}{dt} = \gamma$ $\frac{dP}{dt} = 0$

Substituting these in (c) and (d) and their differentials,

$$0 = A + B + \frac{k}{\mu} \qquad 0 = C + D + \frac{K}{\mu}$$

$$\gamma = -\lambda A - \frac{\mu}{\lambda} B \qquad 0 = -\lambda C - \frac{\mu}{\lambda} D$$

Solving for A, B, C, D,

$$A = \frac{k - \gamma\lambda}{\lambda^2 - \mu} \qquad B = \frac{\lambda(\mu\gamma - \lambda k)}{\mu(\lambda^2 - \mu)} \qquad (j)(k)$$

$$C = \frac{K}{\lambda^2 - \mu} \qquad D = \frac{K\lambda^2}{\mu(\mu - \lambda^2)} \qquad (\ell)(m)$$

Before substituting the experimentl parameters we make further approximations. Thus :- $A = k\,\frac{(1-\frac{\lambda}{\delta})}{\lambda^2-\mu} \simeq -\frac{k\lambda}{\delta(\lambda^2-\mu)}$ since $\frac{\lambda}{\delta} \simeq 10^5$

Therefore $$\frac{A}{C} = -\frac{k}{K}\frac{\lambda}{\delta} = -\frac{\lambda}{\varepsilon} = -\frac{T_2'}{\tau_2} \qquad (n)$$

Also $$\frac{B}{D} = -\frac{\lambda(\mu\gamma - \lambda k)}{K\lambda^2} \simeq \frac{k}{K} = \frac{\delta}{\varepsilon} \approx 1 \qquad (o)$$

since $\lambda k \simeq 5\times10^9$ $\mu\gamma \simeq 10^8$

We now evaluate the exponential indices $-\lambda$, $-\frac{\mu}{\lambda}$

Substituting τ_1, etc.

$$\mu = \left(\frac{1}{\tau_p} + \frac{1}{\tau_a} + \frac{1}{2\tau_2}\right)\left(\frac{1}{T_1} + \frac{1}{2T_2'} + \frac{n}{N\tau_a}\right) - \frac{1}{4\tau_2 T_2'}$$

Neglecting $\frac{1}{\tau_p}$ w.r.t. $\frac{1}{\tau_a}$, $\frac{1}{2\tau_2}$ and dividing by $\lambda = \frac{1}{2\tau_2}$

$$\frac{\mu}{\lambda} = \frac{\tau_2}{2\tau_R T_1} + \frac{1}{T_1} + \frac{n}{N\tau_R} + \frac{\tau_2}{\tau_R T_2'}$$

Neglecting the first term w.r.t. the others, and substituting $\frac{\tau_2}{T_2'} = \frac{n}{N}$ we find

$$\frac{\mu}{\lambda} \simeq \frac{1}{T_1} + \frac{2n}{N\tau_R} = \frac{1}{T}$$

thus defining T.

Finally we require $\frac{k}{\mu}$

$$\frac{K}{\mu} = \frac{\gamma\delta}{\alpha\delta - \beta\varepsilon} = \frac{1}{\tau_p} \frac{\frac{1}{T_1} + \frac{1}{2T_2'}}{\left(\frac{1}{\tau_p} + \frac{1}{\tau_R} + \frac{1}{2\tau_2}\right)\left(\frac{1}{T_1} + \frac{1}{2T_2'} + \frac{n}{N\tau_R}\right) - \frac{1}{4\tau_2 T_2'}}$$

But $T_1 \gg T_2', \frac{n}{N\tau_R}$

therefore $$\frac{K}{\mu} = \frac{1}{\tau_p} \cdot \frac{1}{\frac{1}{\tau_p} + \frac{1}{\tau_R}} = \frac{\tau_R}{\tau_p + \tau_R}$$

Similarly $$\frac{K}{\mu} = \frac{\frac{1}{2T_2'}}{\frac{1}{T_1} + \frac{1}{2T_2'} + \frac{n}{N\tau_R}} \cdot \frac{\tau}{\tau_p} = \frac{\tau_R}{\tau_p + \tau_R}$$

making the same approximations.

Finally, using (h), (i), (n), (o), (p), (q), (r),

$$P = Ae^{-\frac{t}{2\tau_2}} + Be^{-\frac{t}{T}} + \frac{\tau_R}{\tau_p + \tau_R}$$

$$P = -\frac{\tau_2}{T_2'} Ae^{-\frac{t}{2\tau_2}} + Be^{-\frac{t}{T}} + \frac{\tau_R}{\tau_p + \tau_R}$$

Which are the results given in eqs.67, 68, 69.

From (l), (m), we have $\frac{C}{D} = -\frac{\mu}{\lambda^2} \simeq -10^{-7}$

and $$\frac{A}{B} = \frac{A}{C} \cdot \frac{C}{D} \cdot \frac{D}{B} \simeq \left(-\frac{T_1'}{\tau_2}\right)\left(-10^{-7}\right).1 \simeq 10^{-2}$$

Therefore $B \gg A \gg \frac{\tau_2}{T_2'} A$ and the second exponential dominates the first in both equations.

REFERENCES

1. M. Fred, F. S. Tomkins, J. K. Brody, and M. Hammermesh, P.R. 82, 406, 1950.
2. F. D. Colegrove, and P. A. Franken, P.R. 119, 680, 1960.
3. F. Bloch, and A. Seigert, P.R. 57, 522, 1940.
4. I. I. Rabi, P.R. 51, 652, 1937.
5. G. W. Series, Rep. Prog. Phys. 22, 280, 1959.
6. J. Brossel, and F. Bitter, P.R. 86, 308, 1952.
7. J. N. Dodd, and G. W. Series, Proc. Roy. Soc. A.263, 353, 1961.
8. A. V. Phelps, and J. P. Molnar, P.R. 89, 1202, 1953.
9. R. A. Buckingham, and A. Dalgarno, Proc. Roy. Soc. A.213, 506, 1952.
10. M. A. Biondi, P.R. 82, 453, 1951.
11. H. G. Kuhn, and H. J. Lucas-Tooth, J. Sci. Inst. 35, 413, 1953.
12. E. M. Purcell, and G. B. Field, Ap.J. 124, 542, 1956.
13. E. U. Condon, and G. H. Shortley. The Theory of Atomic Spectra. Cambridge University Press, 1959.
14. L. W. Anderson, F. M. Pipkin, and J. C. Baird. P.R. 116, 87, 1954.
15. L. D. Schearer. P.R. Letts. 10, 108, 1963.
16. F. Bloch. P.R. 70, 460, 1946.
17. H. C. Torrey, P.R. 76, 1059, 1949.
18. A. C. G. Mitchell, and M. W. Zemansky. Resonance Radiation and Excited Atoms. Cambridge University Press, 1961.
19. C. W. Allen. Astrophysical Quantities. Athlone Press. 1963.
20. Chapman and Cowling. Mathematical Theory of Non-Uniform Gases.

21. J. N. Dodd, G. W. Series, and M. J. Taylor. Proc. Roy. Soc. A.273, 41, 1963.

22. B. Kibble, and G. W. Series. Proc. Roy. Soc. 1963.

23. M.I.T. Radiation Lab. Series 18. Vacuum Tube Amplifiers, p.395.

24. W. E. Bell, and A. L. Bloom, P.R. 107, 1559, 1957.

25. L. D. Schearer. Advances in Quantum Electronics, p.239. Columbia University Press, 1961.

26. L. D. Schearer. International Conference on Optical Pumping. Heidelberg, 1962. (Unpublished). also, P. R. Letts, 8, 434, 1962, and 9, 502, 1962.

Abstract

The work reported in this thesis consists of an investigation into three aspects of optical pumping in Helium.

(i) Optical pumping in He^4

This work was initially directed towards repeating the observations of Colegrove and Franken (ref. 2), who first reported experiments to produce atomic alignment by optical pumping in He^4. This was achieved, and the theory and experiments were extended to cover the case of polarisation.

The 2^3S_1 term in He^4 is metastable and is used as the ground level in an optical pumping experiment. The metastable atoms are created by exciting a weak electrodeless glow discharge in low pressure He^4 gas. Light of wavelength 10830 Å from a powerful r.f. excited lamp is used to illuminate the sample, which is placed in a weak magnetic field ($\sim$1 G). This excites the transitions $^3S_1 - {}^2P_{0,1,2}$ in the sample. As a result of the non-uniform spectral distribution of the exciting light, the $|J = 1, M_J = \pm 1\rangle$ states of the $^3S_1$ level become more highly populated than the $|1, 0\rangle$ state. Since the atoms in the $|1, 0\rangle$ state are more absorbent to the incident light than those in the $|1, \pm 1\rangle$ states the transparency of the sample increases. This provides a mechanism for the detection of the alignment. In practice magnetic resonance is performed on the atoms in the $^3S_1$ level, thus

equalising the populations of the $|1; \pm 1, 0\rangle$ states. The change in transparency of the sample on resonance is observed.

Polarisation rather than alignment may be produced by illuminating the sample with circularly polarised light. In this case the $|1, 1\rangle$ state becomes more highly populated than the other two.

The line shapes of the polarisation and alignment resonances are quite different, and theoretical reasons are given for this. The line widths of the resonances was found to be about 15 kcs./sec. This width was due to residual field inhomogeneities. The lifetime of the metastable atoms, in the presence of the weak discharge was measured by observing the pumping transient. It was found to be $\sim 10^{-4}$ secs. Possible relaxation processes are discussed. It is concluded that relaxation is mainly the result of collision processes with discharge products.

The spectral profiles of the lamps used were investigated, using a high resolution Fabry-Perot spectrograph. As a result of this investigation a new type of lamp was designed which was effective in reducing self-reversal.

(ii) Optical Pumping in He^3

Polarisation is produced in the $^3S_1$ metastable level of He^3 by a technique similar to that used in He^4. At low magnetic fields the nuclei ($I = \frac{1}{2}$) also become polarised through the hyperfine coupling interaction. Collisions

between metastable atoms and ground state atoms result in the exchange of electrons, and metastability. By this means the nuclear polarisation is transferred to the ground level.

The polarisation may be detected by magnetic resonance in the two hyperfine metastable levels ($F = \frac{1}{2}, 3/2$) or by nuclear resonance in the ground level. In the latter case the depolarising action of the r.f. perturbation is rapidly transferred to the metastable atoms through the mechanism of the metastability exchange process. Thus the nuclear resonance can be detected optically.

Rate equations are developed for a simplified system consisting of two spin $\frac{1}{2}$ assemblies, corresponding to the ground state atoms and the metastable atoms. The polarisations of the two systems are related by spin exchange collisions. Terms are included for the pumping and relaxation processes. Solution of these equations leads to a number of relations between the characteristic times of the pumping and decay transients, which are verified experimentally.

Further rate equations are developed describing the metastability exchange processes for the actual system. It is shown that in equilibrium the metastable atoms and ground state atoms have equal nuclear polarisations. The population distribution among the metastable spin states is similar to a Boltzman distribution, in angular momentum rather than in energy. Using this distribution an expression is calculated

for the nuclear polarisation in the ground level, in terms of the optical nuclear resonance signal. Polarisations of ~4% were achieved. It was found advantageous to use He^4 lamps to pump the He^3 sample.

Longitudinal and transverse relaxation times for the nuclear polarisation in the ground level were measured under different experimental conditions. When the discharge was on, T_1 (~ 10 secs.) was found to be dominated by the exchange collisions with the metastable atoms, which decay very quickly. Without the discharge T_1 was much longer, (~ 160 secs.).

T_2 was measured from observations of the decay of a nutational transient occasioned by a pulse of r.f. at the nuclear resonance frequency. This nutation was observed optically, as before. T_2 (~ .1 sec.) was also found to be determined mainly by exchange collisions with the metastable atoms.

The density of the metastable atoms in the weak discharge was determined by an optical absorption method, using the Fabry-Perot spectrograph. About 1 in 3×10^5 of the atoms, in a 1 mm. Hg. sample, were found to be in the $^3S_1$ metastable level.

The cross-section for metastability exchange was estimated from measurements of T_2 and the density of metastable atoms. The estimate was confirmed from measurements of the line width of the resonances in the metastable levels, which are

broadened by metastability exchange collisions. The measurements of the cross-section by the two different methods gave values:

$$7.9 \pm 2 \times 10^{-16} \text{ cm}^2.$$

$$6.1 \pm 1 \times 10^{-16} \text{ cm}^2.$$

(iii) Modulation experiments

The He^4 optical pumping has some similarities to the Hg. system, used by Series et al. (refs. 7, 21, 22) to study the modulation of fluorescent light, in a double resonance experiment. In their work, excited Hg. atoms were subjected to an r.f. perturbation. As a result of this the wave functions of the excited atoms become coherent superpositions of the unperturbed eigenfunctions. When observed under suitable experimental conditions the light emitted by these atoms was found to be modulated at the frequency of the rotating field, ω_o, and its harmonics.

The work on modulation reported in this thesis was performed with He^4, in which the r.f. perturbation occurs in the lower or absorbing state. It is shown that modulation effects then occur in the absorbed light. The modulation is observed in the fraction of the incident light which is not absorbed by the sample. Again it is necessary to select suitable experimental conditions for observation. It is usually necessary to insert an analyser in front of the detector.

Exploratory experiments show that modulation at frequencies ω_o, $2\omega_o$, $3\omega_o$ and $4\omega_o$ occurs, under a variety of experimental conditions. So far experiments have been conducted at low magnetic fields, so that the frequencies of modulation have been in the kilocycle range.

Tentative theoretical explanations for some of the phenomena are given in terms of the theory of Dodd and Series (ref. 7).

The Hg. and He^4 experiments are not entirely analogous, and phenomena are observed in He^4 which do not occur in Hg. These have their origin in an essential difference between an optical pumping experiment and a double resonance experiment. Optical pumping is a three stage process. Atoms are excited, then they decay and we subsequently observe their absorption properties. In a double resonance experiment atoms are excited once only, and then their emission properties are studied. It is thought that the initial coherence that the He^4 atoms have as a result of the r.f. perturbation may persist throughout the optical pumping cycle. In the double resonance experiment the r.f. perturbation acts once only, i.e. when the atom is in the excited state. It is suggested that experiments at higher magnetic fields, such that $\omega_o \gg \Gamma_{ex.}$ may eliminate these additional effects. (Γ_{ex} is the decay constant of the excited states). Such experiments would be much simpler to interpret.